SOME INVESTIGATIONS OF LOW ENERGY NUCLEAR REACTIONS

by Robert S. Storey

Department of Natural Philosophy

University of Glasgow.

Presented at Glasgow University in November, 1958

as a Thesis for the Degree of

Doctor of Philosophy.

ProQuest LLC.
789 East Eisenhower Parkway
P.O. Box 1346
Ann Arbor, MI 48106 – 1346

PREFACE

In this thesis experiments are described which were carried out by the author between October 1954 and April 1958 in the Department of Natural Philosophy at Glasgow University.

Initially this work was directed towards obtaining more information about the symmetry properties of light nuclei, but later the point of emphasis shifted to the study of nuclear reaction mechanisms and, of course, to the compatability of the various nuclear models with the measured reaction parameters.

Part I consists of a survey of previous techniques used and results obtained in nuclear reaction studies. The various theories of nuclear interactions and of nuclear structure are also discussed. The material presented is drawn from the literature of nuclear physics.

In Part II. 1 an investigation of the 277 kev. resonance for proton capture in ^{14}N is described. This reaction was chosen in order to illustrate nuclear reaction processes in a region of well separated nuclear levels and in order to demonstrate the applicability of the recently developed theory of angular distributions and correlations in obtaining information about such levels. The results presented are original and the experimental work and the analysis were carried out by the author.

In the latter sections of Part II studies of (d,p) reactions are reported. A series of measurements of the angular distributions of the proton groups in $B^{10}(d,p)B^{11}$ had been previously made by Dr. W. M. Deuchars and Dr. K. A. Wallace.

An improved apparatus was developed and used by Dr. Wallace and the author to obtain more accurate distributions and to extend their measurement to lower energy groups in a region of deuteron energy of special interest. The method of analysis used by Dr. Deuchars was applied by Dr. Wallace to the new results. The measurements of the angular distributions in the $Mg^{24}(d,p)Mg^{25}$ reaction and their analysis in terms of a modified stripping theory suggested by Dr. A. H. deBorde were carried out by Dr. Wallace and the author. A latter analysis by the author of one of these distributions in terms of the strong coulomb stripping theory of Martirosyan and of Biedenharn et al. is also reported.

In Part III studies of particle emission in the continuum region are described. The experimental method used in the measurement of the (n,p) spectra and interpretation of the results are original. This is the first systematic attempt to obtain the variation of the absolute value and shape of the cross section for proton emission as a function of proton energy over a range of closely spaced nuclei and at different neutrons bombarding energies. The work described in this part was performed by Dr. A. Ward, Mr. W. Jack and the author, the author taking a major responsibility for the experimental work and the analysis of the results.

New measurements of the decay of fluorescence in CsI(Tl) are described in Part IV. This work establishes a definite variation in the lifetime for different ionizing

particles and provides quantitative measures of this effect at room temperature. Various explanations and applications of this effect are discussed. The author took a full share of the responsibility for this work which was carried out in co-operation with Dr. Ward and Mr. Jack.

In Part V the general implications of the work presented in this thesis are discussed and further experiments which the author believes will enlarge and advance our understanding of this field are outlined.

In the appendices a detailed analysis of geometrical factors in the (n,p) apparatus, and a method of preparing thin plastic scintillators are described. This work was carried out by the author and is original. Although Lagiss (1956) published essentially the same technique for preparing thin plastic scintillators, the author's work on this was completed early in 1955.

ACKNOWLEDGMENTS

The author wishes to thank Professor Dee for making the facilities of his department available for the work described here. He is also indebted to Dr. P. J. Grant for advice given during the first part of this work and to Dr. K. A. Wallace, Dr. A. Ward, and Mr. W. Jack for their co-operation during the latter parts.

The author appreciates the assistance given by Mr. A. Duncan, Mr. R. Irvine and Mr. J. Lloyd, and their assistants in the operation of the accelerators, the construction of the apparatus and the application of the special techniques required.

Financial assistance by the Imperial Oil and Imperial Chemical Industries Fellowship Committees is gratefully acknowledged.

CONTENTS

PART I A REVIEW OF LOW ENERGY NUCLEAR REACTIONS

I. 1 INTRODUCTION

(a) Historical Aspects

The study of the nucleus as a distinct entity began in 1911 when, in order to explain Geiger and Marsden's measurements of the angular distributions of alpha particles scattered by gold and platinum, Lord Rutherford suggested that all of the positive charge and almost all of the mass of an atom were concentrated in a central region or nucleus about 10^{-12} cm. in diameter. Since the mass and charge of nuclei were closely integral multiples of the mass and charge of the hydrogen nucleus or proton, a nucleus was at first thought to consist of protons in sufficient number to account for its atomic number A and of electrons added to reduce its net positive charge to the proper value Ze. However, in bombarding light elements with alpha particles Chadwick discovered the neutron, another particle with about the same mass as the proton but with no charge. Since then (1932) it has been found necessary to modify our original picture of the nucleus and replace the electrons and the proton surplus to the positive charge requirement by N (= A - Z) neutrons.

In recent years much effort has been expended in the measurement and explanation of the detailed properties of the nucleus. The dominant source of information has remained the study of the interactions occurring when two nuclei come into close proximity. Usually a beam of light nuclei with

high velocities are directed into a target consisting of heavier nuclei at rest. The projectiles used are often nucleons; that is, protons or neutrons because their basic nature renders interpretation more definite. However, the next simplest nucleus, the deuteron, has attracted recent interest because of the manner in which the loose bond between its constituent proton and neutron is broken in an interaction at the nuclear surface. The alpha particle, a very strongly bound group of two protons and two neutrons, has also been widely used principally because of its availability. Monoenergetic sources of alpha particles were available before Rutherford's nuclear hypothesis, while similar sources of the other charged particles and neutrons awaited the construction by Cockcroft and Walton and by Van de Graaff, in the early thirtys, of the first two types of a long and continuing series of particle accelerators.

In some senses the problem of nuclear physics is the problem of the description of the mutual forces between nucleons. Some information about the interaction of two nucleons can be obtained by bombarding hydrogen with protons or neutrons at various energies. However, because of the complexity of the forces involved, the incomplete data available, the possibility of many body forces, and the computational difficulties associated with the many body problems, much of the theoretical effort to describe the heavier nuclei in the past has gone into the study of models in terms of macroscopic parameters in analogy with the useful description of matter in terms of a few thermodynamic variables rather than of the set of co-ordinates of position and

motion of the constituent atoms. Assuming such a model, reaction studies require an inquiry into the possibility of an approximate description of the motion of a particular individual nucleon with respect to the rest. Alternatively, such motion might be described as a free orbit in a potential well associated with the whole nucleus (independent particle model) or as highly correlated due to strong interaction with the immediately adjacent nucleons (Bohr compound nucleus model). Unfortunately, the most recent experiments suggest that, although for certain excitation energies and ranges of atomic number accurate explanations are possible in terms of these limiting models, the situation is in general intermediate.

Recently Bruechner and collaborators have started a series of investigations into the relations connecting the commonly used parameters of heavy nuclei with those of the two nucleon interaction with the object of ensuring consistency between measurements in these two fields.

(b) Fundamental Aspects

From the discussion of the previous section it is obvious that the systems of interest consist of groups of nucleons whose members are sufficiently close to each other to interact. Perhaps the most important property of such groups is their stability or time rate of change due to particles or electromagnetic quanta entering or leaving them. We will consider first the ground or minimum energy states of naturally occurring nuclei which are, with a few exceptions, completely

stable. Application of the appropriate boundary conditions to the Schrodinger equation results in an eigenvalue equation for the wave function of the nucleus, each solution of which describes a state with a definite and discrete value of the total energy, the total angular momentum and the parity, and possibly other "constants of the motion" depending on the nuclear model used in the interpretation. These quantities rather than the explicit wave function itself constitute the physically measurable parameters of the system.

As the probabilities for emission or absorption become appreciable this type of description continues to apply, but the total energy is no longer precisely discrete and acquires an uncertainty or total width Γ which, according to the Heisenberg uncertainty relation, equals $\hbar/\tau$ where τ is the average time before a transition occurs in such a system. Since Γ is proportional to the probability for emission it may be split into partial widths or probabilities for emissions of a particular type ($\Gamma = \Gamma_\gamma + \Gamma_n + \Gamma_p + ---$). In general, the average level width will increase with the total energy available; that is, with the increasing instability of the system. Since, as we shall see later, the level spacing decreases with increasing energy the levels eventually overlap and a continuum is reached. The level spacing and hence the energy at which the continuum begins will depend on the atomic number, being many Mev. above the ground state for very light nuclei and only a few Mev. for the heavy nuclei.

As τ approaches τ_d a quantity of the order of

magnitude of the transit time of the group by a nucleon (about 10^{-21} sec.) or equivalently as Γ approaches E which it will as E becomes large or N - Z diverges appreciably from its value on the stability line, a description in terms of the above framework loses its value and one must consider nuclear reactions as such.

A nuclear reaction may be said to occur when a stable group of particles a changes into a second stable group b with different descriptive parameters in the same reference frame. Because of experimental limitations, usually this can occur only when two particles come together initially and accordingly a nuclear reaction may be represented by the form $(A + a) \rightarrow B + \Sigma b_i$ where A and B customarily denote the heaviest particles in each group. In the special case where only the momentum vectors of a and A change the process is spoken of as an elastic scattering. The total energy and momentum of the group is conserved during a transition. There is also evidence for other independent invariant parameters especially in certain types of transition.

Again the most important characteristic of a nuclear reaction is the time taken for it to occur and reactions may be divided into those which are single transitions or direct processes with B and the b_i being produced from a and A during τ_d and those in which a and A combine to form a well defined but unstable nucleus C (which is accordingly called the compound nucleus) and which after a relatively much greater time breaks up to give B and the b_i in one or more random decay transitions. There is

experimental evidence that both types of processes are observed, their relative contributions depending on the particular nuclei and energies involved. In high energy processes some of the b_i may result from a direct effect and some will be emitted only after many transitions have occurred.

The measurements of the cross sections, angular distributions, and excitation functions for nuclear reactions may be interpreted to yield information about the detailed reaction mechanism and about the energy levels of the residual nucleus B and the compound nucleus C (if there is one). If the particle or quanta groups corresponding to discrete levels are resolved by the detecting device, information may be obtained about these particular levels; e.g. energy spin, and parity and about the individual innate transition probabilities or reduced widths. If, on the other hand, there is a continuum of levels or if the levels are experimentally unresolved, information is obtained about average characteristics such as level density or transition probability per unit energy interval.

In the subsequent review sections some of the ideas introduced above will be expanded, but the discussion will be restricted to that which is relevant to the experimental material presented by the author. This material has, of course, been treated in various degrees of detail and from various points of view in many previous works. Among the more general works the author has found useful are those of Bethe,1937, Fermi, Blatt and Weisskopf.[1949] [1952] The relevant sections of the recently published Handbuch der Physik (ed. by S. Flugge) appear to be comprehensive

and its detailed set of references cover most of the important contributions in this branch of physics.

I. 2 EXPERIMENTAL TECHNIQUES

Nuclear reaction experiments are restricted to the measurement of the number and the polarization of emitted particles (or quanta) as a function of bombarding particle energy (excitation function) or of emitted particle energy (spectrum) or of emitted particle angle with respect to the bombarding particle or another emitted particle (angular distributions and correlations). If the absolute flux of bombarding and emitted particles is measured and if the thickness of the target is known then any of the above yields may be transformed into the corresponding cross sections per atom of the target isotope which is an absolute measurement. The magnitudes obtained for these quantities and their interpretation will be discussed in sections I. 3 and I. 4 and the techniques for their measurement in the present section.

We will consider the excitation function first since, unlike the other measurements, the problem is primarily one of a source of bombarding particles of a specified energy. The usefulness of a particular source depends on the range of energies available, the accuracy to which the average particle energy at a particular setting is known and stable, and the degree to which the beam is monoenergetic. The requirements are most stringent for measurements in the discrete energy level range and it is found that the Cockcroft Walton and Van de Graaff accelerators are most satisfactory.

Although neutrons of energies greater than 1 Mev. are available from a number of sources only those produced in

a thin target bombarded with charged particles from an electrostatic accelerator are sufficiently homogeneous for accurate excitation function studies. The reactions commonly used for this purpose are:

$$D + D \rightarrow He^3 + n + 3.28 \text{ Mev.}$$
$$p + T \rightarrow He^3 + n - 0.764 \text{ Mev.}$$
$$D + T \rightarrow \alpha + n + 17.6 \text{ Mev.}$$
$$p + Li^7 \rightarrow Be^7 + n - 1.647 \text{ Mev.}$$

Monochromatic neutrons with energies in the range 6 - 12 Mev. are not readily available because of the lack of a suitable reaction and their use will await the operation of the tandem van de Graaffs now under construction.

A charged particle is detected by means of the photons, ions or chemical changes produced along its path as it slows down due to interactions with the surrounding matter. Detection is more indirect for other types of nuclear radiations, an initial interaction being required in which a charged particle of appreciable energy is produced. A gamma ray may lose all its energy to an electron (photoelectric effect) or be scattered by an electron (compton effect) or change into an electron and a positron when passing through a perturbing field (pair effect). A neutron is detected by observing scattered nuclei (usually protons) or the products emitted following its absorption in a nucleus.

In addition to detecting a particle it may be necessary to know as much as possible about its nature, energy, direction and spin orientation. In a particular experiment some information will be available from previous measurements or may be inferred from the conservation laws or the specific details

such as bombarding energy, geometry, etc., but it may be necessary to make definite measurements to supplement these. Depending on the nature of the detector such quantities as the range (absorbers, photographic emulsions, cloud and bubble chambers), the total light output (scintillating material) or the number of ions produced (ionization chamber, proportional counter) can be measured if the particle is absorbed. If the detector is thin, the particle passes through with a relatively small loss of energy and corresponding quantities such as the energy loss or number of developed emulsion grains per unit length are obtained. Alternatively the deflection of the particle on passing through a known magnetic or electric field may be measured. The energy of the particle can be derived from a quantitative measurement of any of these quantities if its nature is assumed and the required calibrations have been made. Two different types of measurements on the same particle usually determine its nature unambiguously. The average spin orientation of a beam of particles is more difficult to obtain and requires measurement of an angular distribution after a spin dependent interaction has occurred.

Coincidence techniques are required for angular correlations and multiple element spectrometers, and have also been used to measure the lifetimes of some nuclear states. The minimum coincidence time that has so far been achieved is about 10^{-10} sec.

Since nuclear disintegrations are random, measurements of yields, cross sections, lifetimes, etc. will have statistical fluctuations and the magnitudes obtained will

have a relative uncertainty or standard deviation of $N^{-\frac{1}{2}}$ where N is the number of events recorded. Because of this the efficiency of a particular design or type of apparatus is important because it determines the time required for a given accuracy and this time must be minimized to avoid changes due to lack of stability in the apparatus, particularly in the gain and bias of electronic units.

For measurements where a spectrum with considerable structure is involved magnetic deflection systems may be designed to give results with very high accuracy and resolution, but this is obtained at the expense of efficiency and in angular distribution devices such as that of Buechner et al the apparatus becomes very heavy and expensive. Magnetic deflection of monoenergetic bombarding particle beams to separate particles of a different nature is a commonly used technique.

Nuclear emulsions have been much used in reaction studies, particularly those of an initial nature. They are economical in machine running time and convenient to position with respect to the target, but it is difficult to obtain adequate statistical accuracy due to the time spent analyzing each event and it is difficult to study the effects of modifying the apparatus and shielding. The same remarks apply to cloud and bubble chambers except that they are not as convenient for use in the reaction apparatus.

Since the electrical pulse output from scintillation counters and gas filled counting tubes enables an event to be recorded very soon after its occurrence and thus make coincidence

techniques and high statistical accuracy possible, these are the most widely used of all types of detectors. Scintillators have tended to supplant gas tubes recently because they are more convenient to use because the pulse rise time is usually much smaller enabling the use of smaller coincidence time, and because their much higher density results in a much better efficiency and total absorption particularly for high energy particles and gamma rays. Since the measurement of the light output is also a statistical process the resolution depending on the number of photoelectrons produced in the cathode of the associated photomultiplier ZnS(Ag) might be expected to be the best scintillator since it has the highest light output. However, the resolution also depends on uniform light collection which in turn requires the use of a single crystal detector. Since it is very difficult to grow single crystals of appreciable size in ZnS(Ag), NaI(Tl) and recently CsI(Tl) have been used instead. The latter does not require a Protective barrier against water vapour and hence is preferable for detecting short range particles. Its higher density and average atomic number may also make it more desirable for gamma ray studies than NaI(Tl). Their short flucrescent decay times and hydrogen content make organic scintillators valuable in some applications. Anthracene has the highest light output but liquid and plastic scintillators are more frequently used because they are cheaper and more readily obtained in any size or shape.

Gamma ray and neutron spectrometers are usually either of the single detector total absorption or multiple detector telescope types. To get appreciable total absorption and minimum edge effects a very large scintillator is used. It may be surrounded by an anti-coincidence shield to remove edge effects completely and to reduce the background. In this type both the efficiency and the degree of total absorption (or the shape of the contribution to the pulse height spectrum from a monoenergetic source) will vary fairly rapidly with energy. This is particularly so for gamma rays where the magnitude of the contributions from the photo, Compton, and pair effects change rapidly. As well as the total absorption peak there will be two others below it at high energies (due to the escape of one or both of the positron annihilation gamma rays associated with the pair process) and a broad distribution at low energies due to the escape of the Compton gamma ray. Since these contributions also vary with the size and shape of scintillators, standard shapes must be obtained for each crystal for a range of monoenergetic sources for use in analyzing complex spectra. Despite their cost five inch NaI(Tl) crystals are increasingly used because of the high percentage of total absorption pulses obtained.

Unlike the total absorption type in which only a single quantity, the sum of the light outputs from many charged particles, is measured the telescope type measures in as much detail as possible the energies and directions of the

particles proceeding from the first collision. Since it is found that the resolution is poor and the gamma ray background high in liquid or plastic scintillators of sufficient size to totally absorb neutrons the telescope is usually used for neutron spectra despite its very low efficiency.

In accurate nuclear reaction measurements corrections must be made for absorption in vacuum chamber walls, light reflectors, air etc., for finite instrumental resolution in energy or angle, for background (or random coincidence contributions) and for the effects of electronic dead time. These corrections and other details of the apparatus etc. are discussed in the more comprehensive works such as that edited by Segrè (1953) on general experimental methods and that edited by Seigbahn (1955) on gamma ray techniques. Nuclear detectors have been reviewed by Sharpe (1955) and the associated pulse circuitry by Elmore and Sands (1949). Extensive compilations of data on the energy degradation and absorption of radiations in matter are necessary for the design of apparatus and the correction and analysis of measurements. Those of Allison and Warshaw (1953) and Rich and Madey (1954) for charged particles were found most useful by the author. The gamma ray absorption coefficient graphs of Heitler (1944) have been reproduced and extended in many places in the literature.

I. 3 REACTIONS INVOLVING TRANSITIONS BETWEEN DISCRETE ENERGY LEVELS IN LIGHT NUCLEI

The methods by which the cross sections are measured as functions of the variables of the reactions have been discussed in the previous section and their analysis will now be considered. In Section I. 3(a) the application of the well known two stage reaction process with an intermediate compound nucleus and of angular correlation analysis to yield nuclear level parameters and transition probabilities will be discussed. Although the emphasis is naturally placed on the description of the gamma rays of proton capture, particle emission will also be considered because of the author's interest in the possibility of the (d, p) reaction as a compound nucleus process. In Section I. 3(b) the emphasis will shift from the evaluation of nuclear structure and will centre on the description of the complex reaction process which occurs when a low energy deuteron interacts with a nucleus.

(a) The evaluation of the characteristics of nuclear states and the (p, γ) reaction

If it is assumed that the region, where the level width Γ is much less than the level spacing D, is being considered, then the excitation function (after correction for beam inhomegeneity and target thickness) will exhibit well separated peaks, each of which may be fitted by

$$\sigma(p, \gamma) = \pi \lambda^2 (2l + 1) g \frac{\Gamma_p \Gamma_\gamma}{(E - E_R)^2 + (\Gamma/2)^2}$$

and the values of the Γ's and E_R (the resonance energy

corresponding to the energy of particular nuclear state in the intermediate compound nucleus) extracted. This formula is due to Breit and Wigner (1936) and $g = (2j_C + 1) / [(2j_a + 1)(2j_A + 1)]$ is the probability of forming a compound nucleus with spin j_C from two randomly oriented initial nuclei with spins j_a and j_A. The total width Γ is easily obtained since, from the formula, it is just the full width of the peak measured at half maximum height. If the emission of gamma rays and protons is energetically possible then $\Gamma = (\Gamma_\gamma + \Gamma_p) \approx \Gamma_p$ (photon and particle emission compete and Γ_γ is smaller because the coupling between the charge distribution and the electromagnetic field is small) and Γ_γ is proportional to the area under the resonance curve. It is frequently obtained by using a "thick target" (one in which the proton energy loss is much greater than Γ) in which case the yield of gamma rays per proton is $Y = 2\pi \lambda^2 g \Gamma_\gamma / \epsilon$ where ϵ is the proton energy loss per target nucleus.

According to the theory the external energy dependent factors may be removed from a partial width for particle emission by dividing it by $2kv_\ell$ to obtain a reduced width γ^2. k is the wave number of the emitted particle and $v_\ell = (F_\ell^2 + G_\ell^2)^{-1}_{r=R}$ where R is the nuclear radius and F_ℓ and G_ℓ are the regular and special irregular solutions of the radial wave equation for a particle in a Coulomb field. The magnitude of the amplitude of the reduced width depends on the phase relations between

the contributions to the total internal wave function at the nuclear surface. If these are nearly random, γ^2 will be much smaller than $\hbar^2/MR$ the value for a single particle in a potential well. On the other hand values higher than $\hbar^2/MR$ indicate in phase contributions and hence collective motion of the nucleons.

The probabilities for gamma ray transitions are discussed in detail by Blatt and Weisskopf (1952, Chap. XII). It is shown that because of the weak coupling an adequate explanation can be obtained by using only the classical radiation field emitted by a charge distribution with suitable variations in space and time. For the independent particle model the probability of decay by emission of electric radiation of multipole order L is

$$T_E(L) = \frac{4.4(L+1)}{L\,[1.3.5\ldots(2L+1)]^2}\left\{\frac{3}{L+3}\right\}^2\left\{\frac{E}{197\ \text{Mev.}}\right\}^{2L+1}$$

$$\times(R \text{ in } 10^{-13}\ \text{cm.})^{2L}\ \ 10^{21}\ \text{sec.}^{-1}$$

and by emission of magnetic radiation is

$$T_M(L) = 0.45\ (R \text{ in } 10^{-13}\ \text{cm.})^{-2}\ T_E(L)$$

The experimental evidence has been collected by Wilkinson (1956) and put in the form of the ratio $|M(L)|^2$ of the measured T's to the independent particle T's. Extensive data is available only for $|M_E\ (1)|^2$ and $|M_M\ (1)|^2$ which have values extending from 10^{-3} to somewhat greater than one with $|M_M\ (1)|^2$ tending to be the larger. The explanation

of the wide variation is again in terms of the degree of correlation of nuclear motion. Lane and collaborators (Lane and Radicati, 1954, Lane and Wilkinson, 1955) have discussed the values of γ^2 and $|M|^2$ in terms of the type of nucleon coupling and the concept of parentage of nuclear states.

When a reaction occurs the vector sum of the angular momenta both spin and orbital of the initial particles or quanta must be the same as that of the final particles. Similarly the product of the parities of the wave functions describing the separated particles after the collision must be the same as that before the collision. If an intermediate compound nuclear state occurs then the sum and product must give the intrinsic angular momentum and parity of this state. The restrictions on the various nuclear parameters which result from these conservation laws are called selection rules. Their form is fairly obvious but two examples will be given to show the effect of the angular momentum of a particle ℓ and of a photon L on the parity. If we consider the formation of a compound nucleus with spin j_C from a particle with spin j_a and a target nucleus with spin j_A then $|j_C - S| \leq \ell \leq j_C + S$ (if the channel spin $\vec{S} = \vec{j}_a + \vec{j}_A$) and $\pi_A \pi_C = (-1)^{\ell}$. Similarly for the decay of C into C^1 and a photon the selection rules are $|j_C - j_{C'}| \leq L \leq j_C + j_{C'}$, and $\pi_C \pi_{C'} = (-1)^L$ for electric transitions and $\pi_C \pi_{C'} = (-1)^{L+1}$ for magnetic transitions. Similar equations may be written for the components of the angular momentum vectors in a particular direction.

Since monopole radiation (L = 0) is not possible gamma ray emission between $j_C = j_{C'} = 0$ is forbidden. Postulation of a charge independent interaction leads to conservation of the total isotopic spin T and its Z component $T_Z = \frac{N - Z}{2}$ and consequently further selection rules. Comparison may often be made between actual measurements and those to be expected from the conservation of L and S the total orbital and intrinsic angular momenta, and of the total angular momentum j of each nucleon separately and as a result the nucleon coupling may be said to be LS, jj, or intermediate.

It has been seen that for electromagnetic transitions the probability decreases rapidly with increasing L. In a similar manner at the bombarding energies considered here the impact parameters $b = \ell\lambda$ will become greater than the nuclear radius as ℓ increases and the partial cross section for absorption of particles of angular momentum ℓ will accordingly diminish rapidly. For these reasons the contribution from a single particular ℓ and L values will tend to dominate the reaction to a very considerable extent.

The interpretation of measurements of the angular changes in the number of particles or gamma rays emitted in transitions which lead to discrete states is in terms of the theory of angular correlations. The correlation functions in the general case will be very complicated since provision is made for the possibility of external perturbing fields and of polarization phenomena. Fortunately, the precession times due

to magnetic coupling with the electronic structure are much longer (about 10^{-9} sec.) than the lifetimes (about 10^{-15} sec.) of the compound nuclei of interest here. Polarization effects are not usually observed because special techniques are required to produce polarized incident particle beams (see e.g. Zavoiskii, 1957) oriented target nuclei (see e.g. Blin-Stoyle, 1953) and polarization sensitive detectors (see e.g. French and Newton, 1952, Hughes and Grant, 1954. Heusinkveld and Freier, 1952). The cause and magnitude of polarization of particles and quanta produced in nuclear reactions is discussed by Blin-Stoyle (1951), Simon and Welton (1953), Hamilton (1948) and Biedenharn and Rose (1953).

If the angular momentum vector diagram is rigid, i.e. it consists of only three non-zero vectors, then a specified set of vectors will have a unique angular distribution associated with it. That is, if $\sigma(\theta)$ is expanded in terms of powers or Legendre functions of cos θ then the set of coefficients of these functions will be precisely determined. If on the other hand a given resultant vector must be obtained by combining more than two given angular momentum vectors, the diagram loses its rigidity and more than one configuration will be possible. The Legendre coefficients are then only specified within certain limits and a further quantity (e.g. a channel spin mixing parameter) must be specified to fix the distribution uniquely. By comparing measured distributions

with those calculated for certain values of ℓ, L and the various spins and parities, and taking account of the selection rules, intensity limitations for different ℓ and L, and known spins and parities of nuclei taking part in the reaction, the previously unknown value of the spin or parity of some particular nuclear state can be determined at least within certain limits. However, parities cannot be obtained from gamma ray angular distributions because of the different selection rules for electric and magnetic transitions and a polarization measurement is therefore required for this purpose. The values of reaction mechanism parameters may also be determined and compared with those predicted under special assumptions.

The angular distributions and correlations have been worked out in detail for the processes

$$A + a \rightarrow C \rightarrow B + b_1$$

and $$A + a \rightarrow C \rightarrow B + b_1 \rightarrow B + b_1 + b_2$$

(see for example Devons and Goldfarb 1957). The coefficients of the Legendre polynomials are essentially expressed as products of coefficients (Wigner coefficients) for the angular momentum transformations at each stage. However, tedious summations over the magnetic quantum numbers are required and to avoid this Blatt and Biedenharn (1952) have worked out expressions in terms of Racah coefficients. The system and tables of Sharpe et al (1953) have been found to be very convenient and are accordingly used in the analyses presented subsequently in this thesis.

Despite the elaborate formulation of the angular distributions they have some rather simple properties if the incident beam is not polarized. These include symmetry about the incident particle direction, isotropy if the incident or emitted waves are spherical ($\ell = 0$) or if the $(j_c)_z$ are equally probable ($j_c = 0$ or $\frac{1}{2}$). Variation of the distribution with incident particle energy or contributions asymmetric about 90° indicate interference between overlapping resonances and in the second event resonances of different parity. The order k of a Legendre polynomial appearing in a reaction is limited e.g. in a (p, γ) reaction by the formula

$$\text{max.}\ (\ell - \ell^1,\ L - L^1,\ j_c - j_{c'}) \leq k \leq \text{min.}\ (\ell + \ell^1,\ L + L^1,\ j_c + j_{c'})$$

the primes indicating a possible interfering transition. (see Sharpe et al, 1953).

It has been previously seen how the transition parameters γ^2 and T_M or E (L) are related to nucleon motion and similar relations for the parameters of a nuclear state will now be discussed. In order to obtain theoretical predictions for the values of these quantities the nature of nuclear forces must be specified in a quantitative manner. Since these are not directly measurable but rather obtained through the interpretation of two body and nuclear state data simple assumptions must be made and revised after comparison with experiment. The first approximation is that the force should be described by a potential function $V(r_{12})$ where r_{12} is the separation of two nucleons (i.e. a two body, velocity

independant central force). The elementary properties of a nucleus require that the force between two nucleons should be attractive, short range and show saturation. To obtain the last quality, forces of an exchange character are usually assumed. The simplest postulate is to restrict mutual attraction to particles which can exchange their position without altering the wave function (space exchange forces). However, the existence of $^1S - {}^3S$ splitting and of a non-zero electric quadrupole moment in the deutron shows that more complex forces of a spin exchange and spin-orbit nature are required for a complete description. The predictions of nuclear structure arising from these successive approximations have been worked out by Wigner and Feenberg and collaborators (see e.g. Wigner and Feenberg, 1941, Feenberg and Phillips, 1937).

The existence of particularly stable configurations and of similar changes in other nuclear properties for particular numbers of neutrons or protons have lead to the postulation of various shell models. The basic idea is one of a few free nucleons moving in a common potential about an inert core. The single particle model of Mayer 1949 and of Haxel, Jensen and Suess 1949 was the first successful model of this type. A strong spin orbit interaction was postulated but the core included all the paired nucleons and had zero spin like an even-even nucleus. The total orbital angular momentum of the final nucleon accounted for the observed ground state spin in almost

all odd A cases and the magnetic and electric quadrupole moments were also adequately predicted. Since observed energy level spacings are much less than predicted single particle spacings, detailed agreement with nuclear spectra can only be obtained if some of the degeneracies in this extreme model are removed, e.g. by allowing all particles outside the closed shells to have equivalent single particle orbits. The agreement becomes more satisfactory but the calculations are difficult and even in light nuclei are usually restricted to the lowest energy configuration e.g. to 4, $\ell = 0$ nucleons and A - 4, $\ell = 1$ nucleons for $5 < A < 16$. For certain nuclei it is possible to make calculations for other excited configurations (see e.g. Halbert and French, 1957 for A = 15). Midway between closed shells configuration mixing becomes important. The usual type involves interactions between the loose particles or excitation of individual particles in the core and is almost impossible to estimate quantitatively. A second type involving coherent mixing results in a collective excitation of the core. Bohr and Mottleson (1953) have successfully used a model based on this type of motion to explain many nuclear measurements.

(b) Deuteron Interactions

Because the neutron and proton are very loosely bound in the deuteron (ϵ_d = 2.226 ± 0.003 Mev.), and the average separation distance [= $h\,(m_p\,\epsilon_d)^{-\frac{1}{2}}$ = 2.18 x 10^{-13} cm.] is somewhat greater than the range of nuclear forces, the deuteron is expected to have a high probability of breaking up when it comes into the vicinity of the nucleus usually with the absorption of one of the constituent nucleons. This process is commonly known as stripping (Serber 1947). Since the process was first postulated by Oppenheimer and Phillips (1935) many theoretical investigations have been made. These have dealt with the magnitude of this process and with the angular distribution of the emitted particles and the variation of these quantities over a wide range of deuteron energies and target nuclei. A comprehensive description of this material and adequate references are available (Huby 1953) and only those aspects of the theory which apply to light nuclei and low energy deuterons will be discussed here.

Bethe (1937, 1938) discusses the relative contributions of deuteron capture and stripping in light nuclei on the basis that the neutron has to overcome the dissociation energy ϵ_d of the deuteron to enter the nucleus alone while the deuteron has to overcome the potential barrier B. Therefore, stripping is expected to predominate if $B > \epsilon_d$. More detailed

considerations give equal contributions if $\epsilon_d/B = 0.6$ or $B = 3.7$ Mev. which if $r_o = 1.4 \times 10^{-13}$ cm. is the barrier for $Z \approx 10$. Higher kinetic energy helps the deuteron to overcome the barrier but does not effect dissociation. This suggests that capture becomes relatively small as Z and E_d increase, but the magnitude of these contributions in a particular case will depend very strongly on the actual resonances available in the compound nucleus.

In 1950 Burrows et al first measured angular distributions of resolved proton groups using 8 Mev. deuterons. These distributions were similar to those previously measured for unresolved protons using higher energy deuterons; that is, they were in agreement with Serber's idea (Serber 1947) that in stripping the proton retained for the most part its share of the vector momentum of the deuteron and hence had a high probability of being emitted into a forward cone. However, there was one significant difference in that Serber's distributions always have a maximum at 0^o in contrast to one of the Burrows measurements which had a minimum. Theories which explained this difference and which described fairly successfully more recent experiments of the same type were put forward by Butler (1950, 1951) and by Bhatia et al (1952). These are quite different in form, but are similar in content, and yield similar distributions. Unlike an exact

26(a)

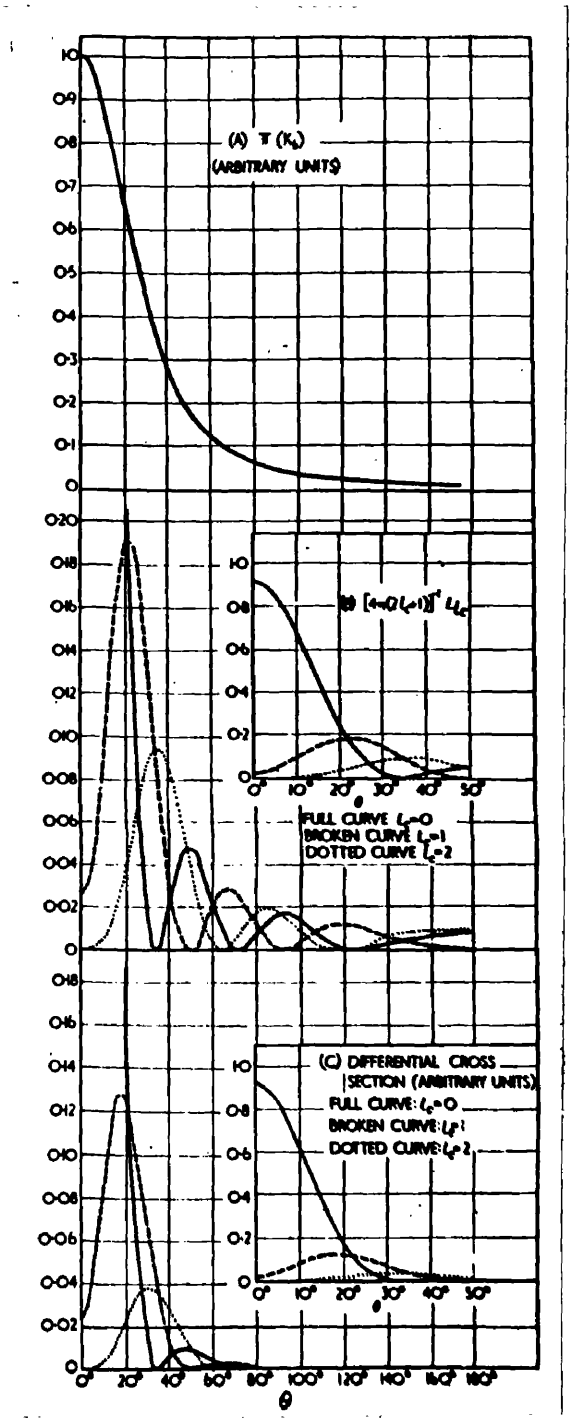

Fig. I.1

The angular variations of $\Pi(K_b)$, L_{l_c} and $\sigma(\theta), (\propto \Pi(K_b) L_{l_c})$ for E_d = 6.9 Mev., E_p = 10.8 Mev. and R = 7.0×10^{-13} cm. calculated according to the formulae of Bhatia et al by Huby (1953).

theory both require specification of a radius at which the deuteron dissociation is said to occur, and when this is used as an adjustable parameter in fitting experimental results, the value obtained for the Bhatia formula exceeds that for the Butler formula (which is in close agreement with the usual nuclear radius) by about 10^{-13} cm. Since the Bhatia formula is easier to apply and interpret, it will be discussed here and used in the subsequent analyses. The differential cross section is given as

$$\sigma(\theta) = \Pi(K_b) \sum_{l_c} P_{l_c} L_{l_c}(k)$$

Since the vector momentum of the proton is the resultant of the internal momentum of the proton in the deuteron K_b plus one half the deuteron translational momentum, and the angle between these is the distribution angle θ, a particular K_b is required for a particular distribution angle and $\Pi(K_b)$ is the probability for this K_b. P_{l_c} is the probability for nucleon capture and is proportional to a reduced width γ^2. $L_{l_c}(k)$ is the probability density that a nucleon c of linear momentum $\hbar k$ will arrive at the nuclear surface with an angular momentum $\hbar l_c$. $L_{l_c}(k)$ will be a maximum at a particular angle specified by applying the classical formula $kR = l_c$. In Fig. I.1 typical predicted variations with θ of $\Pi(k_b)$ and $L_{l_c}(k)$ are shown. It is seen that the $\Pi(K_b)$ variation is essentially that of Serber while the L_{l_c} variation enabled Butler and Bhatia et al to explain distributions obtained when $l_c \neq 0$. Comparison of the measured $\sigma(\theta)$ with these

furmulae allow γ^2 and l_c to be obtained and application of selection rules allows the parity and limits on the spin of the final nucleus to be determined. Further information about the spin can be obtained if necessary through the study of the angular correlations of the proton and a subsequent gamma ray emitted in the de-excitation of the nucleus formed by neutron capture. (e.g. see Satchelor and Spiers, 1952)

Wallace (1957) has made a survey of the manner in which about one hundred experimental distributions for deuteron energies 3 to 20 Mev. agreed with stripping theory. In about 50% of these the agreement was good. In another 20% the agreement remained good if it was assumed permissible to subtract an isotropic background before comparison. In about 20% agreement was poor and in 10% impossible. Most of these results can be explained in terms of break-down of the three major assumptions made: (1) that there is no contribution from the usual compound nucleus process; (2) that the presence of Coulomb effects does not influence the angular distribution and (3) that the effect of interactions between the particles before or after the actual deuteron dissociation is negligible. Many more detailed theories which remove some of the deficiencies associated with these assumptions have been proposed (e.g. Horowitz and Messiah, 1953, Tobocman and Kalos, 1955, Grant, 1954, 1955) but most of these require

elaborate computations and are therefore not readily tested.

It is usually assumed that the compound nucleus contribution, if it occurs, is isotropic and incoherent with respect to stripping, and this is the justification where an isotropic background is removed. There is, however, no general reason for incoherence and isotropy should only occur by chance or possibly in the continuum region. Since the (d,Pγ) correlations show symmetry about the direction of the captured particle, the magnitudes of the contributions symmetrical about the deuteron direction relative to those about the neutron direction indicate the ratio of compound nucleus events to stripping events.

An indication of the importance of Coulomb effects is given by Bowcock (1955). By calculating γ^2 from the high orbital momentum contributions of the deuteron wave, which are less subject to Coulomb distortion, he obtained a value in agreement with that expected, in contrast to the usual discrepancy of at least a factor of two. The same idea has been applied by deBorde (1955) to the angular distributions. Since the Coulomb effect will be greatest for the S wave component, the first order correction will consist of an S Wave phase shift δ. If the S wave and original stripping amplitudes are A and $F(\theta)$ then the modified differential cross section is $\sigma(\theta) = \left| F(\theta) + Ae^{-i\delta} \right|^2$ $= F^2(\theta) + 2AF(\theta) \sin\delta + A^2$. An investigation of the

of the properties of this function reveals that its maxima and minima are simply related to those of the unmodified stripping function. Despite this, considerable changes in the shape are possible, particularly if the coefficient of I is large and negative. Exact theoretical values of A and δ are difficult to obtain but the correctness of this theory may be tested by comparing the δ's obtained for different groups from the same nucleus and with the same entrance channel spin. These should be the same.

Recently Ter-Martirosian (1956) and Biedenharn et al (1956) have considered stripping with strong Coulomb effects. Using the same assumptions and expressions similar to those of Butler the $l_n = 0$ stripping amplitude is obtained as an integral over r from R to ∞ of a function containing the deuteron and proton wave functions ψ_d and ψ_p. Coulomb rather than plane waves are then inserted for ψ_d and ψ_p and it is found that an evaluation of the integral in a closed form is possible only if the lower limit is reduced to zero. In the region of strong Coulomb effects the contributions will be small for r less than R anyway, but the resulting value no longer approaches the Butler value asymptotically as Z approaches zero. Nevertheless, according to Biedenharn it is qualitatively correct showing a maximum at zero. Unfortunately, closed forms are not available for $l_n \neq 0$ either and application of

this treatment to experimental results will be restricted by this difficulty except in the region of very strong Coulomb effects where the distribution becomes only weakly dependent on l_h. The angular distribution obtained for $l_h = 0$ is

$$W(\theta) = \frac{1}{(1+\zeta)^2} \left| {}_2F_1 (i\,\eta_p, i\,\eta_d, 1; -\zeta \right|^2$$

where

$$\zeta = \zeta_0 \sin^2 \theta/2 \text{ and } \zeta_0 = \frac{4k_p\, k_d}{k_\theta^2 + 2\,(k_p - k_{d/2})^2}$$

k_p and k_d are the wave numbers of the proton and deuteron at infinity, η_p and η_d the corresponding Sommerfeld Coulomb parameters ($\eta = \frac{e^2 Z_1 Z_2}{hv}$) and* $k_\theta^2 = \frac{2m_p \epsilon.}{\hbar^2}$

---

*In Ter-Martirosian's paper K_n is the same as ν_n and ζ_0 should be $\frac{4\sqrt{2E_d\,(E_d + Q)}}{(\sqrt{2E_d} - \sqrt{E_d + Q})^2 - E_n}$

I. 4 REACTIONS INVOLVING TRANSITIONS BETWEEN UNRESOLVED ENERGY LEVELS IN HEAVY NUCLEI

It has been seen in section I.1 (b) that as the excitation energy E^* and the atomic number Z of nuclei increase a point is reached where the detector is unable to separate contributions from different levels in the nucleus. This is at first due to finite detector resolution but eventually the levels themselves overlap due to increasing width and density and form a continuum. When only two or three levels contribute, information about the spin, parity, etc. of these levels may be obtained by an extension of the methods discussed in section I.3 to include interference terms. However, in the case of interest here many levels contribute and the only possible analysis is in terms of statistical averages, i.e. the level density as a function of energy, spin, etc.

Bethe (1937) has shown on general thermodynamical grounds that the level density

$$\omega(E^*) = \left[T\left(2 \quad \frac{dE^*}{dT}\right)^{\frac{1}{2}}\right]^{-1} e^S$$

where T is the temperature and $S = \int \frac{dT}{T} \frac{dE^*}{dT}$ is the entropy corresponding to E^*. Values of $\omega(E^*)$ may be obtained from high resolution experiments (see for example, Brown and Muirhead, 1957) or from application of the statistical formula to nuclear reaction data (if this is permissable) and used to obtain explicit information about $E^*(T)$ the equation of state, for comparison with the predictions of various nuclear models.

E^* varies as T^2 for a Fermi gas model and $T^{7/3}$ for a liquid drop model. Bethe has also demonstrated that ω_j, the density of levels of spin j is approximately equal to $(2j + 1)\,\omega_0$. Recently Bloch (1954) has discussed a more elaborate formual $\omega_j = \omega_0\,(2j + 1)\,\exp.\left[-(j + \frac{1}{2})^2 / 2\mu^2\right]$ where μ is a dispersion coefficient and has shown that for a light nucleus and $j = 3$ the second term becomes appreciable at less than 12 Mev. excitation. The level densities derived from experimental measurements and their description by the various formulae and the modifications required are discussed by Lang and Le Couteur (1954) and by Newton (1956). According to the former, a modified Fermi gas formula $\omega_0 \propto \frac{1}{(E + T)^2}\,\exp.\left[2\left(\frac{AE}{f}\right)^{\frac{1}{2}}\right]$ with $f \approx 8$ Mev. gives a satisfactory fit.

In studies of nuclear reactions, $\sigma(E_p, \theta_p)$, (where the subscript denotes an emitted particle), is measured and will depend on the average probability for a transition to a level of the residual nucleus as a function of the energy of this level and on the way the contributions from the various levels and the interference terms between them add together. Until recently these quantities were always described in terms of the statistical model, a full account of which is given by Blatt and Weisskopf (1952). In brief it is predicted that the emission should be isotropic and that the spectrum of emitted particles should be specified by a formula obtained by Weisskopf (1937) on application of the principal of detailed balance, ie.

$$\frac{\sigma(E_p)}{\sigma_r} = \frac{gM\tau_c}{\pi^2\hbar^3} E_p \sigma_c \frac{\omega_R(E_R^*)}{\omega_C(E_C^*)}$$

Here $\sigma(E_p)$ is the cross section per unit energy interval for the emission of a particle of mass M, spin factor g and energy E_p, σ_r is the total reaction cross section, σ_c is the average cross section for the inverse reaction, and τ is the lifetime of the compound nucleus. E_b is the binding energy of the emitted particle. E_R and $E_C^* = E_R^* + E_b + E_p$ are the energies of the residual and compound nuclei respectively and $\omega_R(E_R)$ and $\omega_C(E_C)$ are the corresponding level densities. σ_c is always set equal to $\pi\lambda^2 \sum (2l+1)T_l$ where λ is the wavelength of the emitted particle outside the nucleus and T_l is the barrier transmission coefficient. The following assumptions are also usually made (1) that $\omega(E^*) \propto e^S$ (2) that $S_C(E^*) = S_R(E^*)$ and (3) that $E_p \ll E_C^* - E_b$ and result in $\frac{\sigma(E_p)}{E_p \sigma_C} \propto e^{-E_p/T}$ where $T = \left(\frac{dS}{dE^*}\right)^{-1}_{E^* = E_C^* - E_b}$. Thus T is the temperature of the residual nucleus at maximum excitation and not the temperature of the compound nucleus.

The following fundamental assumptions have been made in the original formula (1) that strong nucleon absorption with consequent independence of formation and decay occurs (back nucleus), (2) that the signs of the reduced width amplitudes Y are random, (3) that $\omega_j = (2j+1)\omega_o$ and (4)

that σ_c is independent of the channel spin S and the total spin j of the system. All of these assumptions are to some extent inaccurate. The work of Feshback, Porter, and Weisskopf (1953, 1954) has shown that moderate nucleon absorption (cloudy crystal ball nucleus) is necessary in order to explain neutron total cross sections. Moderate absorption implies mild correlations of the signs of the Y and hence contributions asymmetric about 90°*. It has already been mentioned that the work of Bloch suggests that (3) is only true as j approaches zero. The known existence of spin orbit coupling implies that the transmission factors. depend on S and j to some extent. Since (3) and (4) are required for isotropy their breakdown leads to angular distributions symmetric about 90°.

The direct effect may be fitted into the above scheme in terms of non-random contributions from levels with energies much greater or less than the average (Brown, 1958). Alternatively the low absorption may be said to result in emission after a very small number of collisions by the incident particle. The question of whether the region in which this process occurs includes the whole nuclear volume or is confined to a surface layer is of considerable interest and this together with other aspects of the direct effect are discussed by Austern et al (1953), Hayakawa et al (1955), Brown et al (1957) and Elton et al (1957).

---

* Strong correlations had been considered instead of assumption (2) but this lead to destructive interference and cross section which were much too small (see Newton, 1952).

The general problem of an adequate descritpion of reactions in the continuum has been discussed very recently by Lane and Thomas (1958).

Experimentally, as theoretically the statistical model appears to be almost correct. Ghoshal (1950) demonstrated that the proportions of the decay products from Zn^{64}, produced either by proton capture in Cu^{63} or alpha particle capture in Ni^{60}, were approximately the same for the same excitation energy. It has also been shown in many experiments (n,p), (n,n^1),(γ,p'), etc. that $\sigma(E_p,\theta_p)$ can be described in terms of two components. One, which is due to the compound nucleus process dominates the spectrum at small values of E_p and has the characteristic Maxwellian energy distribution with isotropy or near isotropy. The other which makes a major contribution at large E_p and forward angles is ascribed to direct processes. Although the relative magnitudes of these contributions vary considerably with the properties of the particular nuclei concerned, the contribution from the latter is usually less than 10% of the total cross section.

I. 5 OUTLINE OF THE PROJECTED RESEARCH

In the preceding sections we have noted two rather general facts about the measurements of nuclear reaction parameters (1) that these may be interpreted to yield information about both nuclear states and about detailed reaction mechansims and (2) that the problem of the interpretation of these results shows considerable differences depending on

whether the mechanism is a direct single stage process or a multiple stage process with intermediate compound nuclei, and on whether the contributions from the individual nuclear states can be resolved or not. The experimental work presented in this thesis has been selected to illustrate by example the various types of problem encountered in the study of low energy nuclear reactions as far as this was possible with the limited time and resources available to the author in hope that thereby insight into the unifying aspects of transitions between nuclear states might be gained.

A (p,γ) reaction was selected for study at the beginning because the interpretation of the measurements was well established (e.g. Devons and Hine, 1949). The angular distributions of the de-excitation gamma rays from the 7.61 Mev. level of ^{15}O were measured because, if the assignment of spin 5/2 for this level (Bashkin) was correct then the captured proton was almost certainly p or d wave and in that event the predicted values of the coefficient of the $\cos^2\theta$ term were sufficiently well separated to allow easy identification of the spins of the 5.27, 6.20 and 6.84 Mev. levels (see Fig. II.3). It seemed desirable, despite the difficulties associated with the low yield and nitrogen target preparation, to have this information for comparative purposes since, as Halbert and French have pointed out, the A = 15 group is one of the few in the p-shell region for which the effects of different configurations in an independent particle sheel model can be obtained without very elaborate calculations.

It has been seen in section I.3(b) that the stripping formulae of Butler and of Bhatia et al are moderately successful and have been widely tested, particularly at high deuteron energies. However, in certain reactions and at low deuteron energies the experimental results are more complex and the required modifications are of considerable interest. Since there was lack of agreement in some respects between the various results which had previously been obtained for the $^{10}B(d,p\gamma)^{11}B$ reaction it seemed desirable to make further measurements with greater accuracy in this case, before proceeding to measure the $^{24}Mg(d,p)^{25}Mg$ reaction. These reactions were chosen so that both of the two principal modifications could be studied independently. These modifications are due to appreciable contributions from the compound nucleus process (for ^{10}B) and to appreciable Coulomb distortions (for ^{24}Mg.).

Previously (n,p) measurements had been concentrated largely on the separation of the contributions from the direct and compound nucleus processes and used nuclear emulsion techniques to make crude measurements of the angular variations of the energy spectra. This method was to a large extent successful in its objective but the rate of measurement was so low that data was obtained with very limited accuracy for only one or perhaps a very small number of isotopes. It was decided that, alternatively, a nuclear counter method could be developed in which the contribution from the direct effect would be very small and which could be used to measure

evaporation spectra rapidly and with high accuracy. This was of considerable interest because it enabled the quantitative study of the small variations in the spectra from adjacent isotopes due to the local variations in binding energy, even or odd numbers of nucleons etc. Since it is also suitable for measuring the changes due to different energies of the bombarding neutron it was decided later to extend the investigation accordingly.

Throughout this work the principal object in the development of the experimental technique has been the removal of backgrounds, due to interfering radiations, in proton spectra. The process for pressing plastic scintillator described in Appendix B was developed in order to make readily available scintillators with minimum thickness for the particle detected so that the background due to gamma rays or neutrons would be a minimum. This was necessary in order to make possible the measurement of the spectra of low energy protons and alpha particles with this scintillator. Since the very heavy elements such as lead and bismuth have low (n,p) cross sections and easily absorb external background protons the problem of obtaining satisfactory resolution from scintillators effectively enclosed in these materials was also studied.

When it became apparent that the CsI(Tl) decay time depended on the nature of the incident radiation this phenomenon was extensively investigated in the work described

in the final section of this thesis because, apart from its obvious interest from the stand point of understanding processes in ionic crystals, it offered a new approach to the complete removal of interfering types of radiation in a manner which had only been possible previously through the use of elaborate and inefficient telescopes.

PART II REACTIONS INDUCED BY CHARGED PARTICLES IN LIGHT NUCLEI

II. 1 RADIATIVE TRANSITIONS FROM THE 7.61 MEV. LEVEL OF ^{15}O

(a) Introduction

Previous measurements of the reaction parameters for the formation of the 7.61 Mev. level of ^{15}O and for its subsequent de-excitation have been summarized by Ajzenberg and Lauritsen (1955) and by Bashkin et al (1955). With the view of reducing the uncertainty of the spin and parity assignments of the levels involved in this process, angular distributions have been measured for the 0.77 and 1.41 Mev. gamma rays emitted in the first transitions of two of the three double cascades which form its accepted discription. The level energies quoted herein are taken from the Ajzenberg (1955) review paper or where possible the recent precise measurements by Marion et al (1955).

(b) Experimental Arrangement

Resonant capture of 277 Kev. protons in ^{14}N was used to produce ^{15}O nuclei in the 7.61 Mev. excited state. The protons after acceleration by the Glasgow University high tension generator were magnetically deflected on to a titanium nitride target which had been previously prepared by heating titanium foil to incandescence in a natural nitrogen atmosphere. Despite the use of a water cooled target holder

the permissible rate of deterioration of the gold-coloured TiN surface layer limited the proton beam current incident on this target to about 40 microamps. A sodium iodide crystal2 in. long and $1\frac{3}{4}$ in. diameter mounted on a DuMont photomultiplier type 6292 served as the gamma ray detector. Because of the low yield of the reaction lead shielding was required to reduce the background activity sufficiently to make measurements possible. After the compromise necessitated by such conflicting requirements, the final design of the angular distribution apparatus provided for a measuring range of 0 to 90 deg. (with respect to the incident proton direction), a detector solid angle of 0.17 steradians, and 1 in. thick shielding. The gamma rays entered the scintillator through a $\frac{3}{4}$ in. diameter hole in the shield. After amplification the spectrum of pulses from the photomultiplier was analyzed and displayed in about 80 channels using a Hutchinson and Scarrott (1951) 'kicksorter'.

A second gamma ray detector, similar to the first, was placed in the plane of the angular distribution apparatus at an angle approximately perpendicular to the proton beam and served to monitor the gamma ray output. In practice the bias on a discriminator in the pulse output circuit was adjusted so that the monitor scaler recorded only pulses corresponding to gamma ray energies greater than about 3.3 Mev. Since the background activity decreases with increasing

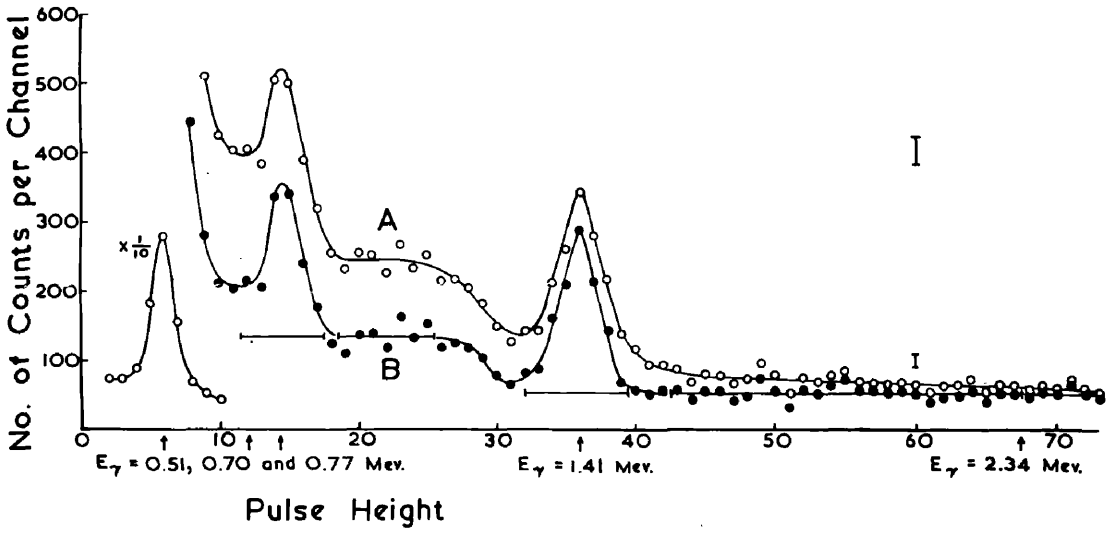

Figure II. 1. Pulse height spectrum of gamma rays at E_p = 277 Kev. and θ = 0 deg. Curve A is the observed spectrum. Curve B has had the background subtracted.

energy until it reaches a small constant value at about 3 Mev., this procedure enabled the use of the higher energy second gamma rays (5.27, 6.20 and 6.84 Mev.) of the three cascades for monitoring and reduced the background corrections in the monitor count to less than 10 per cent. Moreover, the fact that the cutoff was centred in the broad valley of the spectrum between the low and high energy groups of peaks made the total monitor count much less sensitive to small drifts in the gain or bias values.

(c) Angular Distributions

The background activity within the heavily shielded scintillator proved to be isotropic within the accuracy of the experiment. In addition, a 250 kilovolt, 40 microamp beam produced only a very slight increase over the external background present with the H.T. set switched off. Because of this a standard external background was obtained with relatively good statistics, and this, after suitable small modifications depending on the beam current and amplification used in the particular angular measurement, was subtracted from the experimentally observed spectrum to give the spectrum due to the resonant capture of 277 Kev. protons in ^{14}N. A typical pair of observed and corrected gamma ray spectra are shown in Fig. II.1. Note that the low energy corrected spectrum is still superimposed on a background due to the higher energy second transitions in ^{15}O, and that the statistical accuracy

is not sufficient to separate the 2.34 Mev. gamma ray observed by Johnson et al (1952) from this high energy tail.

Since the area of the photopeak of a single gamma ray appears to be less sensitive to errors in background removal than the area of the photopeak and Compton spectrum combined, the former quantity was used in this experiment for angular comparisons. In order to obtain the photopeak area for the 1.41 Mev. gamma ray it is necessary to subtract the contribution of the high gamma rays and for the 0.77 Mev. gamma ray to subtract this last plus the Compton distribution of the 1.41 Mev. gamma ray. Since the high energy tail is fairly closely flat it seemed satisfactory within the statistical accuracy of the experiment to remove a constant value from the 1.41 Mev. gamma ray equal to the average of the 25 channels immediately above it. A similar procedure was followed for the 0.77 Mev. photopeak area. Since measurements with relatively good statistics had shown the Compton distribution of the ^{22}Na 1.28 Mev. gamma ray to be flat within a few per cent after its initial rise, the average of the 7 or 8 channels available in the adjacent flat part of the 1.41 Mev. Compton distribution was removed. Straight lines representing the average values in the regions of averaging and subtraction have been added to Fig. II. 1. It should be noted that this procedure will tend to compensate

somewhat for any errors which may have been made in the subtraction of the external background. Moreover, since the gamma rays are not, in fact, strongly anisotropic and since the procedure adopted is reasonably uniform, a small error in the background removal process should not appreciably distort the angular distributions obtained.

The pulse heights corresponding to the 0.51 Mev. annihilation peak and 1.41 Mev. peak can be used to calculate the energy of the third gamma ray peak in Fig. II.1, since the gamma ray energy is proportional to the pulse height for a sodium iodide detector. The value obtained in this manner is (0.77 $\pm$ 0.02) Mev. Because of this result the third peak is attributed to transitions from the 7.61 Mev. capture level to the 6.84 Mev. level rather than to the weak 6.91 Mev. level reported recently by Marion et al (1955). No definite evidence for a gamma ray transition to this latter level has been obtained by inspection of any of the spectra measured in this experiment or of the spectrum reported by Johnson et al (1952). The maximum possible contribution of such a transition to the calculated photopeak area for the 0.77 Mev. gamma ray depends on the exact energy difference, but is probably less than ten per cent.

The data for the angular distributions were obtained during a single continuous irradiation and the angles were measured in the sequence 90, 60, 30, 0, 15, 45, 75 deg. in

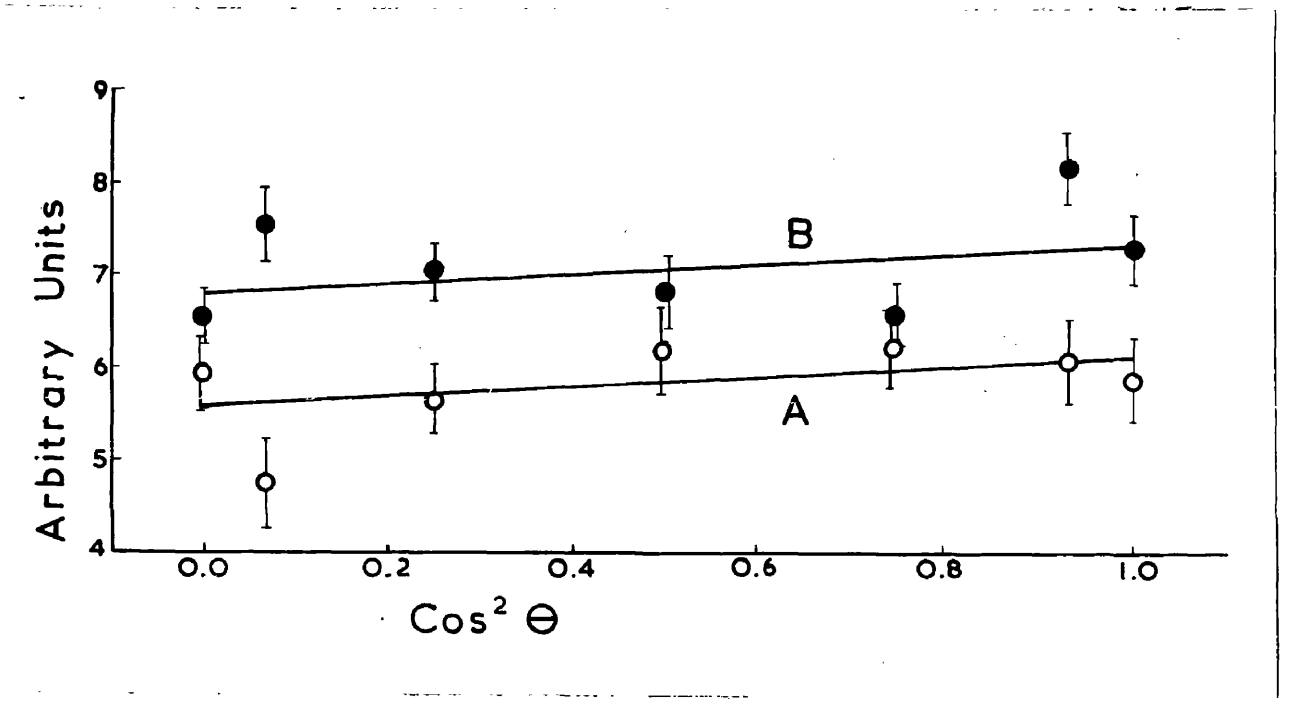

Figure II. 2. Angular distributions.

A - 0.77 Mev. gamma ray.

B - 1.41 Mev. gamma ray.

order to compensate for small long term drifts in the monitor gain and bias. After analysis of the spectra the resulting photopeak areas were corrected to a constant monitor count and plotted as a function of $\cos^2\theta$ in Fig. II. 2. The standard deviations shown in this figure have been computed from the statistics of the averaging and subtraction process used on curve B to obtain the photopeak area. No allowances have been made for inaccuracy in the removal of the external background. Also drawn on Fig. II. 2 are two straight lines which represent the best fit of the function $A + B \cos^2\theta$ to each set of data using the least square method and weighting factors proportional to the total monitor count recorded during the 20 min. counting period used at each angle. The weighting was necessary because appreciable target deterioration occurred during the irradiation. Angular isotropy measurements of the apparatus using the ^{22}Na, 1.28 Mev. gamma ray before the above measurements and the $^{19}F(p,\alpha\gamma)^{16}O$, 6.14 Mev. gamma ray after, were analyzed to give respectively

$$W(\theta) = 1 + (0.012 \pm 0.039) \cos^2\theta$$

and $$W(\theta) = 1 + (0.022 \pm 0.032) \cos^2\theta.$$

The weighted average of these

$$W(\theta) = 1 + (0.018 \pm 0.025) \cos^2\theta$$

was used to correct the distributions of Fig. 2.

Since the target consisted of a 0.020 in. piece of titanium backed by a 0.020 in. piece of copper and placed so

the gamma rays passed through it perpendicularly at the 45 deg. position, the calculated absorption for 0.77 Mev. gamma rays was 4.3% at 45 deg. and 6.0% at 0 and 90 deg. Accordingly, the effect on the ratio B/A was very small and no corrections were made for this effect. After correction for attenuation of the coefficient of the $\cos^2 \theta$ term due to finite angular resolution (see Rose, 1953) the final distributions were

$$W(\theta) = 1 + (0.085 \pm 0.09) \cos^2 \theta$$

for the 0.77 Mev. gamma ray and

$$W(\theta) = 1 + (0.06 \pm 0.09) \cos^2 \theta$$

for the 1.41 Mev. gamma ray.

The contributions from other resonances in O^{15} and O^{16} [from N^{15} $(p + \gamma)$ O^{16}] have been estimated and found to be less than 1% of that due to the 277 kev. resonance for the 300 kev. proton beam used in these esperiments.

Previously, five spectra of the higher energy second gamma rays (5.27, 6.20 and 6.84 Mev.) in the ^{15}O cascades had been obtained. Two of these were measured at an angle of 6° to the proton beam, two at 96° and one at 51°. Accurate decomposition of these spectra into contributions from the three individual gamma rays was not attempted because target deterioration, and small overall gain changes resulted in inadequate resolution and statistics. The total numbers of pulses corresponding to photon energy

loss in the crystal greater than 3.3 Mev. yield on application of the least squares method the angular distribution of the group,

$$W(\theta) = 1 + (0.022 \pm 0.013) \cos^2\theta$$

The angular efficiency of the apparatus although somewhat more uncertain than that described above was probably isotropic within five per cent. The resulting final distribution is, therefore

$$W(\theta) = 1 + (0.02 \pm 0.06) \cos^2\theta$$

The relative intensities of the gamma rays in this grouped distribution may be taken in order of increasing energy as 15 ± 4%, 60 ± 15% and 25 ± 6% (Bashkin et al, 1955) since the variations caused by detection efficiency and the 3.3 Mev. cutoff are small compared to the errors in these results.

The ratio of the intensities of the 0.77 and 1.41 Mev. gamma rays at 0° has been calculated from the coefficients of the photopeak area distribution and the photopeak efficiency function of the detector. The agreement between the 0.37 which was the result obtained and the value 0.40 ± 0.10 quoted by Bashkin et al (1955) for the intensity ratio of the 6.84 and 6.20 Mev. gamma rays supports the double cascades hypothesis as the principal de-excitation process for the 7.61 Mev. level. Only an approximate estimate of the absolute thick target yield of the 1.41 Mev. radiation was made and this was in satisfactory agreement with the $3.8 \pm 1.0 \times 10^{-12}$ gamma rays per proton incident on TiN reported by Bashkin et al (1955)

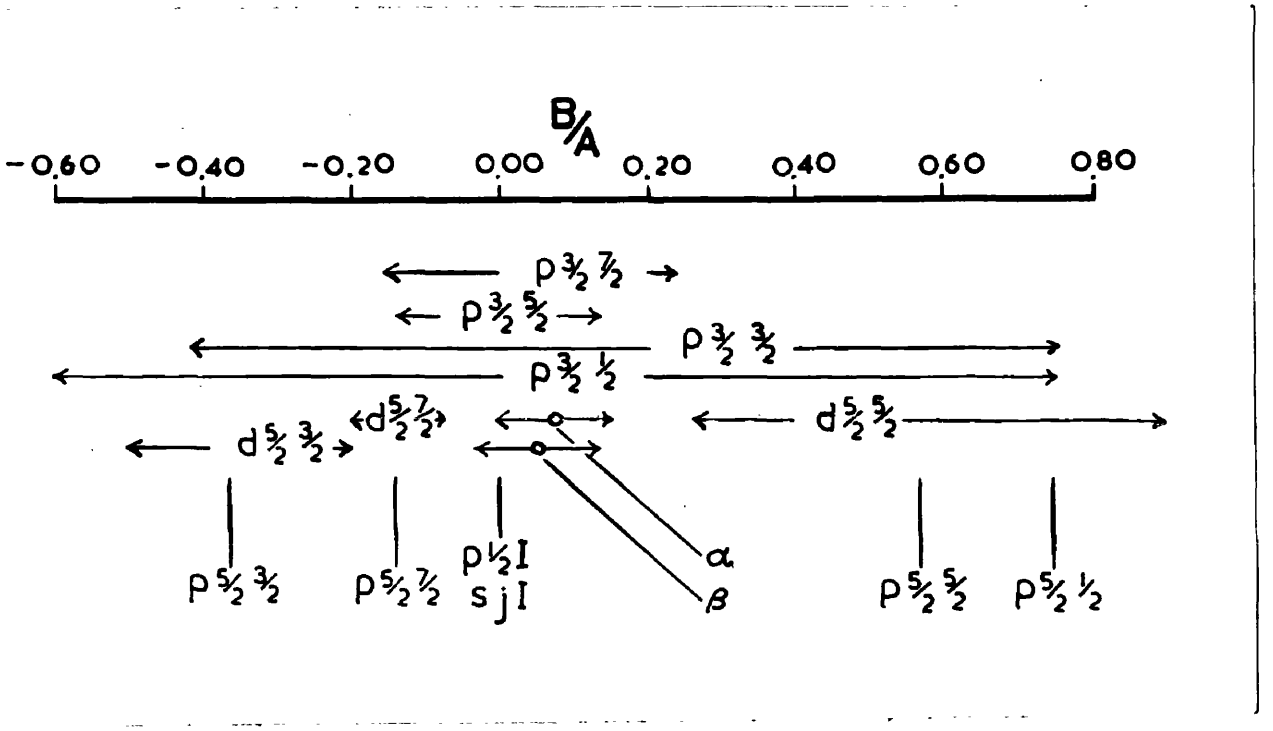

Figure II. 3. Angular distribution ratio B/A for various (l_p, j, I).

α - measured B/A for 0.77 Mev. gamma ray.

β - measured B/A for 1.41 Mev. gamma ray.

for the 6.20 Mev. radiation.

(d) Discussion

Proton capture followed by a radiative transition may be described in terms of the following reaction parameters, S- the entrance channel spin (S = spin of target nucleus ± spin of proton), l_p - the orbital angular momentum of the incident proton, j - the spin of the capture state, and I - the spin of the final state. The angular distributions consistent with some of the more probable sets (l_p, j, I) of values for such parameters in this experiment have been calculated for the lowest order of electromagnetic transition consistent with the j and I values using the tables of Sharp et al (1953). The ratios B/A which define these distributions are depicted in Fig. II.3. For some sets of (l_p, j, I) more than one value of S is possible and this results in a continuous range of ratios. The experimental values of B/A for the 0.77 and 1.41 Mev. gamma rays have been added to Fig. II. 3 over ranges limited by the standard deviations of these results.

The results will now be considered in conjunction with some of the earlier experimental evidence. The latter is displayed in Table II.1. The beta decay measurements support the assumption that the ground state of ^{15}O is $\frac{1}{2}^-$ like that of ^{15}N. The 7.61 Mev. level is assumed, according to Evans et al (1953), to be due to p wave capture and consequently to have negative parity and spin values j limited to $\frac{1}{2}$, 3/2 or 5/2.

Table II.1

Energy Levels (Mev.)	(d,n) Measurements (Evans et al) l_p spin parity					Relative Intensities of transitions from Capture Level (Bashkin et al)
7.61	1		5/2	3/2	1/2 -	
6.84	0			3/2	1/2 +	0.40
6.20	1		5/2	3/2	1/2 -	1.00
5.27	2	7/2	5/2	3/2	1/2 +	0.25
0.00	1		5/2	3/2	1/2 -	0.05

If the assignment is $j = \frac{1}{2}$ or 3/2, a dipole transition to the ground state is possible, and such a dipole transition, as Bashkin et al (1955) have shown, would be expected on the basis of radiative transition probability calculations (Weisskopf, 1951) to have an intensity many times larger than that of the 1.41, 6.20 Mev. cascade instead of the observed ratio of less than 0.05. The calculated disparity factor separating the expected and observed values is of the order of 10^3. Bashkin et al (1955) have therefore chosen 5/2 as the spin of the capture state. If this assignment is accepted then inspection of Fig. II.3 shows that, despite the low yield of gamma rays expected, an angular distribution measurement should easily determine the spin of the 6.20 and 6.84 Mev. levels, particularly since I = 7/2 is very improbable on the interpretation of the (d,n) measurements and I = $\frac{1}{2}$ is also improbable because of radiative transition probability considerations. Unfortunately, the measured angular distributions

are not consistent with any of the lowest order transitions possible for a j = 5/2 level. In an attempt to retain this assignment mixing of quadrupole terms for transitions to I = 3/2 and I = 5/2 was considered. The required quadrupole intensities were 5 per cent and 10 per cent of the respective dipole transitions. Comparison of these values with the Weisskopf predictions gives a disparity factor of greater than 10^6 if the parity of the 6.20 and 6.84 Mev. levels is unrestricted and of the order of 10^9 if the Evans assignments are accepted. Moreover, the calculated distributions of the corresponding second gamma rays (6.20 and 6.84 Mev.) have B/A ratios of - 0.33 or + 0.41 whereas the angular distribution of the high energy group measured as part of this experiment and the comparison of peak heights made by Bashkin et al (1955) tend to favour quite small values of B/A.

On the basis of this evidence the capture state seems to be more probably of spin $\frac{1}{2}$ or 3/2 than of spin 5/2. For the former values of j, the disagreement between the observed and expected intensities of the dipole transition to the ground state may indicate that an appreciable correlation of the nuclear motion is involved in this transition. This is because such correlation would cause the relative probability of emission of electric dipole radiation with respect to that of the other multipole radiations to decrease from that predicted by the Weisskopf rules which assume that only single particles are involved in gamma ray transitions.

Since this work was completed it has become increasingly obvious that the relative probabilities of multipole radiations vary sufficiently widely from the Weisskopf single particle values to invalidate Bashkin's assignment (see Wilkinson 1956). Moreover, Overley et al (1956) have obtained a value of one for the ratio of the intensities at 0 and 90 deg. for both the 0.77 and 1.41 Mev. gamma rays, thus checking the isotropy obtained here. Proton elastic scattering measurements by the same authors are consistent with a $\frac{1}{2}$ + assignment to the 7.61 Mev. level.

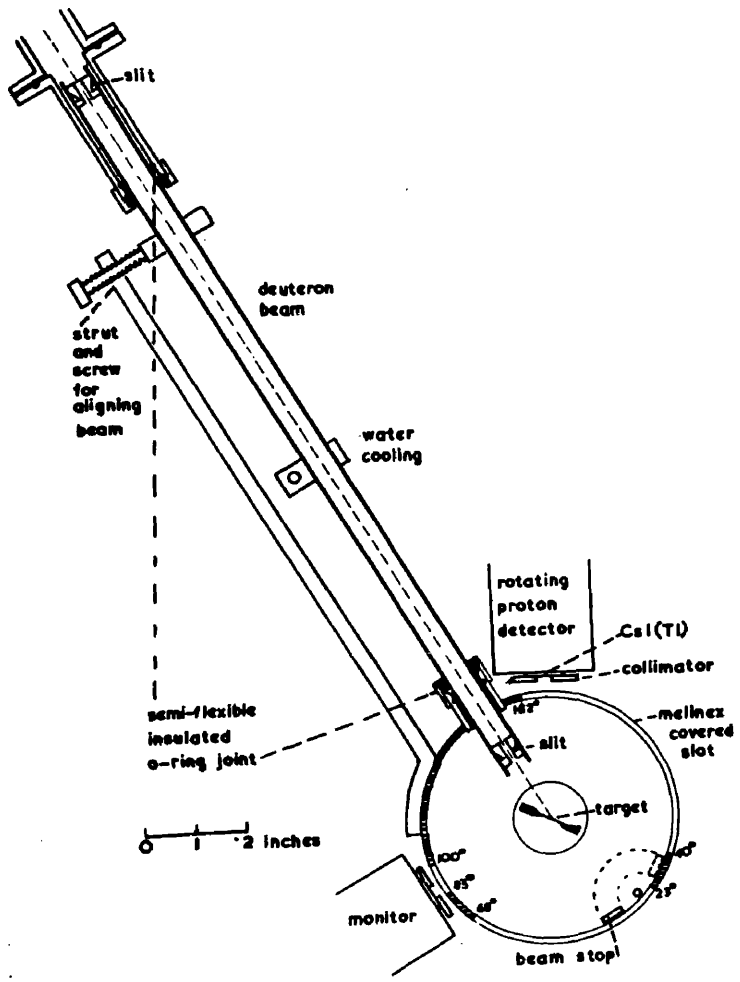

Figure II. 4 The angular distribution apparatus for (d,p) measurements.

II. 2 APPARATUS AND METHOD FOR THE STUDY OF (d,p) REACTIONS

In order to make more accurate measurements of the angular distributions of the protons from the $^{10}B(d,p)^{11}B$ reaction and to extend these measurements to the lower energy proton groups, a new apparatus was designed. It was also used later in the more difficult measurements which were made of the protons from the $^{24}Mg(d,p)^{25}Mg$ reaction.

The previous apparatus is described in detail by Deuchars (1955) and Wallace (1957). It consisted of a cylindrical chamber which was connected by means of pipes with flanged joints onto a part of the resolving chamber of the H.T. set. Two collimating slits were clamped between the flanges. The protons left this chamber through holes at 0, 15, 30 -, -, -, 120 and 135 deg. to the deuteron beam. The holes were nominally 3/8 in. in diameter and their areas were found to vary randomly by $\pm$ 4%. The windows covering these holes and the reflector covering the scintillator were aluminium foils 7 mg. per cm.^{2} thick.

The new apparatus is shown in Fig. II. 4. The insulated joints enabled the beam current to the slits as well as that to the target to be measured. The protons leave the chamber through slots in the curved wall as shown. Since the slot width determined in part the detection solid angle, it was hand filed and checked until it

was constant (at 0.297 in.) to about ± 0.001 in. The distance from the centre of the target to the inner surface of the curved wall was measured, with one end of the chamber removed, and found to be constant(at 6.35 cm.) to within 1%. The lower slit was 1 mm. in width and the upper 2 mm. With a beam of parallel light passing through these slits the strut and screw device was adjusted so that the axis of the two slits passed through the centre of the target. The target was then removed and the 0 deg. position was found accurately as the point where the light beam passed through the slot in the opposite wall. The alignment was checked during the measurements by observing the burn mark on a piece of paper placed on the target holder. This target holder was made of copper and designed so that with a thin target backing (0.0005 in. copper foil) the angular distribution could be measured from 0 to 162 deg. without moving it from the position shown. This required for the monitor and the 0 to 68 deg. section the use of protons which had come through the backing. The overlap between 40 and 68 deg. enabled the symmetry of the chamber to be checked. Provision was made for a removable beam stop to protect the slot window when 0 deg. was not being measured in case the target burned through. The slot window was of melinex (mylar) film 1.7 mg. per $cm.^2$ thick and sealed to the outer surface of the curved wall with 3M cement. Thin mica windows were also tried,

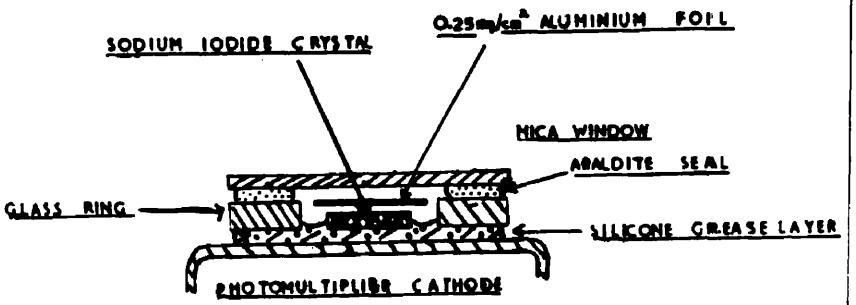

Figure II. 6 The mounting used for the thin NaI(Tl) crystal.*

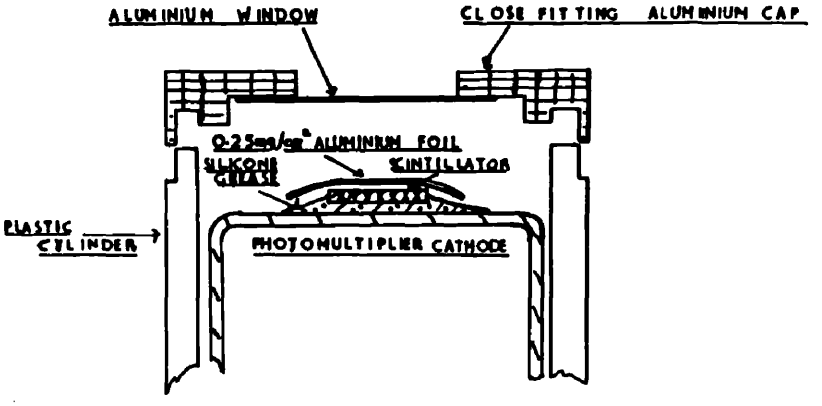

Figure II. 7 The mounting used for the thin CsI(Tl) crystal.*

*In both of these diagrams the thickness of thin layers of material has been exaggerated in order to achieve clarity.

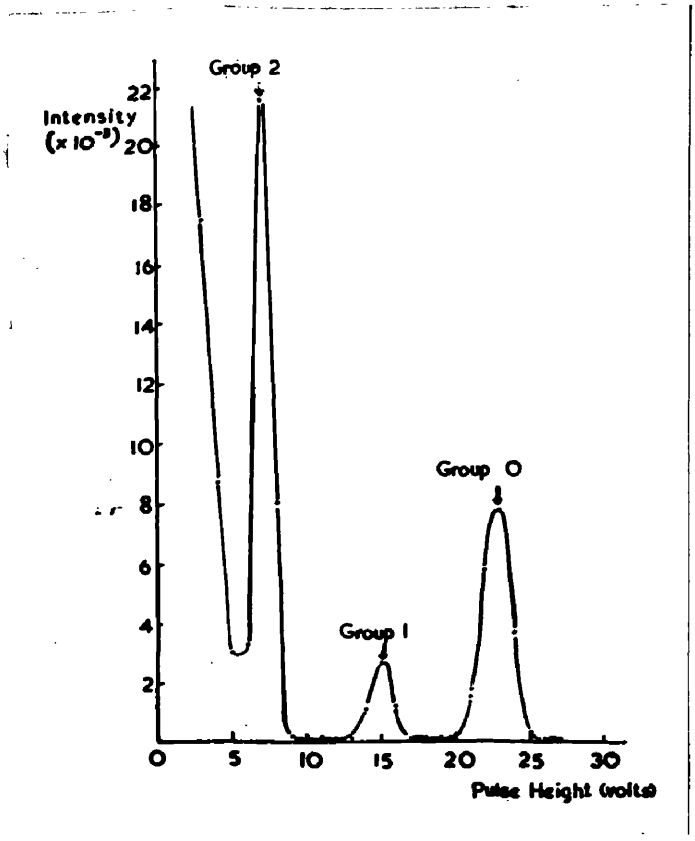

Figure II. 5 The pulse height spectrum of protons from $^{10}B(d,p)^{11}B$ reaction using plastic scintillator.

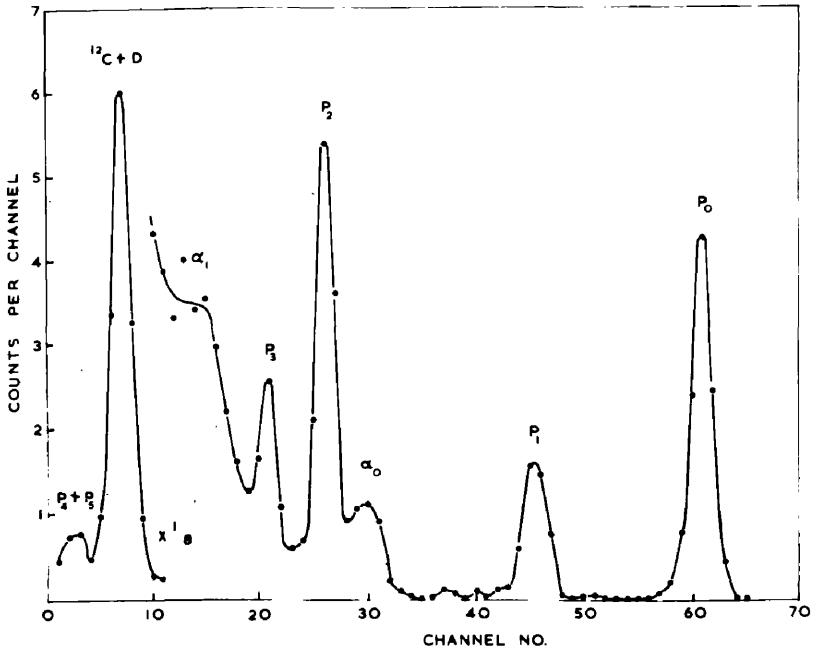

Figure II. 8 The pulse height spectrum from the $^{10}B(d,p)^{11}B$ and the $^{10}B(d,\alpha)^{8}Be$ reactions using CsI(Tl) scintillator. P_i and α_i denote the respective groups. A double group due to D(d,p)T and $^{12}C(d,p)^{13}C$ is also observed.

at first, but these tended to crease and leak when the chamber was evacuated. Previously, the best Deuchars and Wallace measurements had been made with a plastic scintillator detector. This has a background due to neutron scattering by its hydrogen content as well as a low light output. The pulse height spectrum obtained for $^{10}B(d,p)^{11}B$ protons is shown in Fig. II.5. The plastic scintillator used was pressed to a thickness equal to the maximum proton range (for a 9 Mev. proton) using the technique developed by the author and described in Appendix B. Because of their high light output, considerable effort was expended in trying to produce good NaI(Tl) detectors. This was only partially successful because of the deliquescent nature of the substance. One of the more satisfactory mountings is shown in Fig. II.6. In the measurements by the author and Dr. Wallace the angular distribution spectra were obtained using CsI(Tl), a scintillator which had just become available. It is not as brittle and hence more readily shaped than NaI(Tl). Since moisture tight windows were not required, the mounting was as shown in Fig. II.7. Here the light tight window and the aluminium leaf reflector have a total thickness of less than one mg. per cm.^{2}. A CsI(Tl) spectrum from a B^{10} target with minimum absorber is shown in Fig. II.8. The alpha particles from the $B^{10}(d,\alpha)Be^8$ reaction were removed from the spectrum in the angular distribution measurements by placing 0.001 in. aluminium foils between the window and the detector. Since the

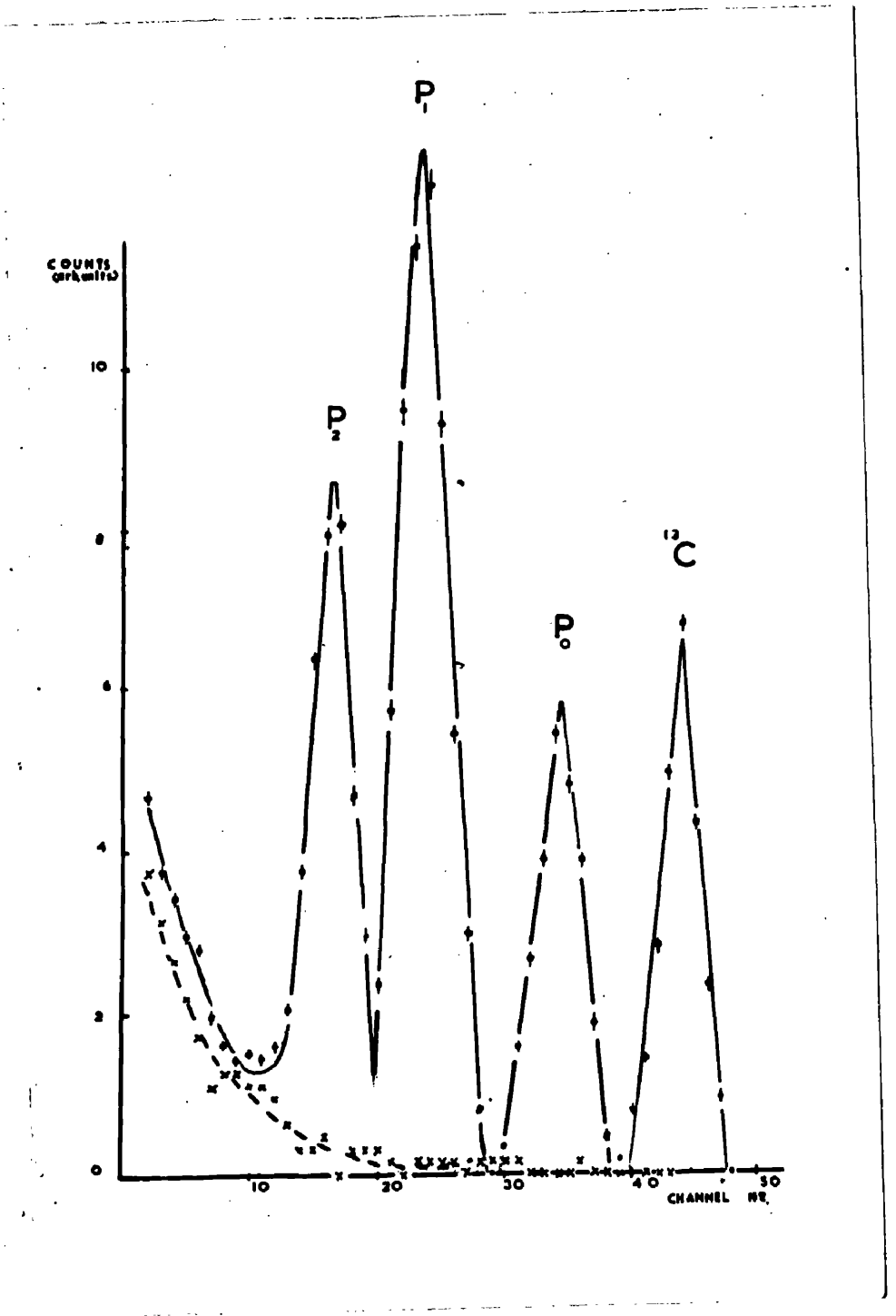

Fig. II. 9 The pulse height spectrum of protons from the $^{24}Mg(d,p)^{25}Mg$ reaction using CsI(Tl) scintillator.

(d,p) reaction has a very low cross section in ^{24}Mg. compared to much lighter nuclei at the bombarding energies used, inpurities were particularly troublesome. The first targets obtained contained ^{6}Li in the very small amounts necessary to produce protons obscurring those from ^{24}Mg. The targets used in the measurements presented gave a spectrum with unidentified alpha particle groups. When the 0.001 in. aluminium foils were put in to absorb these the CsI(Tl) spectrum shown in Fig. II.9 was obtained. The highest energy peak is due to $^{13}C(d,p)^{14}C$ occuring in the inevitable carbon impurity found in accelerators with oil diffusion pumps. The other three were identified as the groups resulting from transitions to the first three levels in ^{25}Mg.

It had previously been demonstrated (see Wallace 1957) that the only satisfactory method of monitoring was to count the protons from the reaction being studied in a fixed counter. Since the only CsI(Tl) crystal available to us when these measurements were made was used for the angular distribution spectra the resolution on the monitor spectra was inferior. This did not matter for ^{10}B because the second and third peaks were well separated and a discriminator could be easily set so that only the protons in the two highest energy groups would be recorded in the associated scaler. Accordingly, a plastic scintillator was used as the monitor crystal. In the ^{24}Mg. experiment,

however, very good resolution is necessary to separate the spectral distribution of $^{24}Mg.$ protons from the ^{13}C contribution at higher pulse heights and the rising background due to ^{12}C and d, (d,p)T protons below. Fortunately, the NaI(Tl) mounting shown in Fig. 11.6 retained sufficiently good resolution long enough for the measurements presented here to be made.

The separated isotope targets used in these measurements were obtained from A.E.R.E. Harwell. The thickness was decided by that required to give a suitable counting rate (for adequate statistical accuracy, but low dead time losses) but had a maximum limit due to the necessity of keeping its effect on the energy resolution of the proton groups negligible. It was about 10 μ gm. per cm.^{2} for the ^{10}B targets and ranged up to 100 μ gm. per cm.^{2} for $^{24}Mg.$ The backing was usually copper because of its heat conducting properties. Thicker backings were used in some of the $^{24}Mg.$ measurements to allow higher beam currents and hence higher yields, but this required measuring the angular distributions in sections with both the monitor and the rotating detector on the target side of the backing and normalizing on overlaps.

The pulses from both the monitor and rotating detector photomultipliers (Dumont 6292) were first passed through cathode followers and linear amplifiers. The proper monitor pulses were then selected with a discriminator (or a single channel analyzer in the $^{24}Mg.$ measurements) and

recorded on a scaler. The rotating detector pulses were analyzed and displayed in about 80 channels using the Hutchison Scarrott "kicksorter". In the experiment these pulse height spectra were recorded for a constant number of monitor counts at each angle. Usually it was only necessary to total the contributions from the kicksorter channels contributing to a peak, but the parts of the spectra in the vicinity of the lowest energy peak required careful analysis to remove other contributions.

Corrections due to the 0.6 msec. dead time of the kicksorter were avoided by keeping the counting rate sufficiently constant. No corrections for angular variations in the efficiency for proton detection were made since a check with the $^{19}F(p, \alpha\gamma)^{16}O$ gamma rays confirmed that these were less than 1%. Since a $\frac{1}{4}$ in. slot mounted on the detector perpendicularly to the chamber slots limited the angular width to about 5 deg., no correction was made for finite solid angle.

The errors are shown in the angular distribution curves of sections II.3 and II.4. They are mainly statistical, but in the case of the lowest energy peaks the uncertainty due to the necessary analysis is large. There are also contributions due to normalizing in the measurements with thick target backings.

In measuring the excitation function for ^{24}Mg. a target of sufficient size to intercept all of the deuteron

beam passing through the slits was used. The apparatus had been constructed so that the target and chamber formed a Faraday cage. The electric charge accumulating from the beam of singly charged deuterons (magnetically resolved) was allowed to pass to earth through a current integrator. The number of pulses passed by a single channel analyzer set across the three groups were recorded for a constant number of current integrator pulses at each deuteron energy. Absolute cross sections at 600 kev. were obtained by using a target of known thickness (50 μ gm. per cm.^{2}) and calibrating the current integator with an ammeter and battery. The pulses were displayed on the kicksorter and the contributions from the three groups carefully separated.

Deuchars and Wallace had measured the angular correlations of the gamma rays from the first two excited states of ^{11}B in coincidence with protons emitted at 45° to the deuteron beam to an accuracy of $\pm$ 6% at points separated by 30° intervals. They used their 3 in. radius proton angular distribution chamber and a 1 μ sec. resolving time. In the measurements of Wallace and the author the proton direction was changed to 65° and a special chamber $\frac{1}{2}$ in. in diameter was constructed. The much larger detector solid angles available, together with the 0.25 μ sec. resolving time used and the better proton resolution, enabled measurement of the gamma rays from the first three

excited states to be made to an accuracy of ± 3% at 15 deg. intervals. In both cases the gamma ray detector was a NaI(Tl) crystal $1\frac{3}{4}$ in. in diameter and 2 in. long mounted on a Dumont 6292 photomultiplier.

Since Jones et al (1952) have shown that these levels all decay by direct transitions to the ^{11}B ground state, the correlations may be derived from the coincidence proton spectra measured for a constant number of gamma counts at each gamma ray detector angle. This is fortunate because the separation of proton groups is much easier than that of gamma rays. Also, since the contribution to the highest energy proton group in such a spectrum will be entirely due to random coincidences, the other proton groups may be corrected for random contributions by subtracting an amount equal to the first group coincidence yield multiplied by the ratio of the singles yield in the group being considered to that in the first group.

II. 3 THE REACTION $^{10}B(d,p\gamma)^{11}B$

(a) Introduction

The principal previous investigations of the angular distributions of the proton groups from the $^{10}B(d,p\gamma)^{11}B$ reaction together with the results of the work presented here are summarized in Table II.2 in terms of the values of the parameters l_n and R necessary to give the best fit to the stripping formula of Bhatia et al (1953). P_0, P_1, P_2, and P_3

Table II. 2

	E_d (in Mev.)	Values of l_n P_0 P_1 P_2 P_3	R (in 10^{-13} cm.)
Evans et al (1954)	7.7	1 1 1 1	6.0
Paris et al (1954)	0.2 - 0.6	1 3 0 1	5.8
Deuchars and Wallace (1955)	0.25 - 0.75	1 3 0	5.8
Wallace and Storey (1956)	0.575 and 0.650	1 3 1 1	5.8

indicate the groups leaving the ^{11}B nucleus in its ground, 2.14, 4.46 and 5.03 Mev. levels respectively. The reaction had also been studied by Redman (1950), Holt et al (1953), Burke (1954), Pratt (1954) and Thompson (1954).

In these angular distributions a slowly varying or isotropic component was found in addition to the stripping component and this was usually attributed to compound nucleus formation. In contrast to the work of Paris et al, the Deuchars and Wallace experiment revealed some indication of a compound nucleus resonance at about E_d = 575 kev.

The angular correlations between the P_1 and P_2 groups and the corresponding gamma rays for the transition to the ground state had been measured by Thirion (1953) and by Deuchars and Wallace (1955). In the Thirion measurements the ratios of the intensities measured at 0 and 90° to the direction of the neutron were found to be 1.05 $\pm$ 0.05 respectively for E_d = 500 kev. In the Deuchars and Wallace experiment isotropy was found within $\pm$ 6% with measurements at thirty degree intervals.

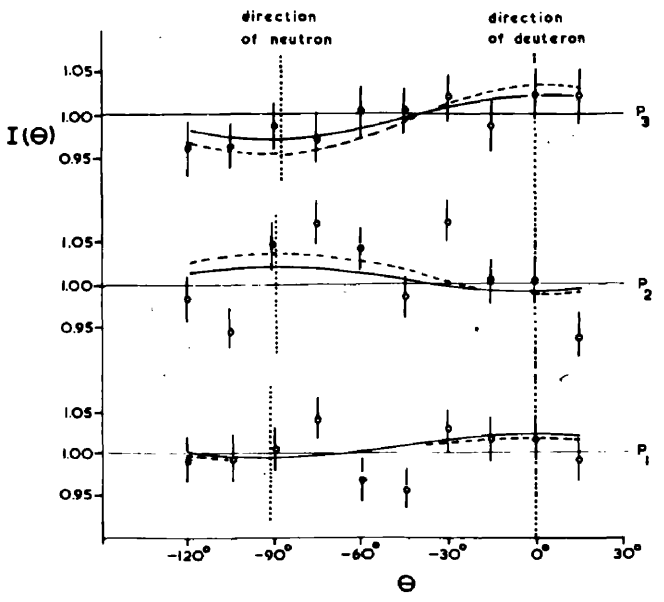

Fig. II. 10 The (d,pγ) correlations of D. & Wallace and the author at E_d = 600 kev. Proton counter at θ = ±65°. The dashed and solid lines correspond respectively to assumptions (a) and (b) of the text and table II. 3.

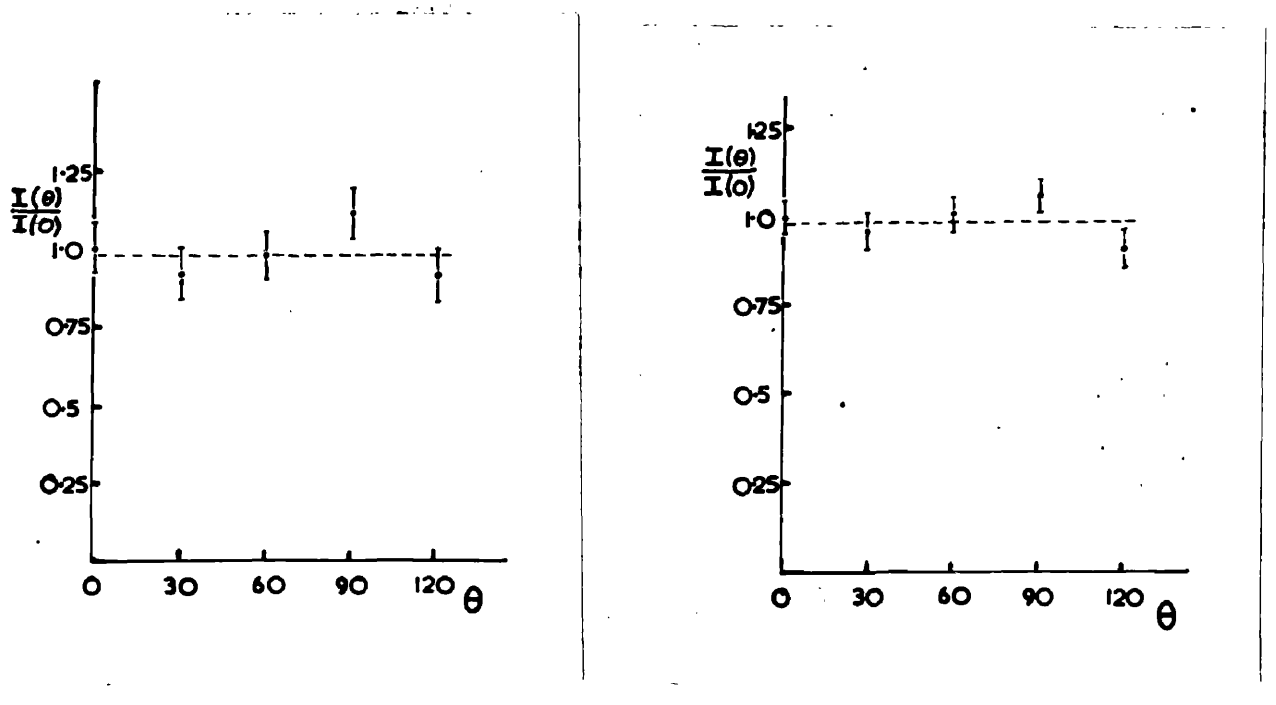

P_1 group P_2 group

Fig. II. 11 The (d,pγ) correlations of Deuchars and Wallace at E_d = 500 kev. Proton counter at θ = 45°, θ is again measured with respect to deuteron direction.

(b) Results and Discussion

The (d,pγ) angular correlations of the present work and those of Deuchars and Wallace are shown in Fig. II. 10 and 11 respectively. The least squares fit of each of the present correlation measurements to $1 + AP_2 (\cos \theta)$ as calculated by Dr. Wallace are given in Table II. 3 for both (a), the pure stripping assumption where θ is measured with respect to the direction of the absorbed neutron and (b) the pure compound nucleus assumption where θ is measured with respect to the deuteron direction. The values of A have been increased by 15% to allow for the finite solid angles subtended by the detectors (Rose, 1953). In respect of the near isotropy of the correlation of the P_1 and P_2 groups these results are in agreement with the previous measurements discussed in section II. 3(a) and have since been confirmed for the P_1 group by the measurements of Gorodetsky et al (1956) using 1.2 Mev. deuterons. The P_3 group correlations does not appear to have been measured by the other workers.

Table II. 3

Proton Group	γ-ray (in Mev.)	Values of the Coefficient A (a)	(b)
P_1	2.14	-0.008 ± 0.03	$+0.016 \pm 0.03$
P_2	4.46	$+0.035 \pm 0.02$	-0.024 ± 0.02
P_3	5.03	-0.050 ± 0.03	$+0.034 \pm 0.03$

It is to be noted that the choice of the proton detection angle at 65° was unfortunate in that it results in the defined direction for the absorbed neutron

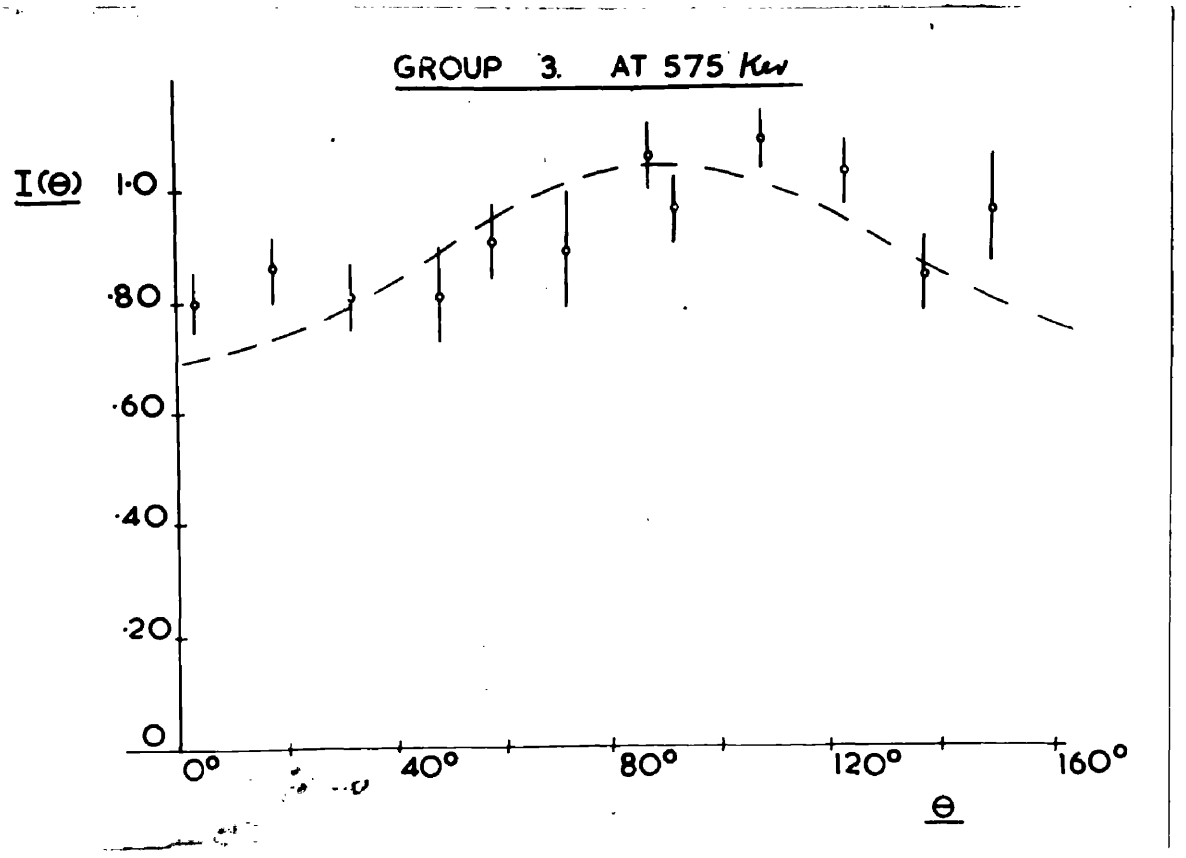

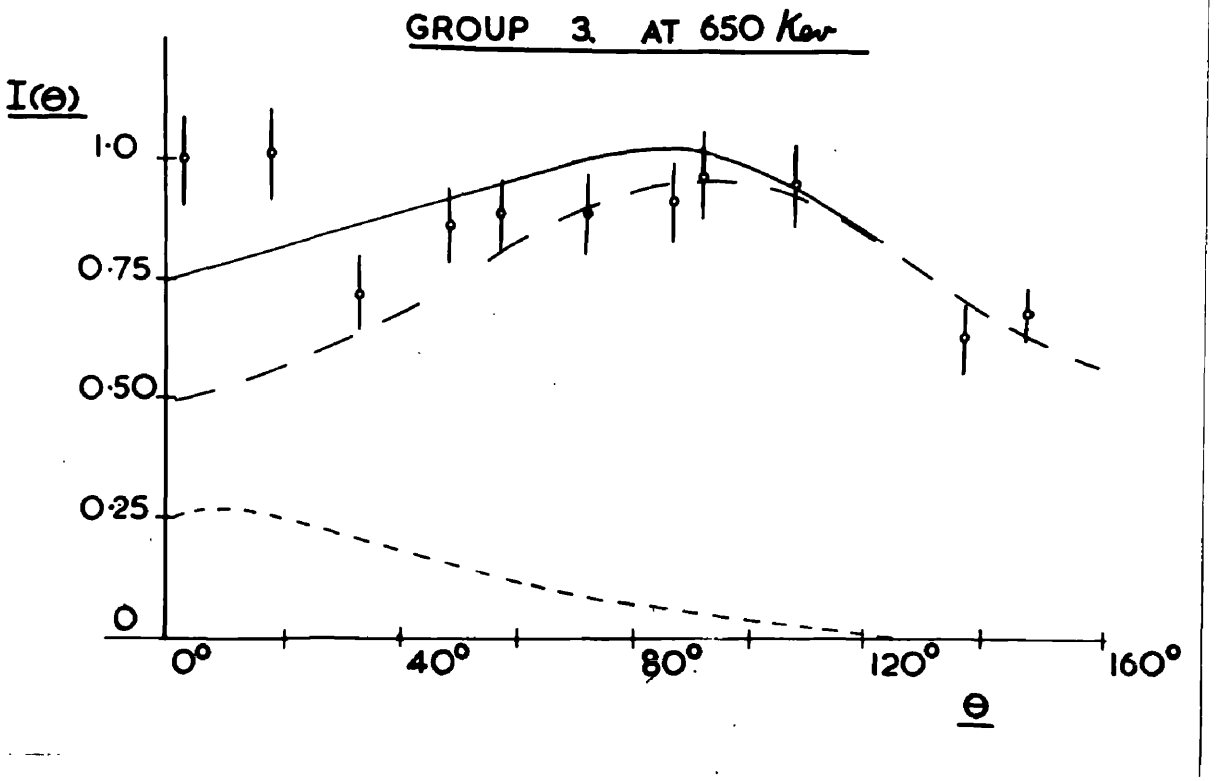

Fig. II. 15 The angular distributions of the P_3 group of protons as measured by Dr. Wallace and the author.

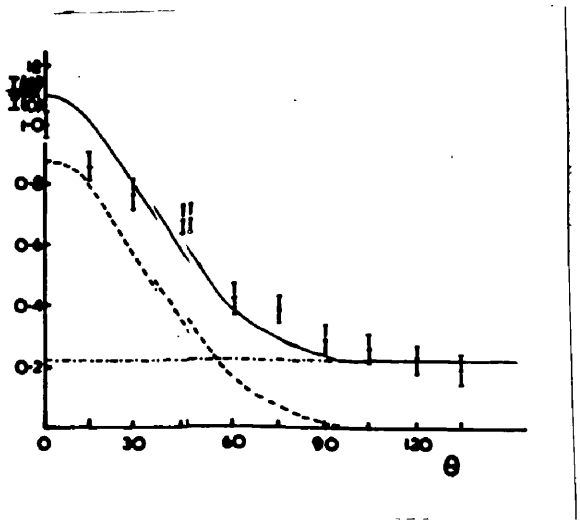

E_d = 575 kev.

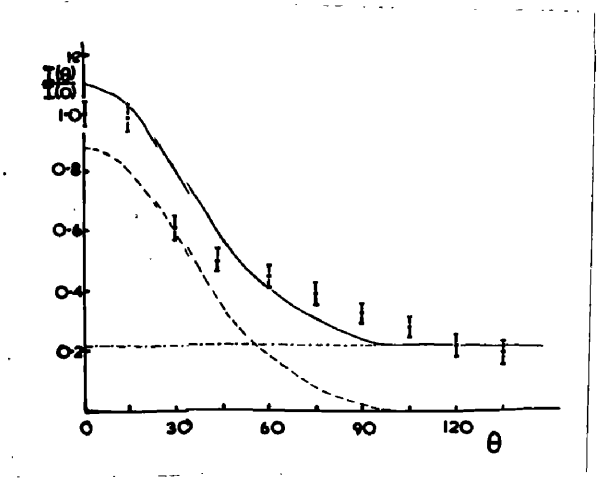

E_d = 675 kev.

Fig. II. 14(b) The angular distributions of the P_2 group of protons as measured by Deuchars and Wallace.

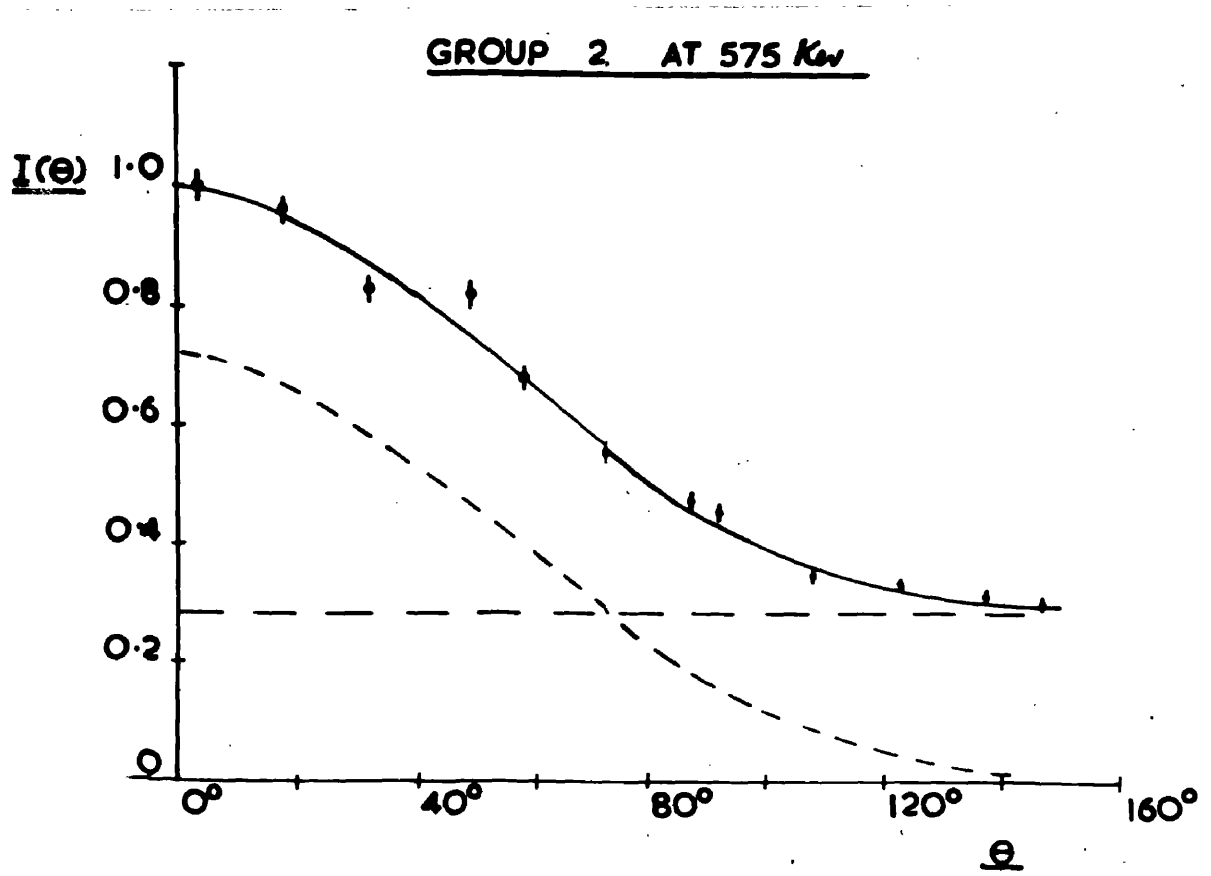

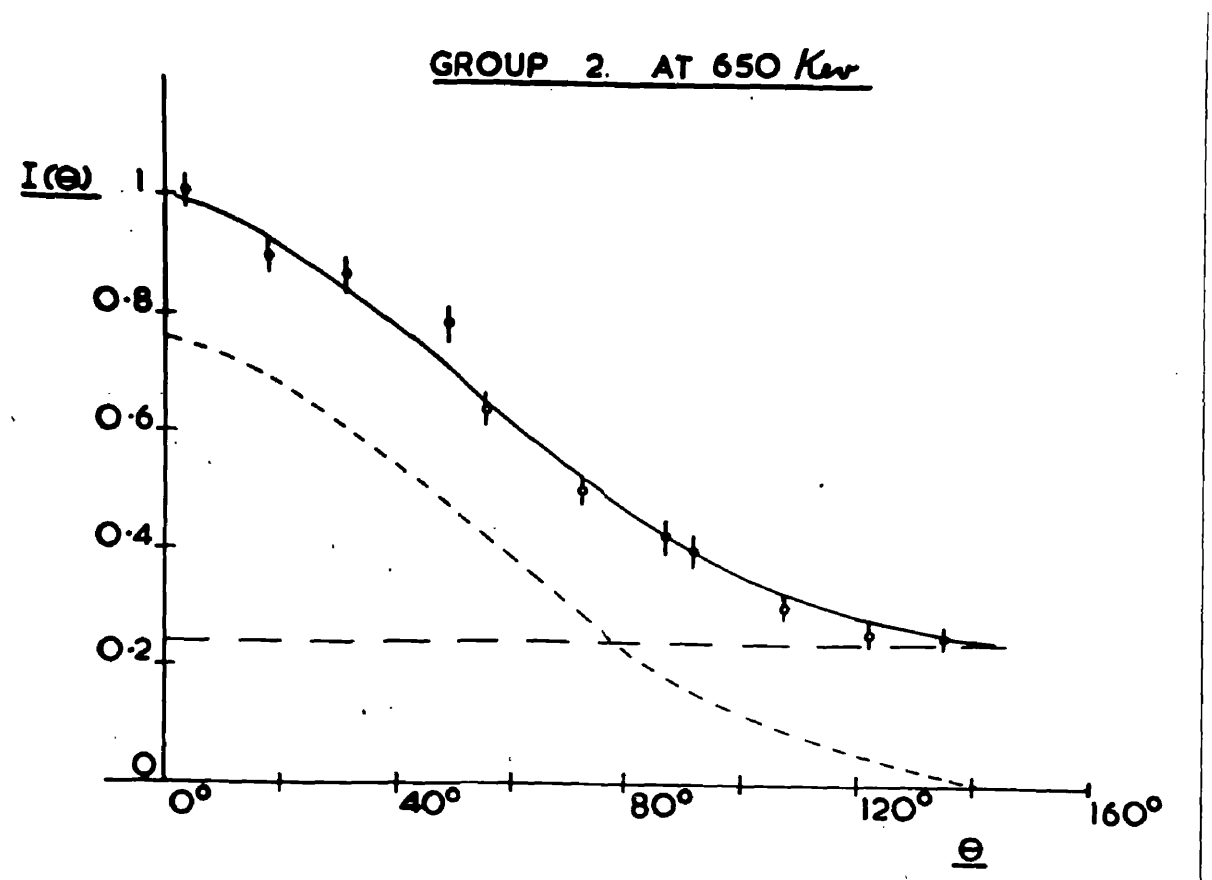

Fig. II. 14(a) The angular distributions of the P_2 group of protons as measured by Dr. Wallace and the author.

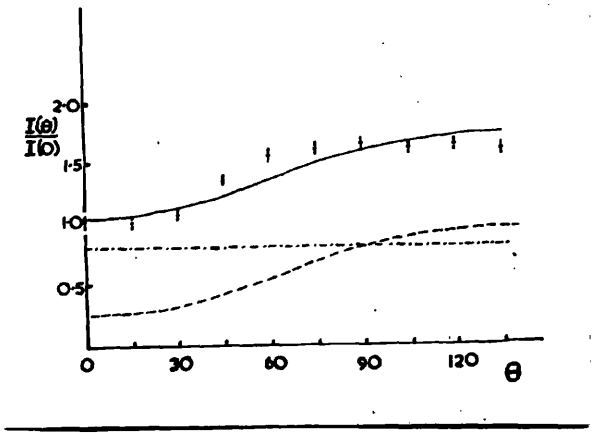

E_d = 350 kev.

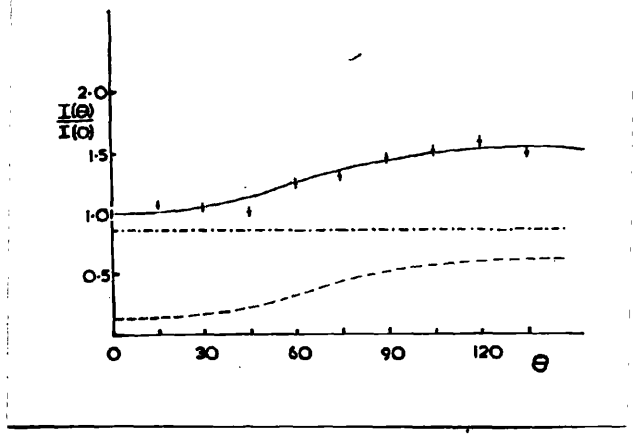

E_d = 500 kev.

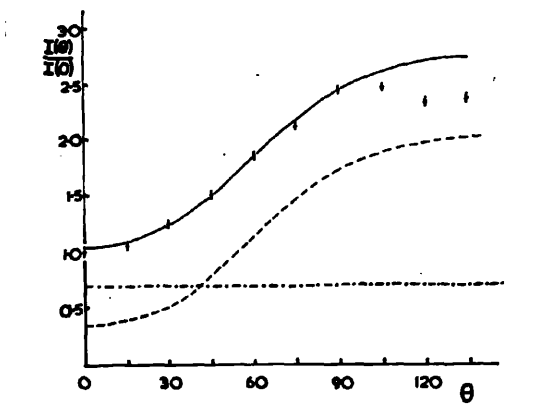

E_d = 575 kev.

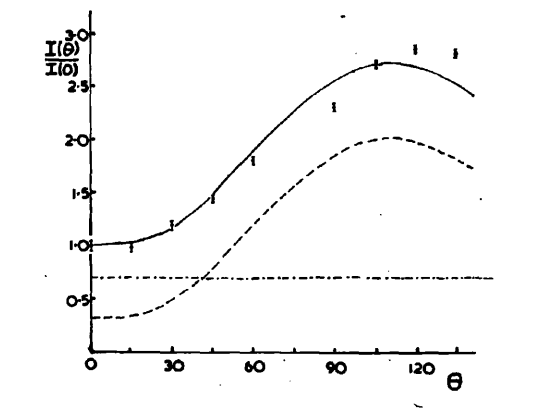

E_d = 675 kev.

Fig. II. 13(b) The angular distributions of the P_1-group of protons as measured by Deuchars and Wallace.

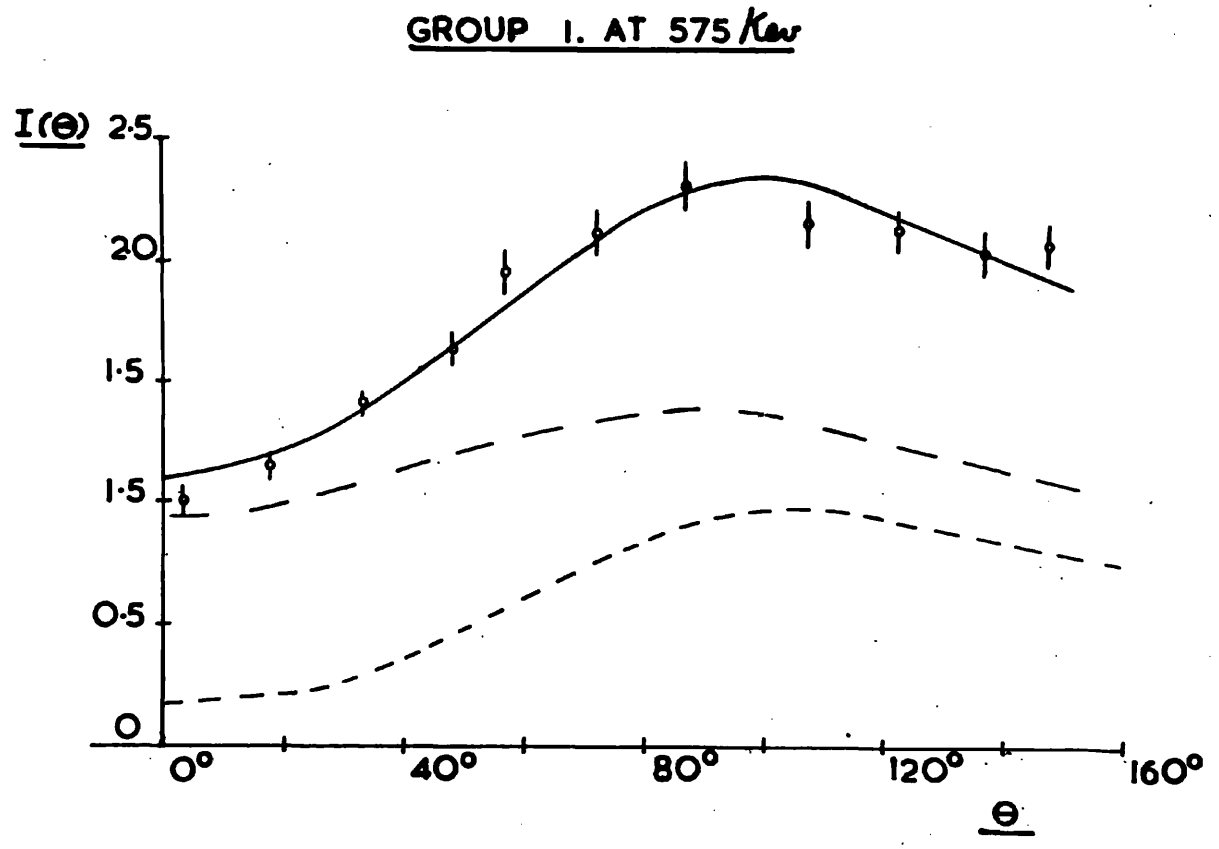

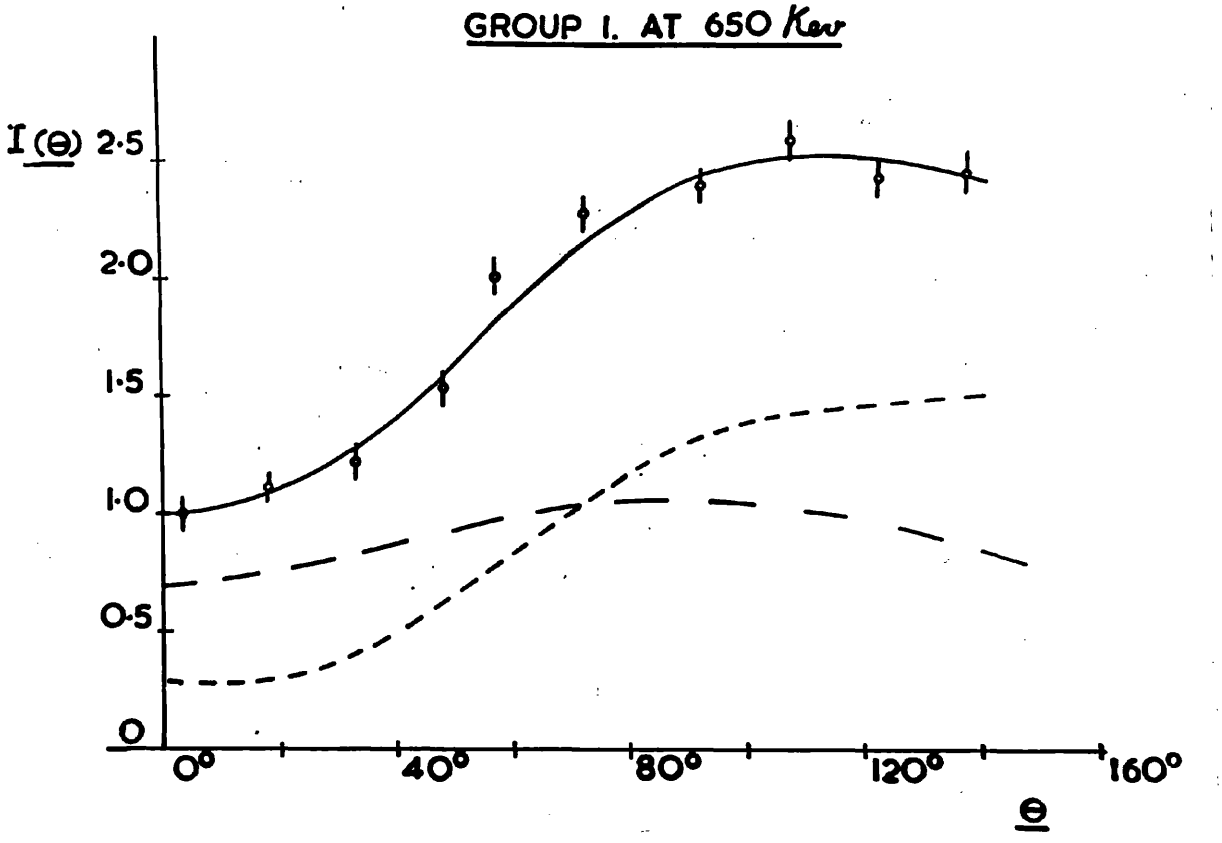

Fig. II. 13(a) The angular distributions of the P_1 group as measured by Dr. Wallace and the author.

62(c)

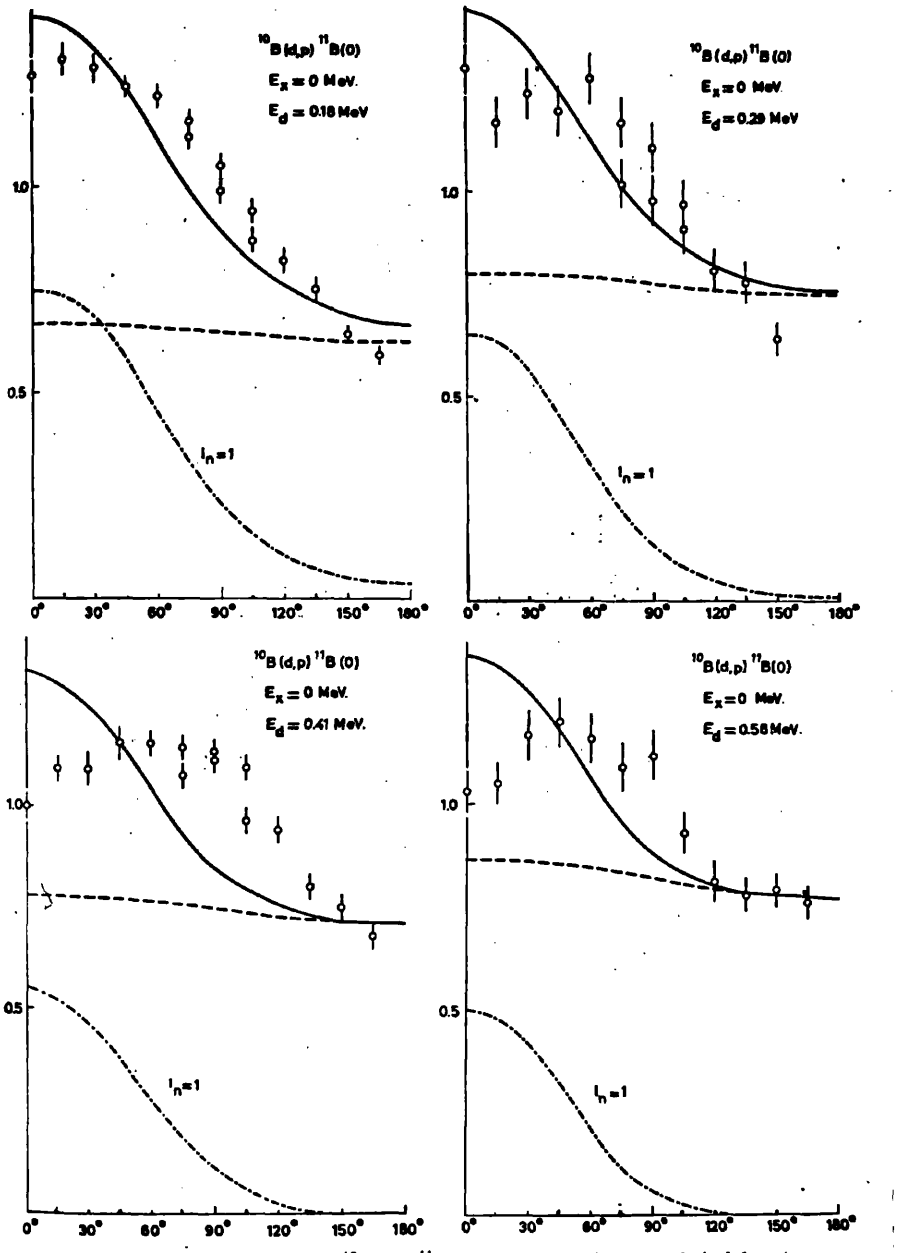

Fig. 1. Angular distributions of $^{10}B(d, p)^{11}B$ group (0) on arbitrary scale in laboratory coordinates. The full curve is the sum of a stripping contribution for $l_n = 1$ (dot-dash curve) and an isotropic contribution for compound nucleus formation (dashed curve).

Fig. II. 12(c) The angular distributions of the P_o group of protons as measured by Paris et al. (1954).

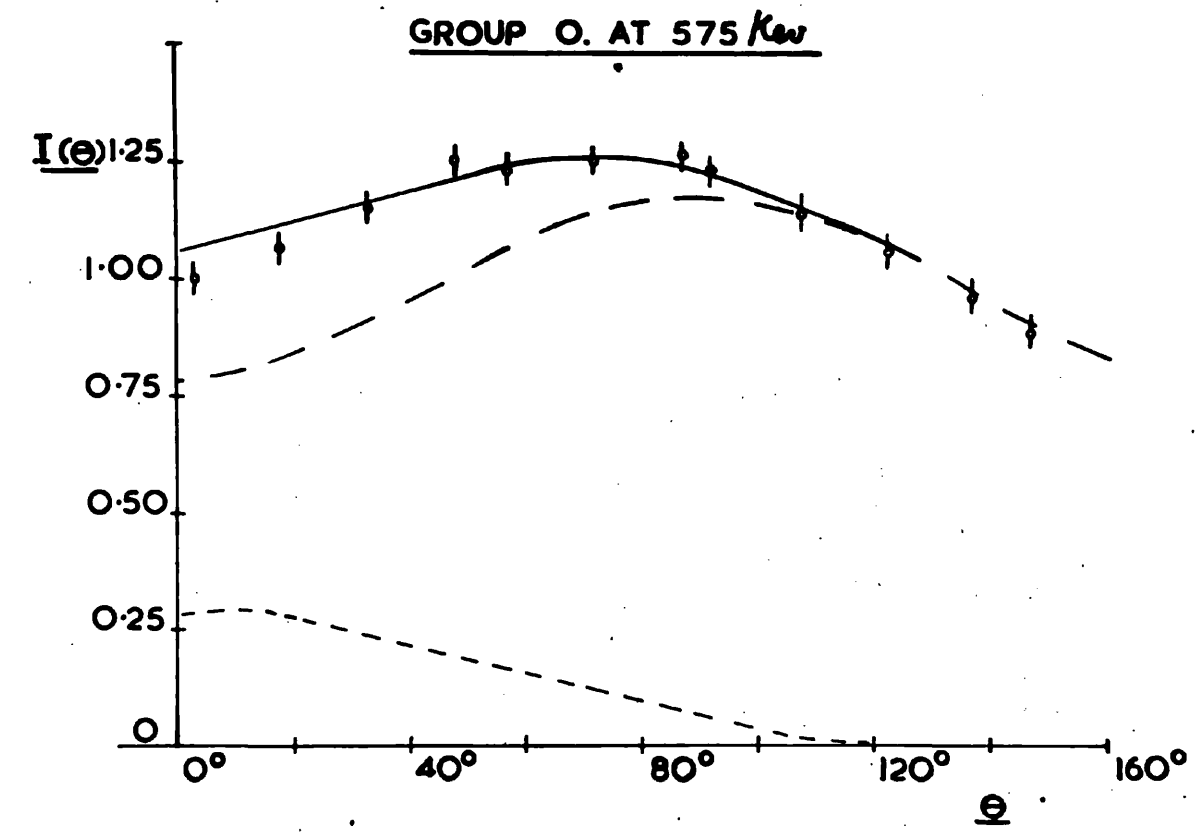

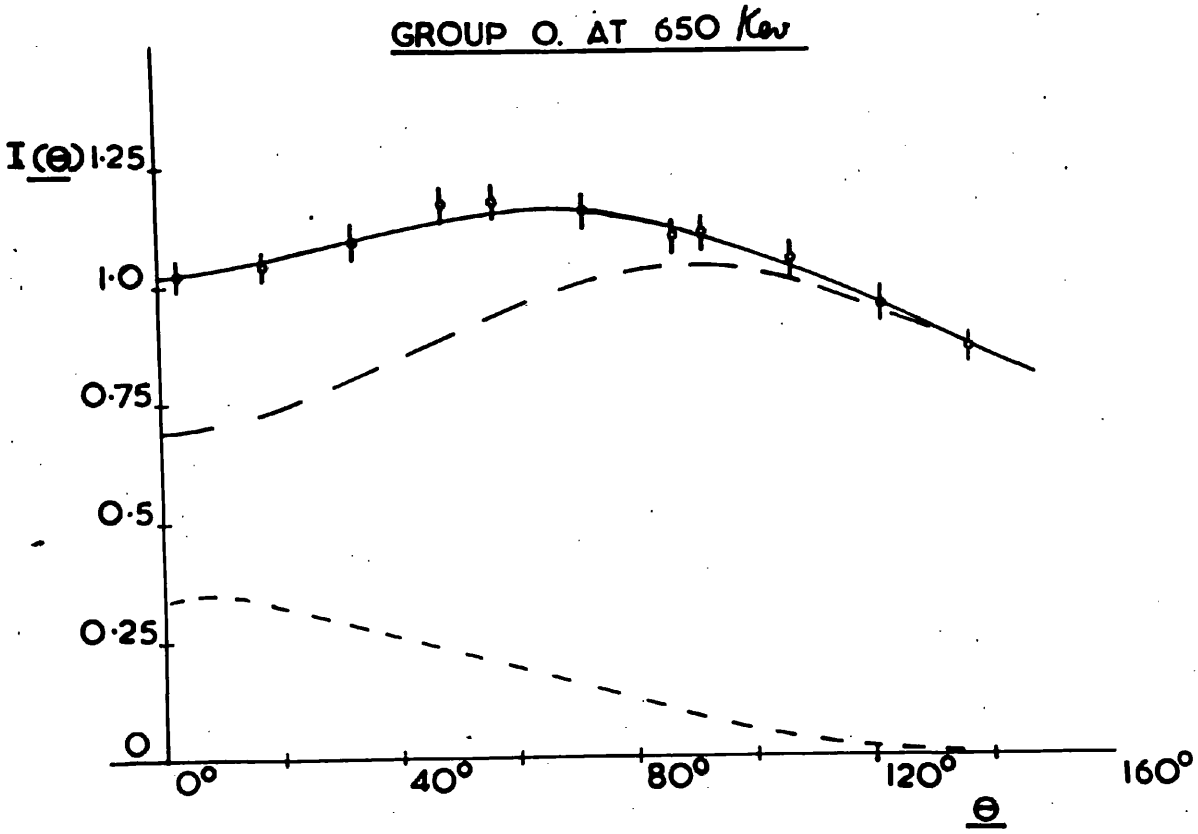

Fig. II. 12(a) The angular distributions of the P_0 group of protons as measured by Dr. Wallace and the author.

being almost perpendicular to the deuteron direction. Since P_2 (cos θ) has an axis of symmetry every 90 deg. a remeasurement with another angle would have been required, had appreciable anisotropies been found, to determine the relative amounts of stripping and compound nucleus.

The angular distributions of the proton groups measured by Dr. Wallace and the author using the apparatus and method described in section II. 2 are shown in Fig. II. 12(a), 13(a), 14(a) and 15 and those of Deuchars and Wallace in Fig. II. 12(b), 13(b), and 14(b). In Fig. II. 12(c) the angular distributions obtained by Paris et al for the P_o group using nuclear emulsions are reproduced for comparative purposes.

In section I.3 the relative importance of stripping, of the compound nuclear process, and of the Coulomb effect on the angular distributions and the expected variation of these quantities as a function of E_d and Z have been discussed. It is assumed that for the present experiment Z = 5 is sufficiently small that a description is possible in terms of the Bhatia et al stripping distribution F^2 (θ) plus an incoherent contribution of the form 1 + AP_2 (cos θ) from deuteron capture in a single level (or a group of levels of the same parity) in ^{12}C.

The details of the results for each group are considered separately in the following sub-sections.

(i) Group O

The angular distributions of this group over

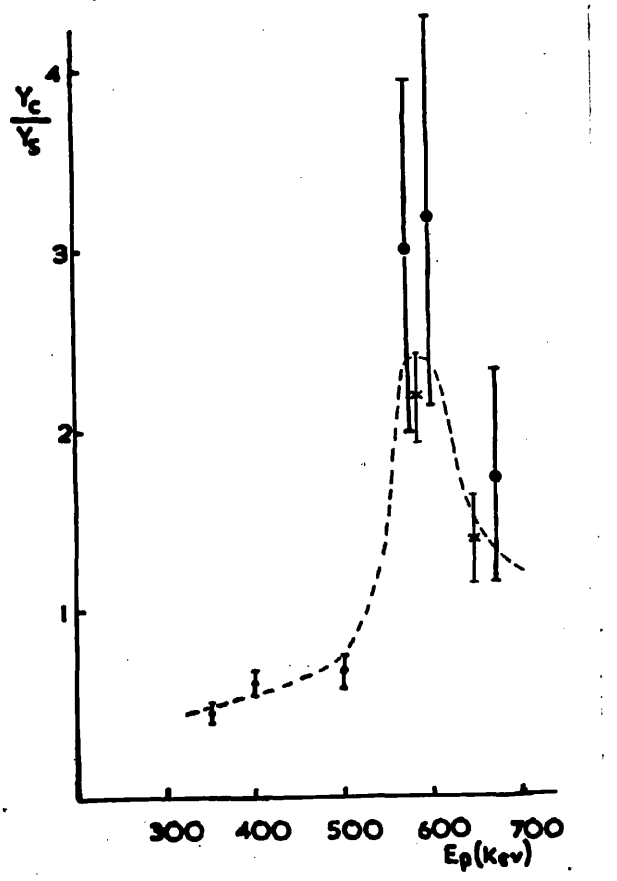

Fig. II. 16(a) The variation of the relative yields from the deuteron capture and stripping processes for the P_o group of protons.

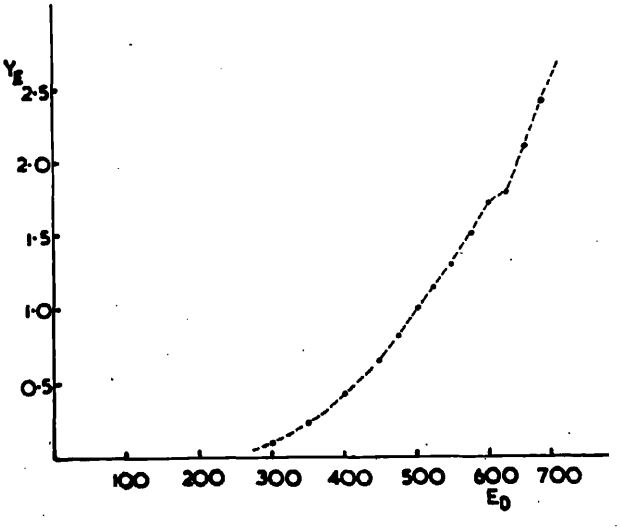

Fig. II. 16(b) The excitation function for the P_o group of protons as measured by Deuchars and Wallace.

the energy range studied can be fitted as the sum of the expected stripping and compound nucleus components with $l_n = 1$, $r = 5.8 \times 10^{-13}$ cm. and $A = -0.25$. The ratio of the integrated contributions from these two modes of reaction varies with deuteron energy as shown in Fig. II. 16(a). The two points on the curve obtained by Wallace and the author establish definitely the resonance nature of the structure at $E_d = 575$ kev. The excitation function for the first group as measured by Deuchars and Wallace is reproduced as Fig. 16(b) for comparison. This resonance for deuteron capture corresponds to a level (or an isolated group of similar levels in ^{12}C) with an excitation energy of 25.7 Mev. Since there is no evidence of a P_1 (cos θ) term in the distribution the parity will be the same for all levels if more than one contribute and will probably be negative since the magnitude of the effect indicates $l_d = 1$. With a purpose of obtaining more evidence about the spin Deuchars and Wallace have searched, unsuccessfully, for the 25.7 Mev. gamma ray corresponding to the transition to the 0^+ ground state of ^{12}C. Unfortunately, little can be inferred from this result/since, because of the competition from particle emission at these high excitation energies, gamma rays of deuteron capture are improbable in any event (see also the experiments of Sinclair (1954) and Allan and Sarma(1955).

(ii) Group I

Fitting the set of angular distributions for this group to the formulae as for group 0 yielded the values of the parameters $l_n = 3$, $R = 5.8 \times 10^{-13}$ cm. and A (the coefficient of P_2 (cos θ) = -0.25. The dependence of the fit on the value of A is not as critical as for Group 0 and the Deuchars and Wallace results were fitted with A = 0. The variation of Y_c / Y_s with deuteron energy is considerably smaller than for group 0. The isotropic angular correlation of the 2.14 Mev. gamma ray indicates either that (1) the spin of the first excited state $J = \frac{1}{2}$ or that (2) $J > 1/2$ and there is a fortuitous mixing of channel spins and gamma ray multipoles in the reaction. Table II.2 reveals that the orbital angular momentum of the captured neutron l_n appears to vary with E_d. At low energies $l_n = 3$ which is compatible with $j = \frac{1}{2}$, but at high energies $l_n = 1$ which required j to be at least 3/2.

Since these measurements were made, Wilkinson (1957) has shown that the 2.14 Mev. gamma is magnetic dipole and has thus removed the second possible explanation of the isotropic angular correlation. Bilanuik and Hensel (1958) have remeasured the high energy angular distributions and confirmed the $l_n = 1$ result of Evans et al (1954). The definite contradiction between this value of l_n and that required by the usual stripping selection rule has resulted in suggestions that the latter be modified. Wilkinson (1957)

has proposed that in this reaction the spin of the proton is reversed in orientation during the stripping and thus contributes an additional angular momentum change of $\Delta S = 1$ to the residual nucleus. Evans and French (1958) suggest that nucleon exchange occurs so that the emitted proton comes from the target nucleus in contrast to the usual concept of stripping and invalidates completely the selection rule. The fact that the sign of the polarization of this proton group is different from that of the other groups from ^{10}B (Hensel and Parkinson, 1958) supports these proposals. Evans and French have been able to show that angular distributions calculated on an exchange basis are not very different from the Butler formula and in the Wilkinson model it appears to be assumed that the angular effect of the occurrence of spin-flip is small. The contributions from these modes of stripping relative to ordinary stripping have not been calculated as a function of E_d and thus it is not possible to check whether these processes are gradually replaced by ordinary stripping at low deuteron energies as required by our results.

(iii) Group 2

The analyses of this group in previous studies gave different results. Evans et al (1954) found $l_n = 1$ and Maslin et al (1956) studying the group going to the mirror residual state in the $^{10}B(d,n)^{11}C$ reaction obtained $l_p = 1$. In contrast at low values of E_d Paris et al (1954) and Deuchars and Wallace (1955) found $l_n = 0$. It now appears

on careful appraisal that in these last measurements where both the $l_n = 0$ and the $l_n = 1$ distributions have their maxima at 0 deg. the results were not sufficiently accurate to differentiate between the two capture angular momenta. The present result gives unambiguously $l_n = 1$ in agreement with Evans et al. Since the compound nucleus contribution remained relatively small at all deuteron energies, it was not possible to decide whether A was non-zero and an isotropic component was used in the analysis.

It is difficult to decide whether the very small anisotropy measured is significant or not. (See Table II.3). Since Jones et al (1952) have shown that the residual state has a spin of 5/2, isotropy can be only fortuitous.

(iv) Group 3

Since this group is small relative to the adjacent spectral contributions the errors are large and no detailed analysis was made. The resemblance of these results and those of Group 6 suggests a predominant contribution from the compound nucleus, a stripping contribution possibly with $l_n = 1$ and a spin of 3/2 for the 5.03 Mev. level.

As in the case of Group 2 the significance of the very small correlation anisotropy is in doubt.

II. 4 THE REACTION $^{24}Mg.\ (d,p)^{25}Mg.$

(a) Introduction

The available numerical data describing this reaction are given in Table II. 4. In the experiments of Holt et al (1953)

Table II. 4

Group		P_o	P_1	P_2
Q in Mev.		5.10	4.52	4.12
Measurements				
(a) Holt et al, (1953) E_d = 8.2 Mev. Bhatia et al analysis	l_n	2	0	2
	R in 10^{-13} cm.	5.5	7.4	5.5
(b) Wallace and Storey (1956) E_d = 0.65 Mev. Bhatia et al analysis with modification due to deBorde	l_n	2	0	2
	R in 10^{-13} cm.	6.7	6.7	9.5
	in deg.	+78	-52	0
	$\sigma(\theta)$ in 10^{-7} barns per sterradian *	2.4	8.0	6.0
Residual States Endt and Braams (1957)	energy	0	0.58	0.98
	spin and parity	5/2+	$\frac{1}{2}$+	3/2+

* (θ) was measured with the proton counter at 65° to a beam of deuterons with an energy of 0.6 Mev.

the two highest energy groups were fitted with the Butler formula plus a small isotropic background. Since the target used was of natural magnesium the third group effectively coincided with the first group from $^{26}Mg.(d,p)^{27}Mg.$, Q = 4.207 Mev.

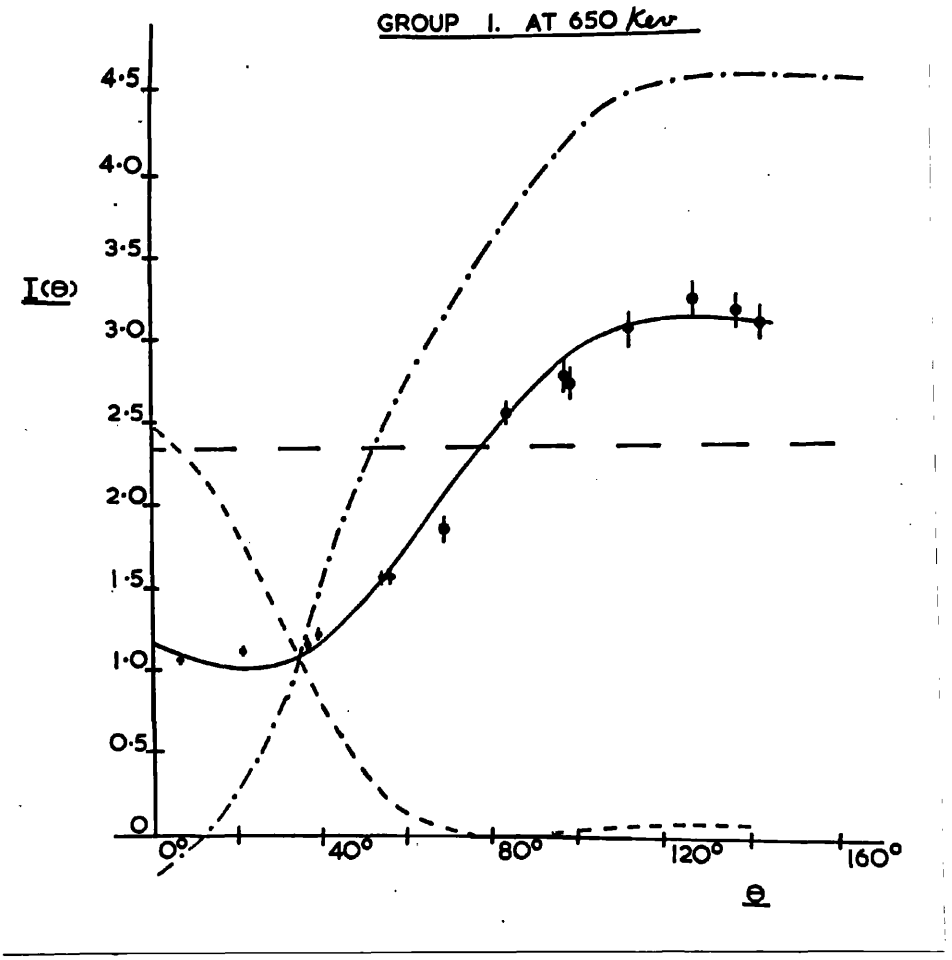

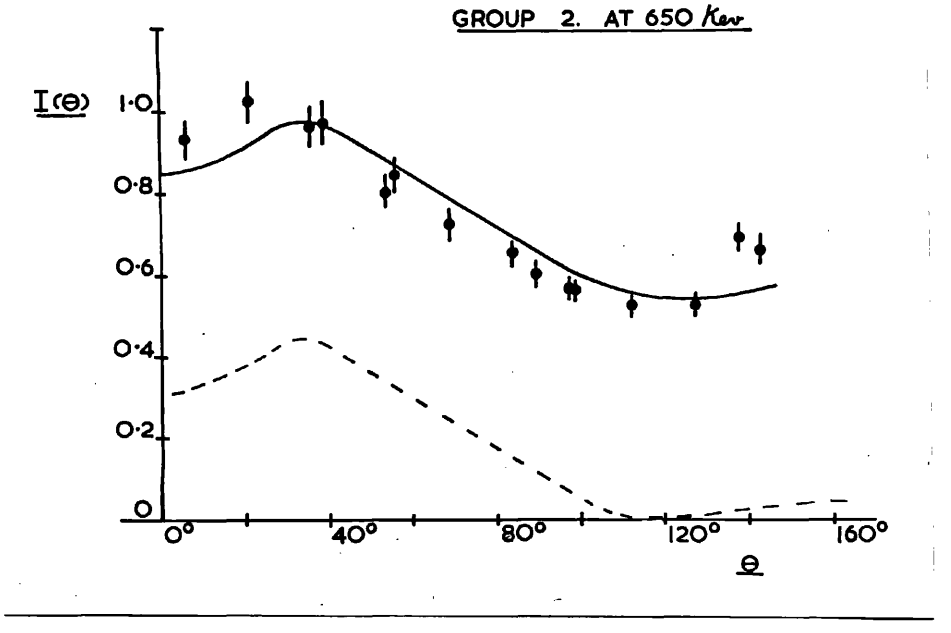

Fig. II. 18 The angular distributions of protons from the $^{24}Mg(d,p)^{25}Mg$ reaction.

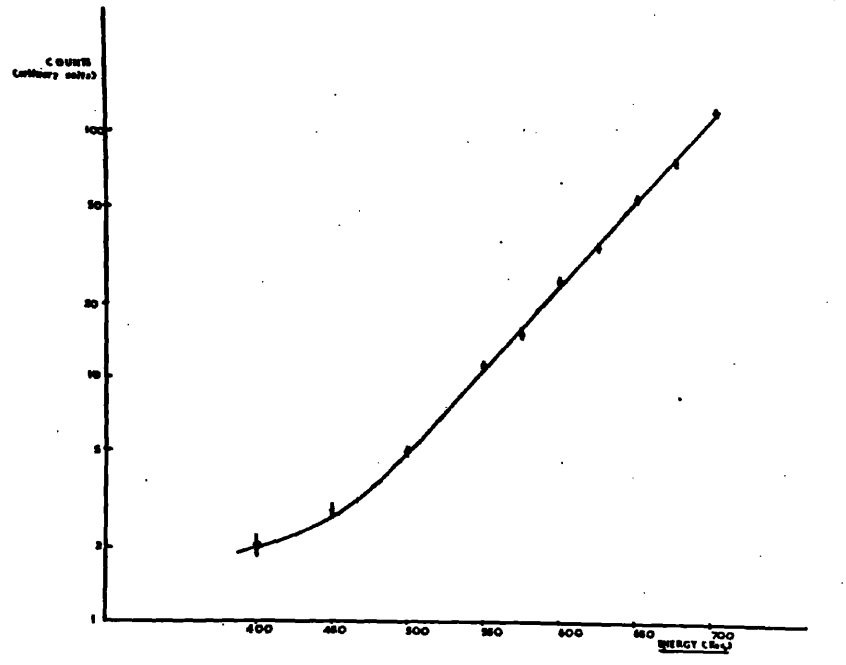

Fig. II. 17 The total yield of the first three proton groups in $^{24}Mg(d,p)^{25}Mg$ as a function of E_d.

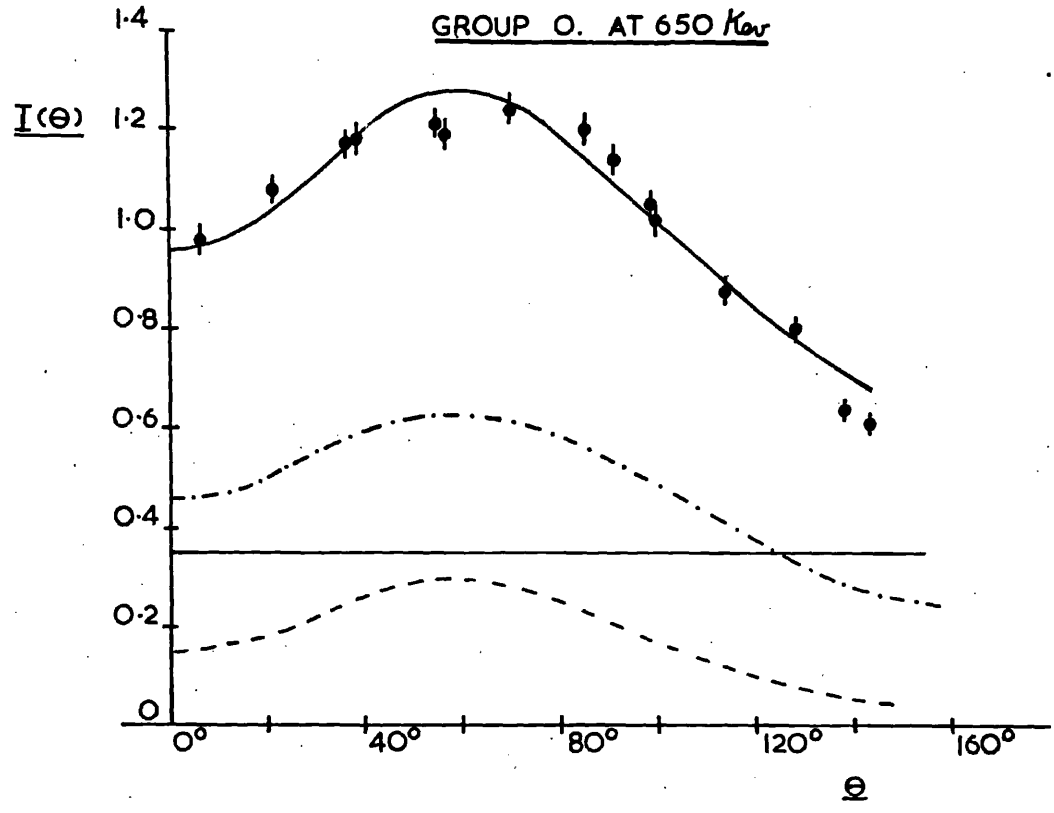

Fig. II. 18 The angular distributions of protons from the $^{24}Mg(d,p)^{25}Mg$ reaction.

This angular distribution appeared to have $l_n = 0$ and $l_n = 2$ components. Holt et al showed that in the ^{26}Mg. reaction $l_n = 0$ and therefore, attributed the other component to ^{24}Mg.

(b) Measurements and Interpretation

The excitation function and the angular distributions as measured by Dr. Wallace and the author are shown in Fig. II. 17 and Fig. II. 18 (a, b and c) respectively. The apparatus and method used is described in section II. 2.

It has been seen that in the $^{10}B(d,p)^{11}B$ reaction the compound nucleus and stripping contributions are of the same order of magnitude. In the present study the charge Z of the nucleus has been increased from 5 to 12 while the deuteron and proton energies (E_d and E_p) used remained roughly constant. According to the discussion of section I.3 (b) this should result in the relative contributions of the compound nucleus decreasing. The fact that the total cross section decreases by three orders of magnitude (see Table II. 4 and Wallace, 1956) suggests that this relative decrease is very considerable. No indication of capture resonance structure appears in the excitation function which rises smoothly and steadily. The change of Z at constant E_d, E_p will have another effect as well, the Sommerfeld parameters η_d, η_p which measure the magnitude of the Coulomb effect also increase considerably.

For these reasons we have chosen to assume that the description of the angular distributions should be in terms of the Bhatia stripping formula with modifications due to

Coulomb effects. The relative magnitude of the effects is uncertain. Accordingly an initial description in terms of weak Coulomb effects due to deBorde (1955) was applied by Dr. Wallace and the author. This is described in the present section. More recently, in view of the failure of the parameter δ to remain constant independent of the group measured as required by deBorde (see Section 1.3 (b) the author decided to apply the strong Coulomb theory of Ter Martirosyan (1956) and of Biedenharn et al (1956). The details of this last analysis are given in section II. 4 (c)

In accordance with the formula of deBorde each of the distributions has been divided into three components (1) the usual Bhatia stripping formula $F^2_{R,l_n}(\theta)$ denoted on the graphs by a dashed line, (2) a multiple of the Bhatia stripping amplitude $2A \sin \delta \times F(\theta)$ denoted by a dash-dot line and (3) an isotropic term A^2 denoted by a solid line. The values of R, l_n and δ required for the best fit are given in Table II. 4.

In the Group I diagram (Fig. II. 18 (b) $2A \sin \delta$ is displaced upwards by 3.5 units. It is to be noted that the stripping amplitude changes sign after the first minimum in $F^2(\theta)$.

The variation of the proton energy with angle is considerable in the D(d,p)T reaction due to large centre of mass effects and in the forward 45 deg. it tends to overlap Group 2 rendering the results increasingly uncertain as the angle decreases to zero. This curve has been fitted by $l_n = 2$.

because the selection rules and agreement with Holt et al (1953) required it but the value of R necessary is almost 50% greater than for the other groups. It is difficult to understand why this should be so. Since R is an average interaction radius it might be expected to vary with E_d or l_d (from classical closest distance of approach or impact parameter considerations. It may be that it is associated with the fact that the first two proton groups have corresponding single particle residual status, while the third residual state has a more complex structure. (Possibly it is the first member of a rotational series based on the 0.58 Mev. level.) These last properties are deduced by analogy from those of the mirror states in ^{25}Al which has been extensively studied by Verma and Jack (1956) and by Litherland et al (1956) using the (p, γ) and p, $p^1\gamma$) reactions.

In general it may be said that the experimental measurement cannot be fitted by a pure stripping curve or even with the addition of the usual isotropic background (with the exception of the P_2 group). They may be fitted with the modified formula but δ has not the expected constantcy and the situation is approached where the curves may fit only by reason of having introduced a further degree of freedom.

(c) <u>An Alternative Interpretation</u>

In view of the different values of δ obtained, the author decided to investigate the agreement of the experimental angular distributions with the strong coulomb theory of Ter Martirosian (1956) and of Biedenharn et al (1956) as far as

that was possible. The best fit for the $l_n = 0$ transition to the first excited state of ^{25}Mg as the sum of the strong coulomb stripping formula and a small isotropic compound nucleus contribution is shown in Fig. II. 19. The required hypergeometric function $_2F_1$ (0.855i, 3.60i, 1, - $\zeta(\theta)$ was evaluated as a function of θ by using equation 5.3.16 of Morse and Feshbach (1953) and calculating sufficient terms in the series expansion to give 1% accuracy. The result gives $I(180^\circ)/I(0^\circ) = 5.0$. As an approximate check this ratio was evaluated for the corresponding asymptotic expression (η_d and $\eta_p \rightarrow \infty$) and a value of 5.9 obtained.

As has been mentioned in Part I the corresponding angular distributions for $l_n \neq 0$ are not readily available. If the angular position of the characteristic maximum in these distributions is denoted by θ_m, then the only indicator of the value of θ_m is through its classical identification with ϵ, the orbit eccentricity, that is $\sin(\theta_m/2) = 1/\epsilon = (1 + l_n^2/\eta_d \eta_p)^{-1/2}$. Substitution of $l_n = 2$ and proper values of η_d and η_p would predict peaking at about 80 deg. for the other two proton groups which is probably in adequate agreement with the 30 deg. and 60 deg. experimentally observed (when the quality of this estimate is considered).

The advantage of this treatment lies in its lack of parameters such as R, A and δ whose value is not known with sufficient accuracy from other data to give a rigid theoretical curve. Admittedly the ratio Y_c/Y_s is such a parameter but

it is quite small and may be unnecessary since the present results except for the two points between 0 and 30 deg. could be equally well fitted with just the strong coulomb stripping curve.

Comparison of the results of the two different interpretations considered here suggests that the coulomb effects in this experiment were too strong to be accounted for by the deBorde approximation.

PART III PARTIAL EVAPORATION OF HEAVY NUCLEI

III. 1 A MODIFIED EVAPORATION MODEL

(a) The General Model

The formulae required for the discussion of this work have already been discussed in section I.4. They will be reproduced here in outline for convenience. The differential cross section for particle emission in the statistical model is given by the formula

$$\frac{\sigma(E_p)}{\sigma_r} = \frac{g.\tau_c}{\pi^2\hbar^3} E_p \sigma_c \frac{\omega_R(E_R^*)}{\omega_c(E_c^*)} \qquad \text{III (1)}$$

which reduces to the corresponding spectral shape,

$$\log \frac{\sigma(E_p)}{E_p \sigma_c} = -E_p/T + \text{const.} \qquad \text{III (2)}$$

if the following simplifying assumptions are made (a) $\omega(E^*) \propto e^S$, (b) $S_c(E^*) = S_R(E^*)$, and (c) $E_p \ll E_c^* - E_b$.

The general thermodynamical formula for level density is

$$\omega(E^*) = \left[T(2\pi \frac{dE^*}{dT})^{\frac{1}{2}}\right]^{-1} e^S \qquad \text{III (3)}$$

and experimental results have been fitted to some extent to the semi-empirical formula

$$\omega_o \propto \frac{1}{(E^*+T)^2} \exp. \left[2\left(\frac{AE}{f}\right)^{\frac{1}{2}}\right] \qquad \text{III (4)}$$

In these formulae the subscripts C and R denote compound and residual nuclei respectively, E_p is the energy of the emitted particle and E^* that of an excited nucleus, which has corresponding level density, lifetime, temperature and entropy. ω, τ, T and S. σ_r is the total reaction cross section and σ_c is required by the principal of detailed balance to be the averaged cross

section for the formation of the compound nucleus in the inverse reaction. In practice it is always set equal to

$$\pi \lambda^2 \sum_l (2l+1) T_l \qquad \text{III (5)}$$

where $T_l(E_p)$ is the transmission coefficient for a particle of angular momentum l incident on a repulsive potential barrier of the form.

$$V = -V_o \quad , r < R$$

$$V = \frac{Z_p Z_T e^2}{r} \quad , r > R$$

Experimental neutron spectra are usually converted to $\log \frac{\sigma(E_p)}{E_p \sigma_c}$ and plotted as a function of E_p (e.g. Graves and Rosen, 1953) and a temperature T is accordingly obtained as the reciprocal of the slope of the best straight line through the points (equation III (2)). Because of the effect of the Coulomb term in σ_c the present experimental results (section III.2) and most others where proton emission is measured do not satisfy assumption (c) of eqn. III.2. Since this assumption has allowed III.2 to be obtained using only the first term of a Taylor series expansion, the second term + $\frac{E_p^2}{2} \frac{d^2S}{dE^2}$ will now be considered $\frac{d^2S}{dE^2}$ is negative, since eqn. III (4) implies $S \propto E^{\frac{1}{2}}$. On the plot mentioned above inclusion of this term results in the theoretical prediction falling more and more below the limiting straight line as E_p increases. The present experimental values, however, show very little tendency

to diverge from the straight line and many other proton measurements show the opposite effect a considerable rise about the line at large E_p. This latter is probably due to an appreciable contribution from the direct effect caused by the use of higher bombarding energies or more forward angles of detection. Many other authors (Colli et al, 1957); Thomson, 1957; Gugelot, 1954) have also pointed out that there seems to be more correspondence between results from different experiments when the energy spectra are plotted against emitted particle energy rather than residual nucleus excitation energy as would be expected from eqn. III (1).

It is important to note at this point that the general form of eqn. III (1) is due to the principal of detailed balance and hence in all probability is correct. The insertion of III (5) for σ_c and $\omega(E_R^*)$ for the density of states of the residual group immediately after emission is, on the other hand, probably only accurate for a strong coupling or absorption i.e. a black nucleus. Since a method of inserting values more characteristic of a moderate absorption into this detailed balance formula, was not obvious to us, we decided to attempt to obtain the same effect by a more direct calculation. It was assumed that the long mean free path and weak coupling would allow a particle inside the nucleus to approach the barrier and pass through without its total energy being modified by interaction with other nucleons. Thus the spectrum of particles outside would have the same shape as the distribu-

tion inside. This internal distribution of particles was expected to conform to that of a gas with weak coupling i.e. the lower energy region might be distorted due to degeneracy, but the high energy tail was probably closely Maxwellian (see Ter Haar, 1954, page 91). Since the predicted spectrum corresponded to this tail it would accordingly satisfy eqn. III (2) with a well defined T characteristic of the nucleus from which evaporation occurred.

According to this concept

$$\frac{\sigma(E_p)}{\sigma_r} = \sum_l N_l(E_i) \frac{\Gamma_{esc.,l}(E_i)}{\Gamma_{col.,l}(E_i) + \Gamma_{esc.,l}(E_i)} \tau_c \qquad \text{III (6)}$$

Here $N_l(E_i)$ is the number of collisions per unit time inside the nucleus which result in a specific type of particle P acquiring an internal kinetic energy E_i per unit energy interval. $\Gamma_{col.}$ and $\Gamma_{esc.}$ are the probabilities per unit time (multiplied by $\hbar$) that this particle suffers further collisions and that it escapes. $\Gamma_{col.} \gg \Gamma_{esc.}$ The mean time the particle spends at this energy is therefore $\Gamma_{col.}/\hbar$ and the distribution in energy of such particles is $\rho(E_i) = \frac{N(E_i)\ \Gamma_{col.}}{\hbar}$ III (6) may therefore be written

$$\frac{\sigma(E_p)}{\sigma_r} = \sum_l \rho_l(E_i)\ \Gamma_{esc.,l}(E_i)\ \frac{\tau_c}{\hbar} \qquad \text{III (7)}$$

It can be shown that $\rho_l(E_i) = \frac{\lambda_i^2}{\pi^2}(2l+1)\,\rho(E_i)$ III (8)

and that

$$\Gamma_{esc.\ 1}(E_i) = \frac{\hbar v_i}{2R} T_1 \qquad \text{III (9)}$$

and hence that

$$\frac{\sigma(E_p)}{\sigma_r} = \frac{2}{3}\sqrt{\frac{2}{M}}\frac{\tau_c}{V} E \sigma_c \frac{\rho(E_i)}{\sqrt{E_i}} \qquad \text{III (10)}$$

It is seen that eqn. III (10) is essentially the same as III (1) except that

$$\frac{\omega_R(E_R^*)}{\omega_C(E_C^*)} \left[\frac{MV(2ME_i)^{\frac{1}{2}}}{2\pi^2\hbar^3}\right]$$

has been replaced by $\rho(E_i)$. The former is the ratio of densities of initial and final states. The quantity in the square brackets is the density of states of the emitted particle. It is believed that our assumption is accordingly equivalent to one in which the density of final states is obtained from the instantaneous non-equilibrium groups of nucleons which subsequently relax to form the residual nucleus. The idea of a relaxation time long compared with the transit time of the nucleon through the nucleus is in agreement with length of the mean free paths associated with moderate absorption. It is also to be noted that in III (10), τ_c is now a measure strictly of barrier transmission factors i.e. it is defined by eqn. III (5) and hence the assumption of complete absorption of all particles passing through the barrier into the nucleus as required to ensure the proper inverse cross section in the detailed balance formula is no longer necessary.

(b) A Particular Model

The first order approximation for the compound nucleus (a mixture of weakly interacting particles obeying either Fermi-Dirac or Bose-Einstein statistics) is now used to evaluate $\rho(E_i)$ in eqn. III (10) and obtain "theoretical" values for cross-sections and energy spectra in nuclear reactions. We use the usual theory (see for example Land, 1955) for gases in thermal equilibrium at temperature T.

In general

$$\rho(E_i) = g\, 2\pi V \left(\frac{2M}{h^2}\right)^{3/2} \epsilon^{\frac{1}{2}} \exp. \left[\frac{-(\epsilon - \mu)}{T}\right] \qquad \text{III (11)}$$

where $\exp.\left[\frac{\epsilon - \mu}{T}\right] \gg 1$. μ is the free energy per particle and ϵ is the particle energy measured from the lowest level of this type of particle in the nuclear well.

We now define E_B as the depth into the well to the top of the unexcited distribution and E_o as the height from the bottom of the nuclear well to the bottom of the unexcited distribution for each type of particle in the nuclear well. Then

$$E + E_B = \epsilon - \mu_o \; ; \quad \epsilon = E_i - E_o$$

where μ_o is the value of μ at T = 0. μ_o = 0 for particles obeying Bose-Einstein statistics and μ_o = the "Fermi Energy" for particles obeying Fermi-Dirac statistics. Substituting these relations into eqn. III (11) and then inserting the values of $\rho(E_i)$ obtained into eqn. III (10) gives the following general expression for $\sigma(E)$ applicable to all types

of particles for this particular model

$$\frac{\sigma(E)}{\sigma_r} = \frac{16}{3}\frac{g^M \tau_c}{\pi^2 \hbar^3} E \sigma_c (1 - E_o/E_i)^{\frac{1}{2}} \exp.\left[- F(N) + \frac{E_B}{T} + \frac{E}{T}\right] \quad \text{III (12)}$$

In eqn. III (12), N is the number of particles, of the type emitted, of mass M in the compound nucleus and for Fermi particles,

$$F(N) = \frac{\mu_o - \mu}{T} = (0.825\ T/T_o + 1.22\ (\frac{T}{T_o})^3 + - - -) \quad \text{III (13)}$$

where $T_o^{3/2} = \frac{188N}{AM^{3/2}}$, and exp. $\left[- F(N)\right] \to 1$ as $T \to 0, (< T_o)$

For "Bose" particles,

$$F(N) = \frac{\mu_o - \mu}{T} = \log\left[\frac{1}{2.2126}\ (\frac{T}{T_o})^{3/2}\right] + 0.923\ (\frac{T_o}{T})^{3/2} + 0.034(\frac{T_o}{T})^3 + - - - \quad \text{III (14)}$$

where $T_o^{3/2} = \frac{110N}{AM^{3/2}}$; and exp. $\left[-F(N)\right] = 1$ when $T < T_o$

(In the expressions for T_o, A and M are in A.m.u., T_o is in Mev.)

A completely general expression for the temperature T as a function of E_c^* is difficult to obtain but the following relations are applicable in the limits indicated -

For "Fermi" particles -

$$E^*\ F.D = \frac{\pi^2}{4}\frac{NT^2}{T_o}\ (1 - \frac{6}{40}\ \pi^2\ \frac{T}{T_o} + - - -);\ T < T_o \quad \text{III (15)}$$

$$E^*\ F.D = \frac{3}{2}\ NT;\qquad T >> T_o$$

For "Bose" particles

$$E^*_{B.E} = 0.77\ NT\ (\frac{T}{T_o});\ T \leq T_o \quad \text{III (16)}$$

$$E^*_{B.E} = \frac{3}{2}\ NT\ (1 - 0.462\ (T_o/T)^{3/2} - 0.0225\ (T_o/T)^3 + - -);\quad T > T_o$$

where $E_C^* = E_{B.E}^* + E_{F.D.}^*$

The calculation of the most probable mass distribution is not carried out here but we would like to draw attention to the similarity between this problem and the equilibrium theory of the natural abundance of the elements. In the equilibrium theory it is assumed that the elements were formed in an assembly of fundamental particles at a high temperature and density, and expressions are obtained (Ter Haar, 1954, Chap. XIV) for the mass distribution in such an assembly. Although the density of the compound nucleus is considerably higher than that required in the equilibrium theory to explain the natural abundance of the elements the temperatures are similar and it might be expected that a calculation of the mass distribution in the compound nucleus will result in a distribution which decreases rapidly with particle mass. If this result were obtained, it would suggest that in the gas model used here, the gas is mainly a Fermi gas of neutrons and protons plus increasingly smaller numbers of particles with increasing mass.

At a given nuclear temperature the principal factor governing the yield of a particular particle is $e^{-F(N)}$. In order that the yield be appreciable the population N for this particle must be sufficiently large that F(N) will not diverge much from zero. As an example a very approximate calculation has been made. If T = 1.5 Mev. and A = 60 A.M.U., then $F(N) < \frac{1}{2}$

required N to exceed $1\frac{1}{2}$ for neutrons or protons, 1 for deuterons, 8 for He^3 or H^3 and 20 for Li^5 and He^5. Since the population falls with increasing M it is seen that the evaporation cross sections vary rapidly diminish as M exceeds a few A.M.U. The alpha and deuteron values are lower because they are Bose particles. Deuteron emission is probably relatively much smaller than indicated here because of its unusually small binding energy.

III. 2. THE MEASUREMENT OF THE CROSS SECTION FOR PROTON EMISSION AS A FUNCTION OF PROTON ENERGY FROM SEVERAL ISOTOPES AT DIFFERENT EXCITATION ENERGIES

(a) Introduction

The first studies of the (n,p) reactions induced by fast neutrons were made by Waffler (1950) and by Paul and Clarke (1953) who obtained values of the total cross section by measuring the activity of the residual nuclei. However, if the emitted protons can be detected and their energy measured more direct and detailed information is obtainable. Nuclear emulsions have been used for this purpose by several authors (Allan, 1957, Brown et al, 1957, March and Morton, 1958 a,b) but the time required for scanning the emulsions and measuring the proton tracks has severely restricted the number of different targets studied and the statistical accuracy obtained.

Fairly recently Colli et al (1958) have shown that scintillation counters can be used successfully in measure-

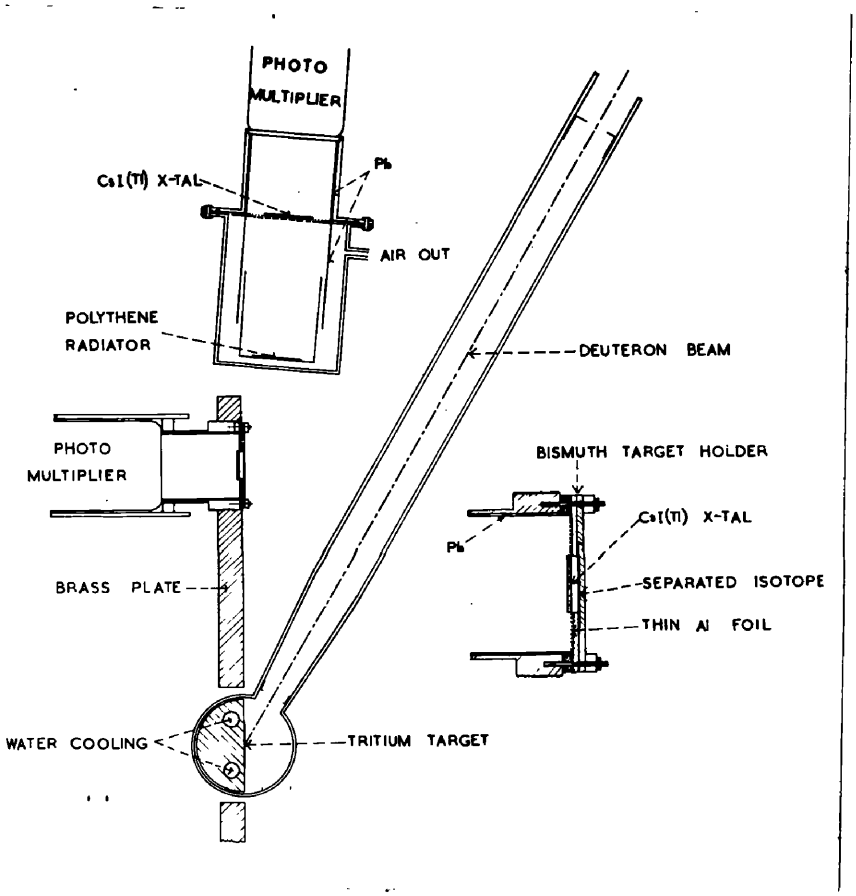

Fig. III. 1 Apparatus used for measurements of proton energy spectra from n,p reactions.

Inset - Crystal - Target assembly, twice scale.

ments on fast protons from targets bombarded by 14 Mev. neutrons. This technique required rather large areas of separated isotopes, and the full use of available intensities of neutron fluxes is apparently prevented by a relatively large random rate of coincidences. A technique similar to that of Colli has been described by Jack (1958) which avoids these difficulties, but both techniques have really been developed to estimate the contribution of "direct" effects in reactions by measuring proton energy spectra at small forward angles. The technique which is described here has been developed to measure directly the energy spectra and cross sections averaged over almost a 4π geometry. Small forward angles are avoided, and it is therefore hoped that the measured energy spectra correspond closely to the emission of particles from compound nuclei formed by capture of the incident neutron.

(b) Experimental Method

Fig. III. 1 is a diagram of the apparatus used for measurements of cross sections and energy spectra of protons in (n,p) reactions at incident neutron energies of 13.0 and 15.7 Mev. Measurements were also made at 14.1 Mev. and in this case the brass screening plate was 7.5" long, that is twice as long as that shown in Fig. III. 1. It will be seen that the purpose of the apparatus is to attenuate the neutron flux reaching the CsI(Tl) crystal used to detect protons from n,p reactions in the completely exposed separated isotope target, without introducing too large a gap between the two.

To avoid slow changes in relative positions, the apparatus was made very rigid, but the apparatus can rotate with respect to the deuteron beam in order to give a range of neutron energies, and the position of the complete crystal-target assembly (shown enlarged in the inset of Fig. III. 1) can be varied in a direction perpendicular to the parallel planes containing the CsI(Tl) crystal, separated isotope target, brass plate and tritium target. For the latter movement, the crystal-target assembly had fine screw threads on the rim which fitted into corresponding threads in the brass plate; by rotating the assembly the crystal and the separated isotope target were moved at a fixed distance from each other an accurately known distance into the brass plate.

The CsI(Tl) crystals were obtained from the Harshaw Chemical Co. Ltd. The thickness of the crystals used were chosen as a compromise between edge effects for the highest proton energies and the achievement of a low background rate. At 14.1 Mev. the crystal was 0.035" thick and at 13.0 and 15.7 Mev. the crystal was 0.045" thick. In the experiments, the crystal was mounted quite rigidly with 0.005" platinum wire at a distance of 1.6" from the glass top of the Du Mont 6292 photomultiplier, primarily to avoid background due to (n,p) reactions in the glass, but we have also found that this improves the energy resolution (probably because of non-uniform response across the photomultiplier cathode). Also to reduce background, the brass outer casing around the crystal was lined with thin lead. A very thin layer of aluminium was

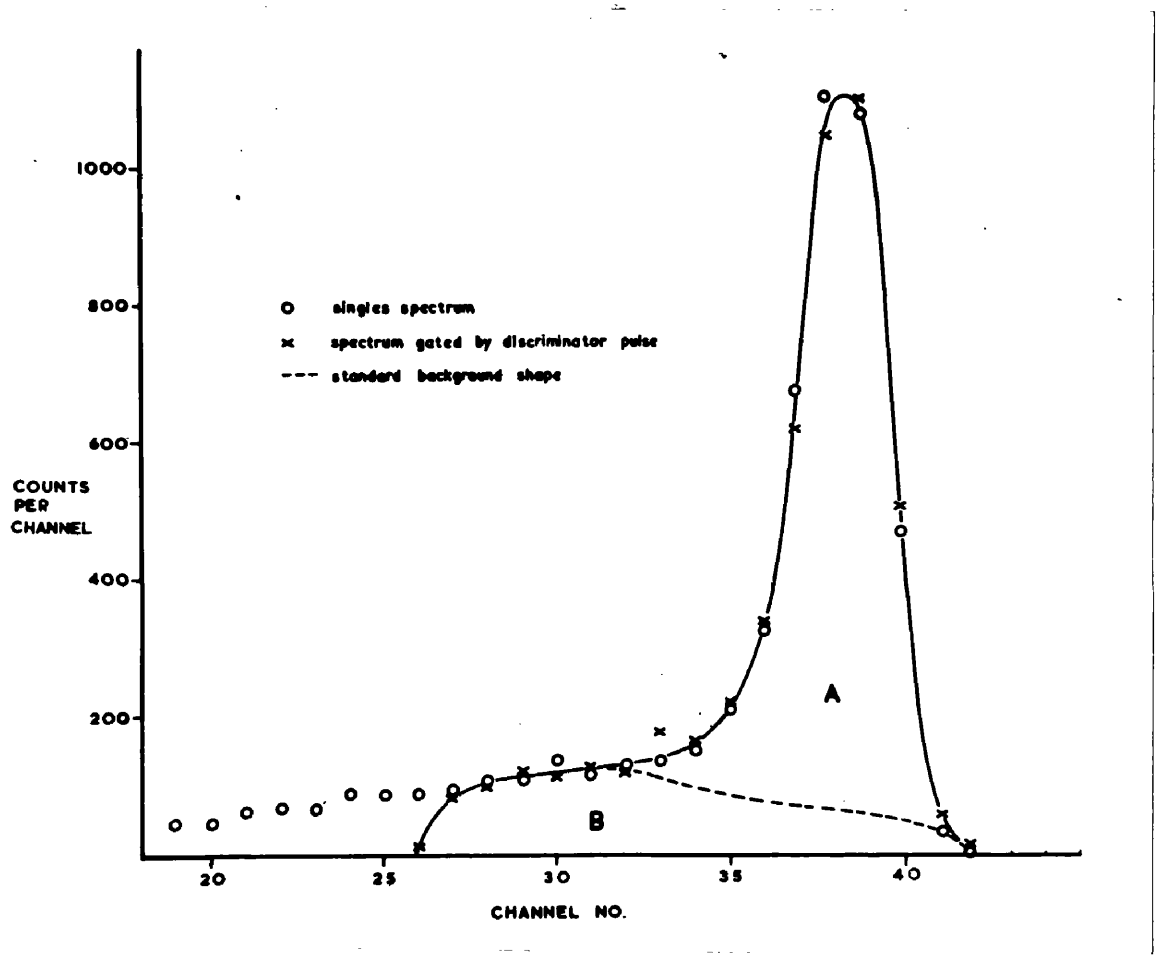

Fig. III. 2 Pulse height distributions in monitor.

The background shape is obtained by removing the radiator.

The ratio $\frac{A}{A+B}$ was evaluated from these curves and used as a factor in calculating the absolute efficiency of the monitor.

evaporated onto the surface of the lead and a very thin aluminium foil was placed immediately behind the crystal, to act as light reflectors. Platinum was used as the backing material for the separated isotope target which was clamped between a ring and a disc of bismuth to achieve rigidity and maintain a low background. To change targets, the target holder was removed as a unit from the crystal-target assembly and replaced accurately in the same position relative to the crystal. In the experiments the gap between crystal and target was kept fixed at 2 mm.

The neutron monitor shown in Fig. III. 1 was designed to correspond to the accurate computations of Bame et al (1957) which allowed us to obtain absolute values for the (n,p) cross sections. A typical pulse height distribution for 14 Mev. neutrons is shown in Fig. III. 2 and it can be seen that the peak due to knock-on protons from the polythene radiator gives this type of monitor a high stability. The air was removed to avoid a small background due to (n,p) and (n,d) reactions in nitrogen. As in the (n,p) detector the use of very heavy elements is required in order to give a sufficiently low background.

Before carrying out measurements of (n,p) spectra, the apparatus was checked and the best position of the crystal-target assembly obtained, relative to the brass plate, by observing the number of counts in the CsI(Tl) crystal for a fixed neutron monitor count as the crystal-target assembly was rotated. A typical result is shown in Fig. III. 3, the

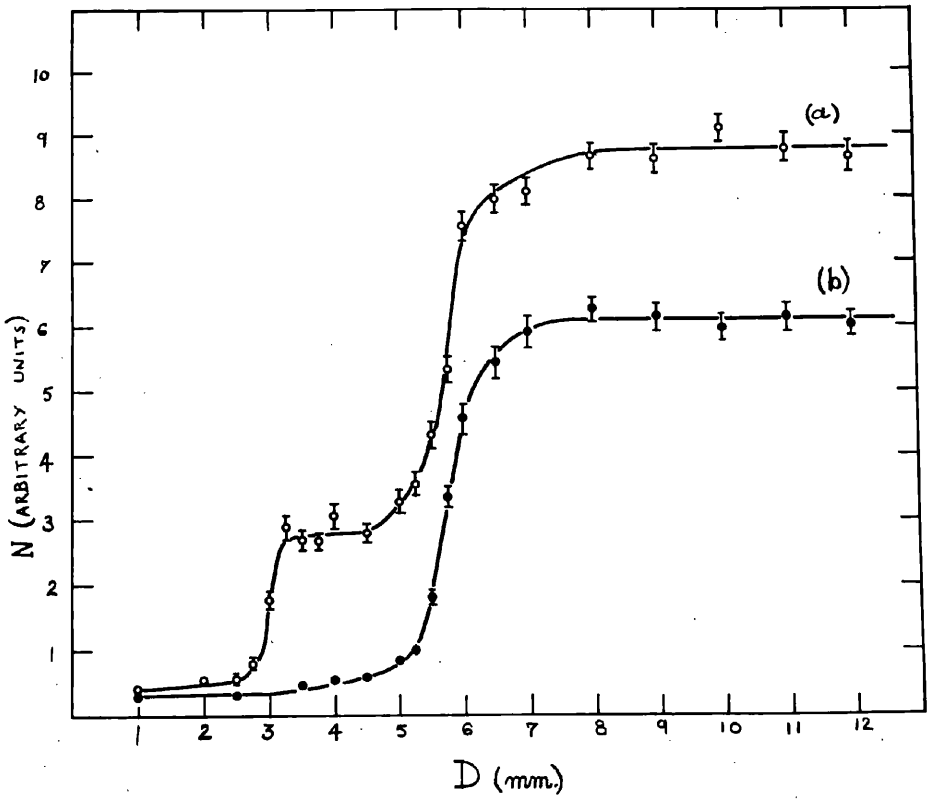

Fig. III. 3 N, the number of counts corresponding to all protons of energy $\gtrsim 8$ Mev., for a fixed number of monitor counts, plotted as a function of the position of the crystal with respect to the brass plate. The zero of the abscissa scale is not significant.

zero of the abscissa scale is not significant. The curve labelled b was obtained for no target, and the curve labelled a for a 15 mg/cm^2 target of ^{58}Ni. The bias on the scalar recording counts was set at approximately 8 Mev. No appreciable change was found in the positions of the edges when these runs were repeated, and a position about halfway along the lower plateau in curve (a) (D = 4 mm.) was chosen for the experiments. Fig. III. 3 was obtained for the longer brass plate. Defining the attenuation as the ratio of the ordinates at D = 1 mm. and D = 8 mm. in curve b, the attenuation of the plate 7.5" long was 20:1 and of the plate 3.75" long about 3:1. The flat plateaus observed in figure 3 show that there is little evidence of appreciable scattering by the brass plate increasing the neutron flux above that measured on the monitor. The rounding off of the edges is attributed to residual misalignment of the planes containing the crystal, brass plate and tritium target. Much of the width in the edge of the curves is due to the finite thickness of the CsI(Tl) crystal.

The separated isotope targets were obtained from Harwell A.E.R.E. and were all about 15 mg/cm^2 mounted on a 0.0005 inch platinum backing. Preliminary runs using platinum foils were made to ensure that the background remained unchanged when the platinum foil was inserted into the target holder. Three runs were made at each neutron energy for the targets ^{54}Fe, ^{58}Ni, ^{64}Zn, and three runs were made at 14.1 Mev. for ^{27}A , ^{54}Fe, ^{56}Fe, ^{58}Ni, ^{59}Co, ^{60}Ni, ^{63}Cu, ^{64}Zn and ^{65}Cu. Each

run required about half an hour and between runs the gain of the photomultiplier was checked using a ^{137}Cs source of gamma rays. The position of the peak in the neutron monitor was frequently checked. The results of each run were first plotted separately to check for consistency, then averaged. The background was measured six times at intervals between measurements for the same neutron flux as in each of the target runs, and each background was plotted separately before they were all averaged. The pulses from the photomultipliers were clipped to 2 μs, amplified and the pulse height distributions measured on a 100 channel pulse height analyser. Pulses from the monitor were fed to a rate meter so that the neutron flux could be maintained constant. The neutron energies 13.0 and 15.7 Mev. were obtained by making measurements at forward and backward angles to the incident deuteron beam at 600 Kev. The neutron energy of 14.1 Mev. was obtained by making measurements at 90° to the incident deuteron beam at 160 Kev. The thickness of the tritium targets used was about 70 Kev. at both energies; the corresponding spread in neutron energy was about 0.1 Mev. Beam currents were of the order of 100 μ amps on the tritium target which was 1" in diameter. All the runs at 14.1 Mev. were made using the same tritium target and the neutron yield remained at about 5.10^9 neutrons per sec into 4π . The end points of the (n,p) spectra were not used to calibrate the crystal. Instead, an independent calibration was made using proton groups from the

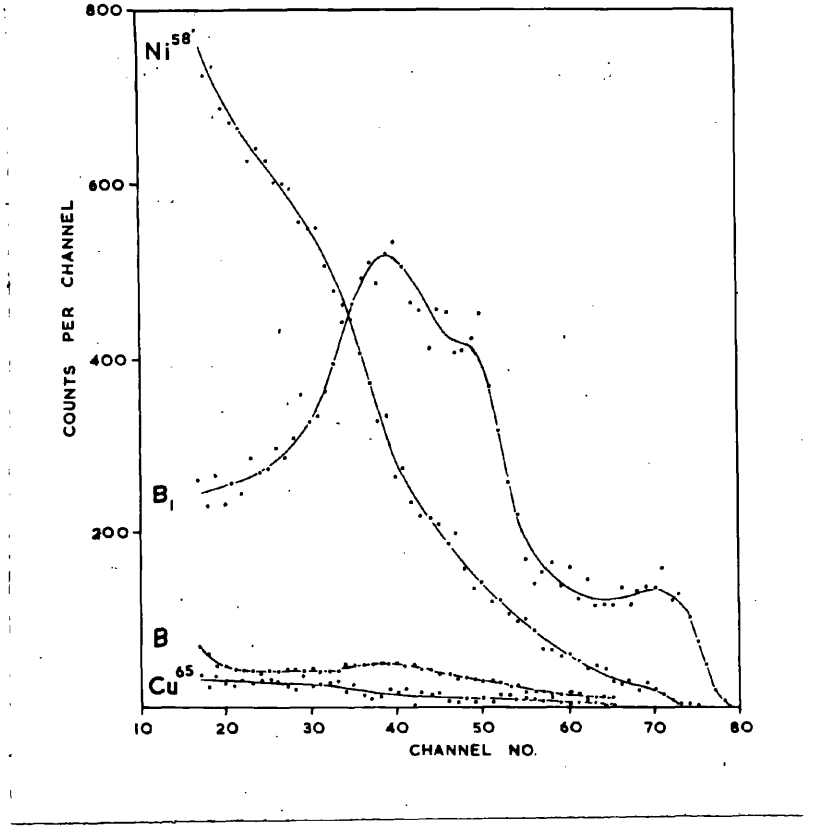

Fig. III. 4 Typical pulse height spectra for the longer screening plate. B denotes the normal background during the experiment. B_1 is the background with the CsI(Tl) crystal unscreened. The channel number is proportional to the proton energy loss in the scintillator and channel 75 is equivalent to 15 Mev.

reactions $^{3}He(d,p)^{4}He$, $^{10}B(d,p)^{11}B$, and $^{2}H(d,p)^{3}H$. It was found that the response of the crystal was linear over the range of proton energies measured in the n,p spectra and the calibration was used to check for consistency by comparing the measured and expected Q values for the n,p reactions.

The yield of pulses per voltage channel for E_n = 14.1 Mev. and 40,000 monitor counts (a typical run) is given in Fig. III. 4 in order to show the shape of the background and its size relative to the spectra from the separated isotope targets. The spectra of ^{58}Ni and ^{65}Cu (with background subtracted) were chosen for display because the yields were the greatest and the least respectively from the targets used. The background for D = 9 mm. (see Fig. III.3) is also shown to illustrate the improvement due to screening. The most of background is caused by the reactions in nitrogen and (n,α) reactions in CsI(Tl) and hence further improvements would require evacuation of the chamber and use of a screen with a greater attenuation factor.

(e) Results and Discussion

The results of measurements of energy spectra at 14.1 Mev. are shown in Fig. III. 5, in which for convenience the ordinates of the curves are arbitrarily displaced. The points shown have been corrected for small effects due to finite thickness of the separated isotope target and the CsI(Tl) crystal.* $\sigma(E)/E\,\sigma_c$ is the cross section per unit energy divided by the barrier transmission factor. The values of σ_c

*The corrections to the cross sections for these geometrical effects are discussed in detail in Appendix A.

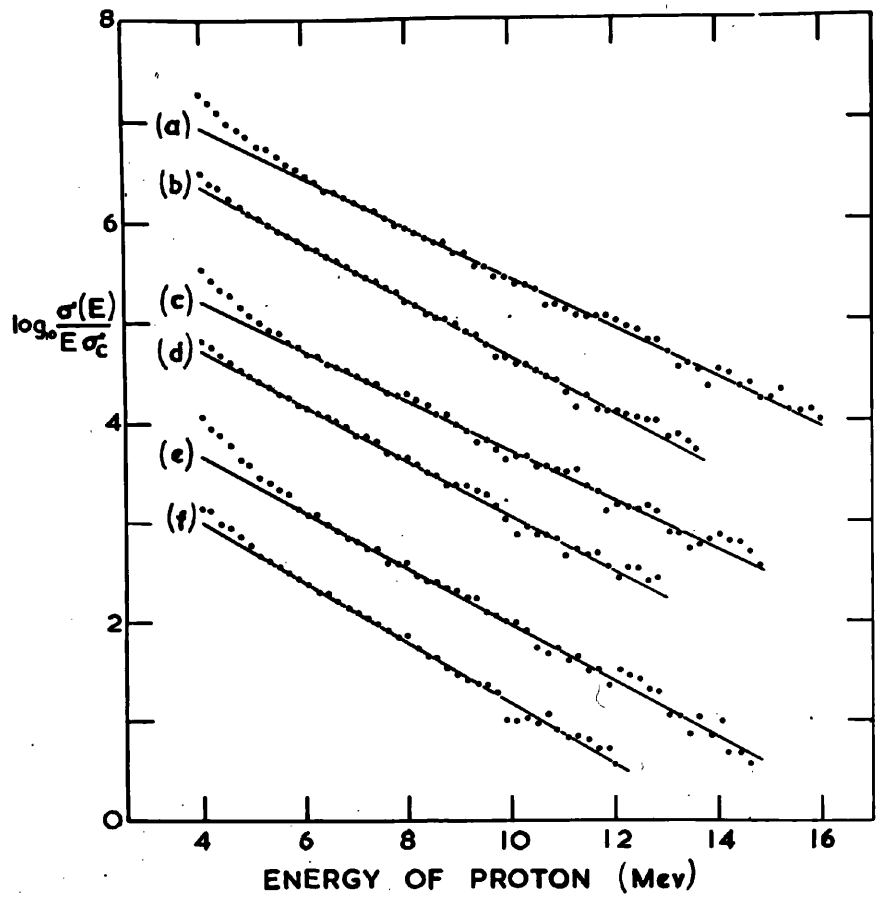

Fig. III. 6 The modified (n,p) spectra for E_n = 12.9 and 15.7 Mev.

(a) ^{58}Ni E_n = 15.7 Mev.

(b) ^{58}Ni E_n = 12.9 Mev.

(c) ^{54}Fe E_n = 15.7 Mev.

(d) ^{54}Fe E_n = 12.9 Mev.

(e) ^{64}Zn E_n = 15.7 Mev.

(f) ^{64}Zn E_n = 12.9 Mev.

The curves are displaced arbitrarily with respect to the ordinate scale for convenience.

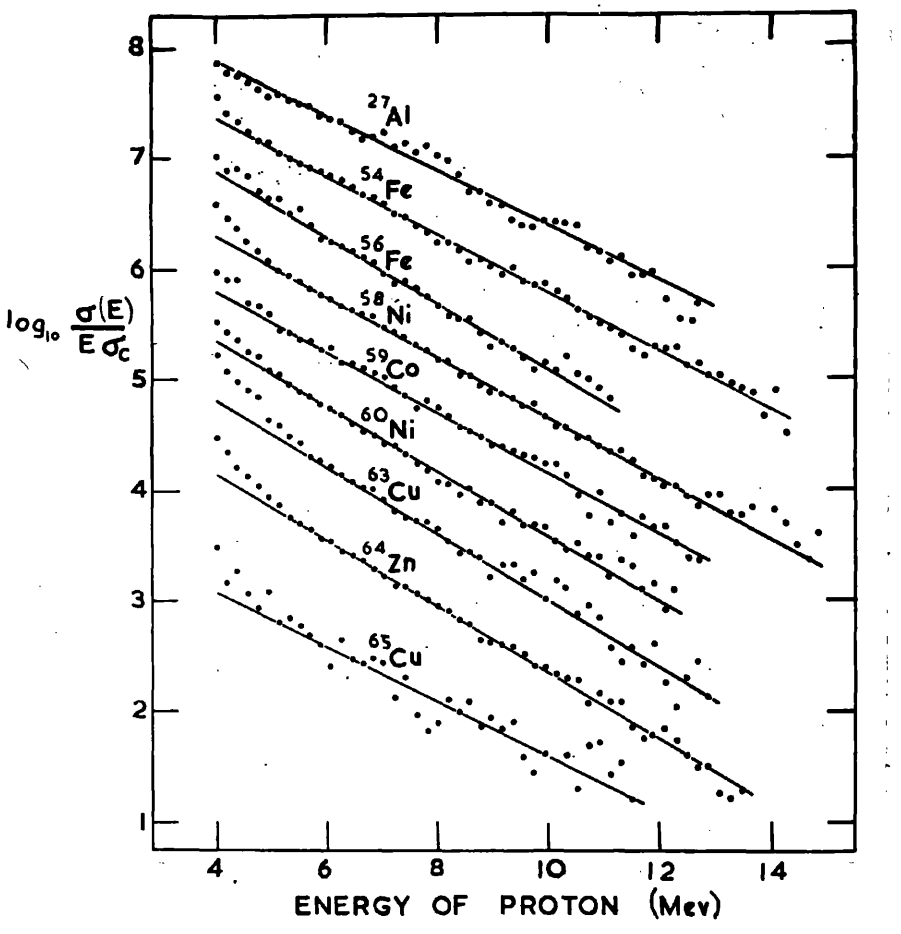

Fig. III. 5 The modified (n,p) spectra for E_n = 14.1 Mev. The curves are displaced arbitrarily with respect to the ordinate scale for convenience.

were obtained from the tables of Blatt and Weisskopf (1952), using a value for $r_o = 1.5\ 10^{-13}$cm. E is the energy of the emitted proton. The measured energy spectra at 13.0 and 15.7 Mev. are shown in Fig. III. 6 and again the ordinates of the curves are displaced arbitrarily. The full lines in Fig. III. 5 and III. 6 are the best straight lines which can be drawn through the points above about 6 Mev. The temperatures T of the compound nuclei shown in table III. 1 were obtained from the reciprocals of the slopes of these lines. The values of the integrated cross sections $\sigma(n,p)$ in table III. 1 were obtained by extrapolating the straight lines in Fig. III. 5 and III. 6 back to zero proton energy, and assuming that the angular distribution of the protons in (n,p) reactions is isotropic. The rise in the experimental points above the straight line below 6 Mev. proton energy is attributed at least partly to the reaction (n,np). The relative errors in the values of $\sigma(n,p)$ in table III. 1 at the same neutron energy are about $\pm$ 5% but the absolute value of the cross sections may be in error by as much as $\pm$ 20% due mainly to uncertainty in the absolute efficiency of counting protons from the targets. The errors in the values of T are only about $\pm$ 3% if the barrier transmission factor is not grossly wrong.

For each value of T in table III. 1 there is a corresponding value of the excitation energy E_c^* of the compound nucleus formed in the reaction. If the range in E_c^* were wide enough the nuclear equation of state could be found directly

Table III. 1

Target Isotope		Al^{27}	Fe^{54}	Fe^{56}	Ni^{58}	Ni^{60}	Co^{59}	Cu^{63}	Cu^{65}	Zn^{64}
T(Mev)	E_n=13.0		1.58		1.54					1.42
	E_n=14.1	1.75	1.65	1.45	1.575	1.48	1.59	1.44	1.76	1.45
	E_n=15.7		1.76		1.74					1.54
E_c^*(Mev)	E_n=13.0		22.24		21.94					20.87
	E_n=14.1	21.80	23.37	21.71	23.07	22.60	21.56	21.98	21.07	22.00
	E_n=15.7		24.96		24.66					23.59
σ(n,p)	E_n=14.1	90	333	90	534	158	75	149	30	257
in mb.	E_n=15.7		561		754					344

for each compound nucleus, according to the general solution (eqn. III (10). Since this is not possible we compare the experimental values of T with the particular model chosen in section III. 1 since this gives some relation between values of T for different compound nuclei.

Since the values of T in table III. 1 are fairly close to those expected from a pure Fermi gas of neutrons and protons only, the nuclear equation of state obtained from eqn. III (15) and III (16), Part I is:

$$E_c^* = \frac{\pi^2 N}{2} \frac{T^2}{T_o} + \frac{3}{2} nT \qquad \text{III (17)}$$

where N = number of neutrons or protons, assumed equal, and n = total number of other types of particles, assumed small. We also assume that the mass distribution inside the compound nucleus is such that the number of particles of a given mass

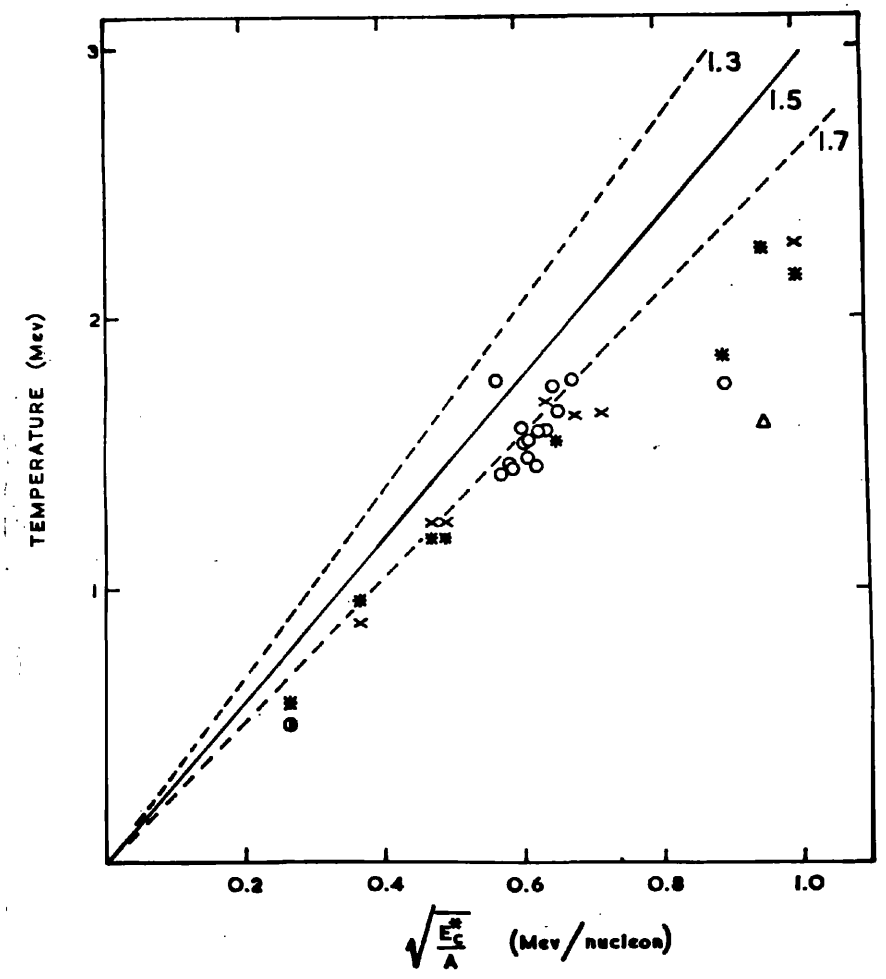

Fig. III. 7 The energy spectra from different nuclear reactions are fitted to the formula $\frac{\sigma(E)}{E\,\sigma_c} \propto e^{-E/T}$ The temperatures T obtained are plotted as a function of $(E_c^*/A)^{\frac{1}{2}}$ where E_c^* is the excitation energy of the compound nucleus and A is the mass number. The full line is the temperature predicted for a pure Fermi gas with radius parameter $r_o = 1.5 \times 10^{-13}$ cm. The broken lines correspond to $r_o = 1.3$ and 1.7×10^{-13} cm. ○ - present work n,p; × - Gugelot p,p'; △ Zucker $^{27}A + ^{14}N$; ◑ - Sargent and Bertozzi γ,n. ✱ Temperature predicted for a nucleus consisting of neutrons and protons and four other particles when $r_o = 1.5 \times 10^{-13}$ cm.

decreases rapidly with increasing mass of the particles.

If n = o, eqn. III (17) reduces to the usual expression for a Fermi gas of neutrons and protons only -

$$E_c^* = \frac{AT^2}{f} \qquad \text{III (18)}$$

where $f \approx 8.8$ Mev. if $r_o = 1.5\ 10^{-13}$ cm.

The filled in circles in Fig. III. 7 are the values of T in table III. 1, the full line is the theoretical value corresponding to eqn. III (18) (the dotted lines correspond to eqn. III (18) if $r_o = 1.3$ and $1.7\ 10^{-13}$ cm.) and the asterisks are approximate theoretical values obtained from eqn. III (17) if n = 4. Clearly the introduction of small numbers of light particles other than neutrons or protons has the effect of lowering the theoretical values to the experimental points.

The value of $r_o = 1.5\ 10^{-13}$ cm. is the value used to obtain the barrier transmission factor σ_c for a square well (as defined in section III. 1) which gave a good fit to the measured energy spectra. However, it is known from the electron scattering experiments of Hofstadter (1956) and theoretical estimates (see for example Brueckner, 1955) that the effective nuclear volume corresponds to a somewhat smaller value of r_o than is used to obtain σ_c. The theoretical lines in Fig. III.7 will therefore have steeper slopes and the values of n will be somewhat higher although never very large. Clearly the concept of having other types of particles inside the compound nucleus in the theory section III. 1, which is necessary to explain the emission of such particles (e.g. deuterons or alphas) is also

useful in explaining the fact that the experimental temperatures are less than those expected for a pure Fermi gas of neutrons and protons.

To compare the experimental values of $\sigma(n,p)$ in table III. 1 with the theory, eqn. III (12), is integrated to obtain:

$$\frac{\sigma(n,p)}{\sigma_r} \propto T^2 \bar{\sigma}_p \exp\left[-\frac{1}{T}(B_p + P_p)\right] \qquad \text{III (19)}$$

where

$$\int_0^{E\,max} E\,\sigma_c\, e^{-E/T} dE = \bar{\sigma}_p \int_0^{\infty} E\, e^{-E/T} dE = T^2 \bar{\sigma}_p$$

Carrying out the corresponding integration for the emission of neutrons from the same compound nucleus, and using the approximation that the integrated cross section for emission of neutrons, $\sigma(n,n^1)$ equals $\sigma_r - \sigma(n,p)$ we obtain the relation:-

$$\frac{\sigma(n,p)}{\sigma(n,n^1)} \approx \frac{(n,p)}{\sigma_r - \sigma(n,p)} \approx \frac{\bar{\sigma}_p}{\bar{\sigma}_n} e^{-\frac{1}{T}\left[(B_p - B_n) + (P_p - P_n)\right]} \qquad \text{III (20)}$$

In eqn. III (20), $\bar{\sigma}_p$, $\bar{\sigma}_n$ and T vary slowly for neighbouring isotopes and for the values in table III. 1 we can write

$$\log \frac{\sigma(n,p)}{\sigma_r - \sigma(n,p)} \approx \text{constant} - \frac{1}{T}\left[(B_p - B_n) + (P_p - P_n)\right] \qquad \text{III (21)}$$

In these equations B_p and B_n are the experimental binding energies of protons and neutrons in the compound nucleus, and P_p and P_n are the pairing energies which must be added to the experimental binding energies to make them coincide more closely to E_B defined above eqn. III (12). (P_p and P_n are not the actual pairing energies of the last proton and

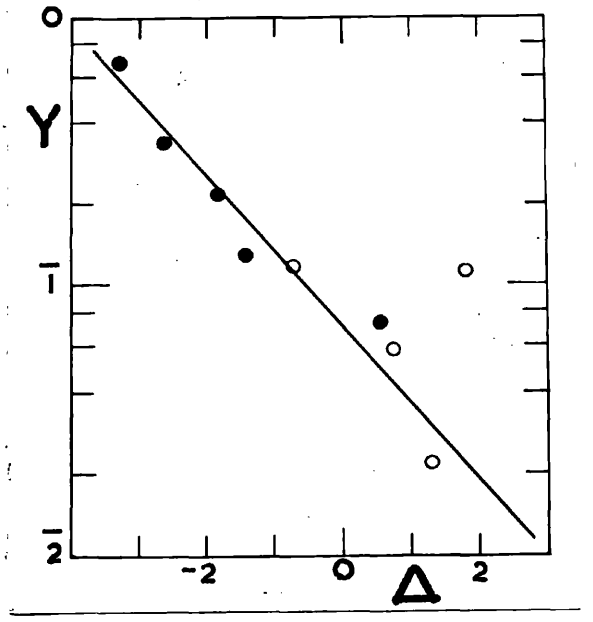

Fig. III. 8(a) $Y = \log_{10}\left[\sigma(n,p)/\ \sigma(n,n')\right]$ plotted as a function of Δ (in Mev.) = $B_p - B_N + P_p$ where B_p and B_N are the binding energies of a proton and a neutron respectively in the compound nucleus and P_p is related to the pairing energy. (see text)

● - target nucleus even-even.

○ - target nucleus odd-even.

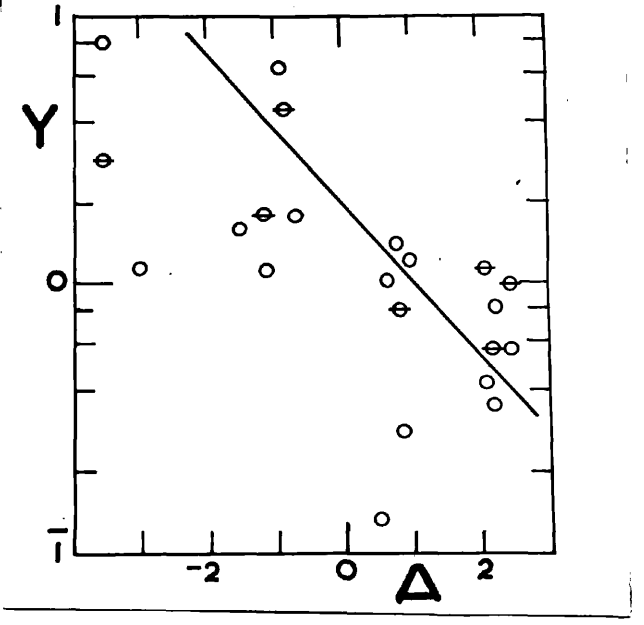

Fig. III. 8(b) $Y = \log_{10}\left[\frac{\sigma_1(n,a)}{\sigma_1(n,n')} \cdot \frac{\sigma_2(n,n')}{\sigma_2(n,a)}\right]$ plotted as a function of $\Delta = (B_{a1} - B_{n1}) - (B_{a2} - B_{n2})$ B_n and B_a are the binding energies of a neutron and an alpha particle in the compound nucleus; the (1) and (2) refer to two neighbouring nuclei. ⊖ Paul and Clarke (1), Forbes (2); ○ Paul and Clarke (1), Paul and Clarke (2); △ Conner (1), Forbes (2)

neutron but rather the lack of pairing energy relative to the other neutrons and protons).

From eqn. III (21), table III. 2 has been constructed giving the ratio of the terms $\exp\left[-\frac{1}{T}(P_p - P_n)\right]$ for different types of compound nuclei and the corresponding residual nuclei in (n,p) reactions, using values of T = 1.5 Mev. and $P_p = P_n = 2$ Mev. The latter was the average value obtained by comparing our results with III (21). The "values" in brackets are taken from the survey of the available data on the apparent level density of residual nuclei, by Brown and Muirhead (1957). While Newton (1956) has shown that the empirical ratios of Brown and Muirhead can be reasonably explained by inserting the pairing energy into level density expressions used in applying the Weisskopf theory, it is very satisfactory that the theory presented in section III. 1 should also give an explanation of this effect on (n,p) reactions.

Table III. 2

Compound Nucleus		$-\frac{1}{T}(P_p - P_n)$		Residual Nucleus	
p	n			p	n
odd	even	1	(1)	even	even
odd	odd	3.6	(5)	even	odd
even	even	3.6	(5)	odd	even
even	odd	13	(12)	odd	odd

In figure III. 8(a) the measured values of $\sigma(n,p)$ in table III. 1 are plotted as $\log_{10} \frac{\sigma(n,p)}{\sigma(n,n')}$ against Δ, where Δ equals $B_p - B_n$ for odd-odd compound nuclei (open

circles), and equals $(B_p - B_n) + P_p$ for even-odd compound nuclei (full circles). The value of P_p, which is due to the pairing energy effect (see Part I) was obtained by letting $P_p = \frac{1}{2}B_p(A + p + n) + \frac{1}{2}B_p(A - p + n) - B_p(A + n)$ where $B_p(A + p + n)$, $B_p(A - p + n)$ and $B_p(A + n)$ are the binding energies of protons in the corresponding nuclei and A is the atomic weight of the target nucleus. The values of B_p and B_n where taken from the compilation of Way, (1955). The full line in Fig. III. 8(a) corresponds to a value of T = 1.55 Mev., the average of the values of T in table III. 2 obtained from the measured energy spectra. The agreement between theory and experiment in Fig. III. 8(a) is good, and can probably be made better by reducing the experimental error and evaluating the pairing energy term more accurately.

(d) Discussion of Similar Measurements

Since the theory presented in Part I is applicable to all reactions involving the formation of compound nuclei, we have selected some of the experimental results of others, and without changing the published values, have rearranged the material so that it can be compared more conveniently with the theory. We must point out that the values of temperatures T of the compound nuclei are those obtained by us, and are not stated by the various authors whose published work we have used in drawing up Fig. III. 8(b), III. 9, and III. 10.

Fig. III. 8(b) has been obtained from absolute cross sections for (n,α) reactions at an incident neutron energy of

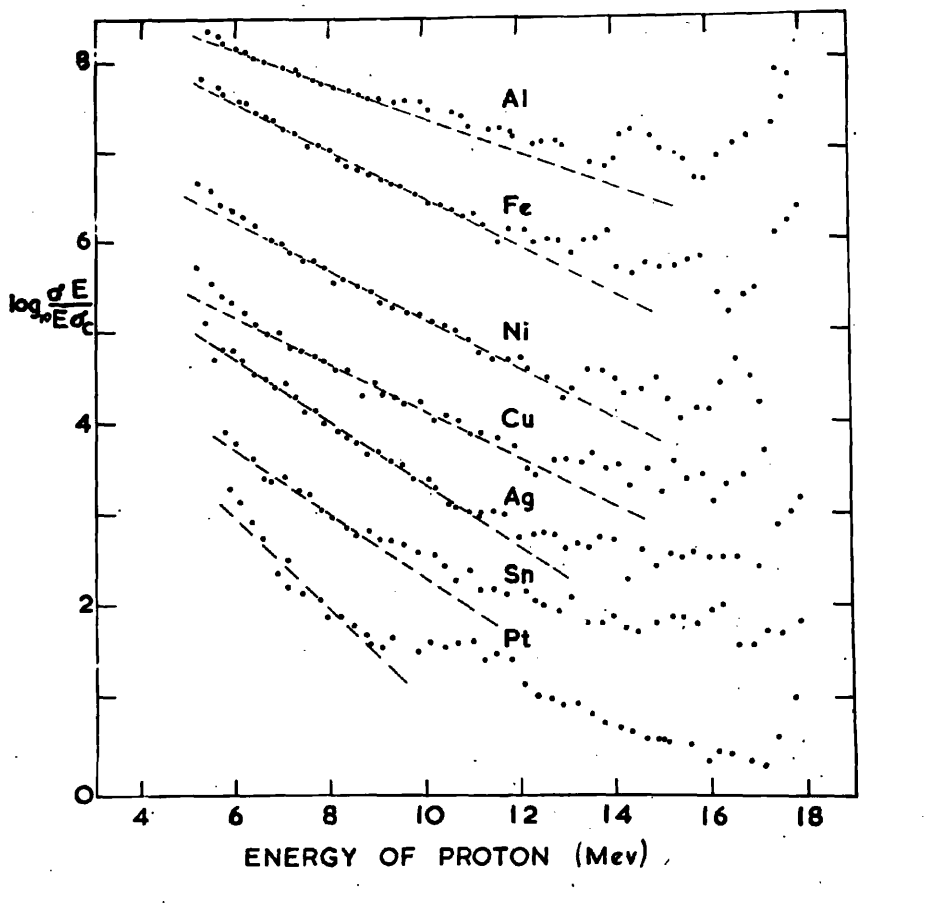

Fig. III. 9 The modified (p,p') spectra for E_p = 18.2 Mev. as obtained from the measurements of Gugelot (1954). The curves are arbitrarily displaced with respect to the ordinate scale.

14 Mev. by Paul and Clarke (1953), Forbes (1952) and Conner (1953). We find a theoretical relationship between the values, which cover a wide range in the periodic table, in the same way as was used to derive eqn. III (20): i.e.

$$\frac{\sigma(n,\alpha)}{\sigma(n,n^1)} \approx \frac{\sigma(n,\alpha)}{\sigma_r - \sigma(n,p)} \approx \frac{\sigma_\alpha}{\sigma_n} e^{-\frac{1}{T}(B_\alpha - B_n)} \qquad \text{III (22)}$$

where B_α is the experimental value of the binding energy of the alpha particle in the compound nucleus.

By taking the ratio to the nearest element for which an experimental value of $\sigma(n,\alpha)$ is available, the coulomb terms roughly cancel out and we obtain:-

$$\log \frac{\sigma_1(n,d)}{\sigma_1(n,n)} \frac{\sigma_2(n,n^1)}{\sigma_2(n,\alpha)} \approx \text{constant} - \frac{1}{T}\left[(B_{n1} - B_{\alpha 1}) - (B_{n2} - B_{\alpha 2})\right] \qquad \text{III (23)}$$

by neglecting the pairing energy terms for simplicity. In deriving eqn. III (23) considerably greater approximations have been made than for eqn. III (22) but it is doubtful whether it is worth being more precise at this time as there are considerable differences in published experimental values of (n,α) cross sections. For some of the points plotted in Fig. III 8(b), $\sigma(n,n')$ is equated to σ_r as we were unable to find a value for $\sigma(n,p)$. The full line in Fig. III.8b corresponds again to a value of T = 1.55 Mev. Despite the approximations and the experimental errors, there again appears to be reasonable agreement with the theory of section III. 1.

In Fig. III. 9 we have redrawn the measurements by

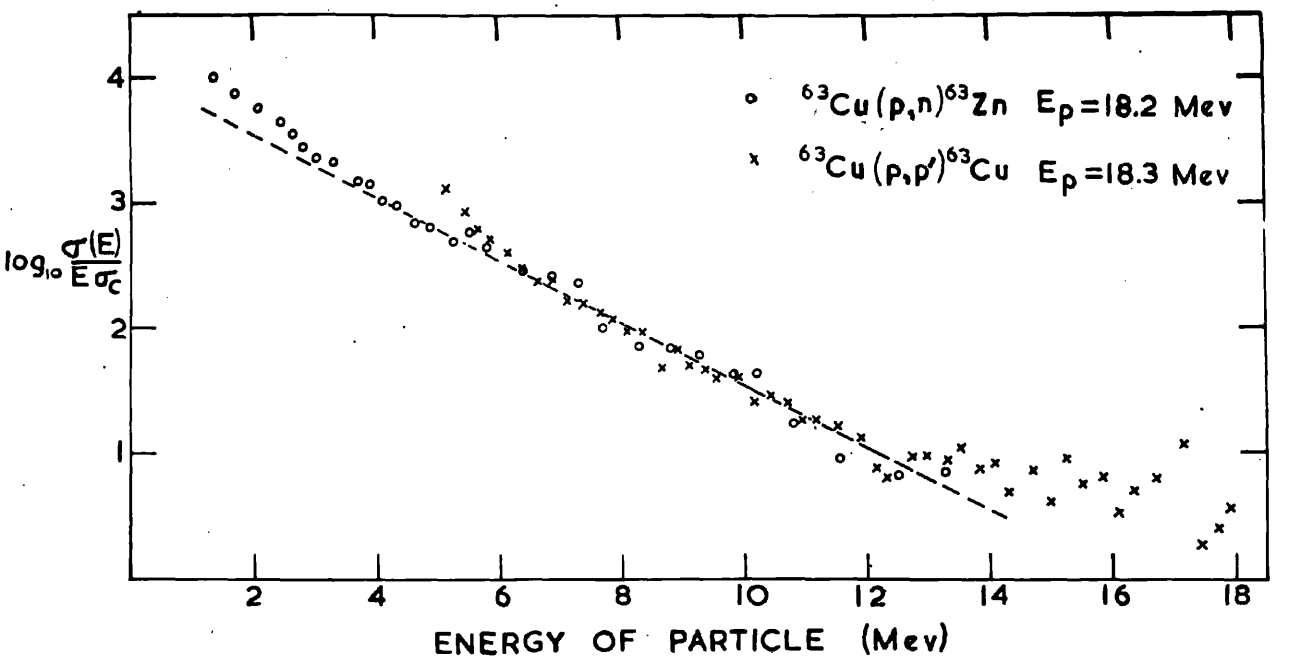

Fig. III. 10 Modified spectra obtained from the measurements of Gugelot (1954) and Thompson (1957)*

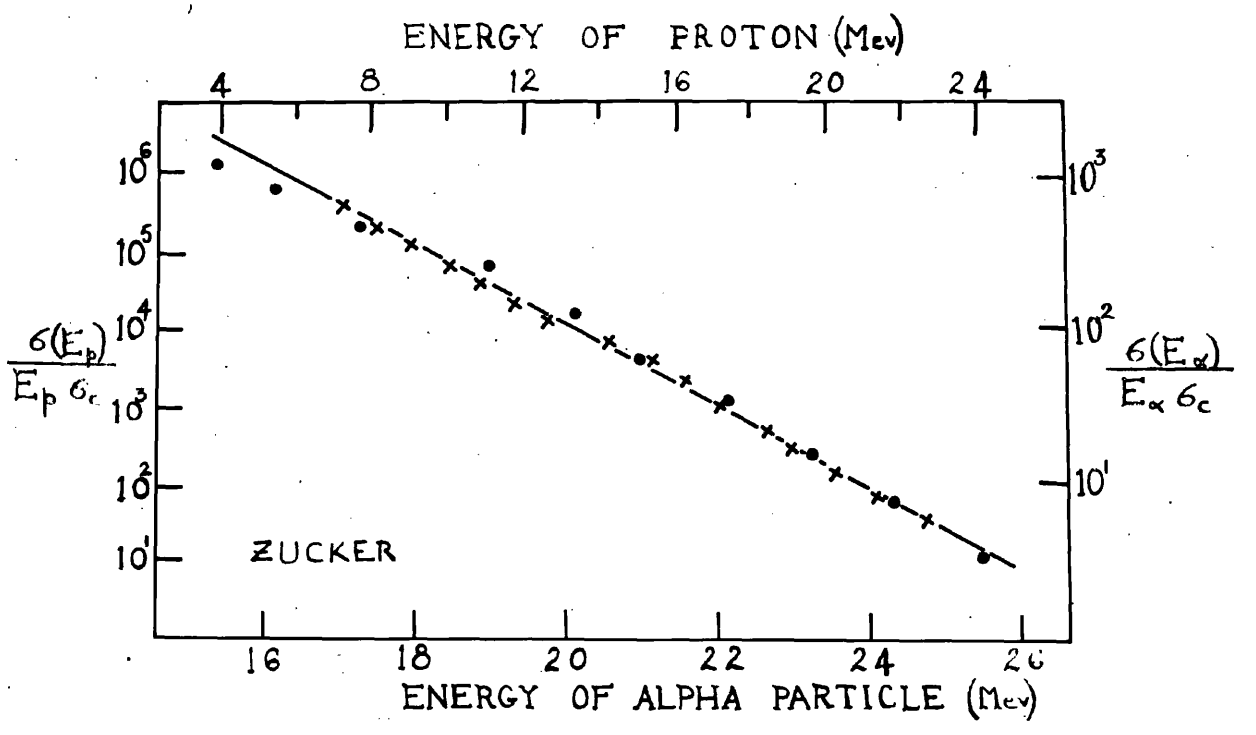

Fig. III. 11 Modified spectra obtained from the measurements by Zucker (1958) of the charged particle evaporation from Ca^{41}.* X - proton spectrum, ● - alpha particle spectrum

*The curves are arbitrarily displaced with respect to the ordinate scale.

Gugelot (1954) of proton spectra at 150° in (p,p') experiments at an incident proton energy of 18.2 Mev. Ignoring the direct effect (Cohen, 1957) at the higher emitted proton energies, we have obtained values of the temperatures T of the compound nuclei, and these are plotted as crosses in Fig. III. 7. The full lines in Fig. III. 9 have been drawn to obtain the temperatures, and the ordinates of the curves are arbitrarily displaced for convenience. While there is considerably more uncertainty in obtaining temperatures from (p,p') experiments due to the apparently greater contribution from the direct effect when the incident and emitted particle is the same, it can be seen from the crosses in Fig. III. 7 that Gugelot's results can be used to obtain temperatures similar to those found by us in (n,p) reactions.

In Fig. III. 10 we have redrawn the results of Gugelot (1954) and Thomson (1957) for Cu(p,p') and Cu(p,n) at incident proton energies of 18.2 Mev. and 18.1 Mev. respectively. As would be expected from the theory of section III. 1 the temperatures are the same when deduced from the parts of the spectra less likely to be affected by multiple particle emission or direct effects. The value of the temperature deduced from the straight line in Fig. III. 10 is also plotted in Fig. III. 7.

Zucker (1958) has measured the energy spectra of protons and alpha particles from ^{41}Ca at an excitation energy of 39.3 Mev. formed by bombarding ^{27}A with ^{14}N ions. We have plotted his results against emitted particle energy in Fig. III. 11 and again it will be noticed that the temperature of the compound nucleus is essentially the same when deduced from the spectra of either emitted particle. The value of the temperature obtained from Fig. III. 11 is plotted as a triangle in

Fig. III. 7 and is considerably lower than the values of temperature obtained from (n,p),(p,p') and (p,n) experiments. Possibly this is due to considerably greater "surface oscillations" occurring during the emission time in this type of reaction in which two large nuclei fuse together.

In Fig. III. 7 we have also included a value of T obtained from the energy spectra of Sargent and Bertozzi (1957) for the reaction (γ,n) in gold and tantallum. The value is shown by a half filled circle and appears to be consistent with the general trand of values obtained from other reactions.

(e) Application of the Detailed Balance Formula to Experimental Results

The analysis of the results presented here has been carried out in terms of the description of evaporation theory proposed in section III. 1. The desirability of the proposed formulae relative to the usual detailed balance formula of Weisskopf has also been discussed in the same section. However, some details of application of the later formula to experimental measurements have become apparent during this work and they will be discussed in the present section.

At first it should be pointed out that while the usual formula III (2) with assumption (c) removed is not adequate this may be because of assumption (a) i.e. $\omega(E^*)=e^S$. The author has shown that if the measured $\sigma(E_p)$ for a ^{58}Ni target is fitted to formula III (1) with $\omega_R(E^*) \propto (E^*_R)^{-2} \exp\left[2\left(\frac{\Delta E^*}{f_1}\right)^{\frac{1}{2}}\right]$ the level density parameter f_1 is well defined

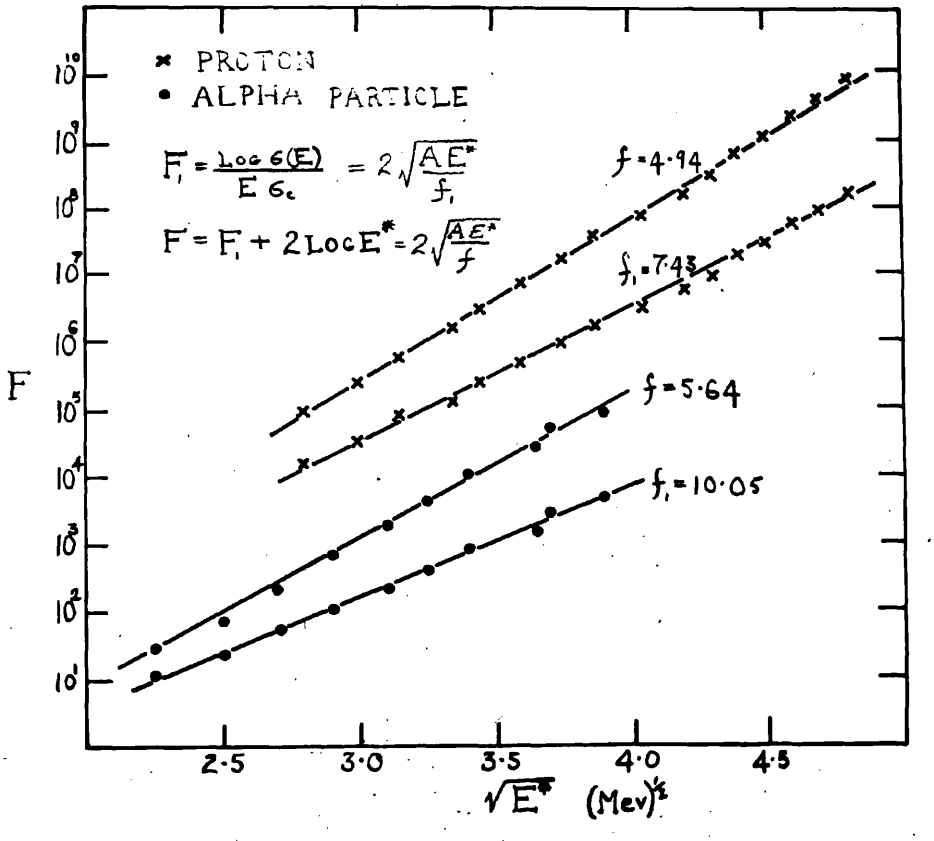

Fig. III. 12 An illustration of the method of obtaining the level density parameter by application of the detailed balance formula. The experimental data used is that of Zucker (1958) for evaporation from ^{41}Ca.

and equal to 10.3 Mev. in approximate agreement with Lang and Le Couteur (1954). Thus it is seen that the $(E_R^*)^{-2}$ variation is important. When this type of analysis is applied to the results of Zucker (1958) for the proton and alpha particle spectra from ^{41}Ca values of $f_1 = 7.43$ and 10.05 respectively are obtained. The latter results and the method of analysis as depicted in Fig. III. From this it appears that to test accurately the validity of inserting $\pi\lambda^2 \sum(2l + 1)T_l$ and $\omega_R(E_R^*)$ into the detailed balance formula it is necessary to show the existence of an adequate formula for ω as a function of E^*, A and other variables such as even or odd neutron and proton numbers i.e. a formula in which the coefficients f are constant. This seems to be possible only by the tedious method of successive approximation and fitting and will require revision as the range of E^* and A are extended. (See Lang and LeCouteur, 1954).

(f) Conclusions

The agreement between many experimental results and the theory presented in section III.I is sufficiently good to encourage the belief that the concepts of impulsive emission through a static nuclear surface barrier followed by a relatively long relaxation time for the residual nucleus to reach an equilibrium energy distribution, are valid in a description of the emission of particles from compound nuclei.

It is expected that further experimental results will be found to be consistently explained by reasonable modifications and

developments in the particular models used to obtain the equilibrium properties of compound nuclei and the probability of transmission of particular particles out through the surface berrier.

PART IV THE VARIATION OF THE DECAY TIME IN CsI (Tl) FOR PARTICLES OF DIFFERENT IONIZATION DENSITY

IV. 1 (a) Introduction

In the scintillation counter the light produced by an ionizing particle in the fluorescent material is converted by the photomultiplier into an electrical pulse with the same time variation. It is generally believed that the decay time of the fluorescence is independent of the nature of the radiation detected and therefore, that only information about the energy loss occuring can be derived from the pulse. For this reason, it is necessary, when the type of particle cannot be deduced with certainty indirectly, to measure pulse heights produced by the same particle in at least two separate scintillators. However, this usually results in an apparatus with much reduced efficiency. Accordingly, in many measurements of weak reactions the experimenter is often confronted with the difficult problem of choosing between a low statistical accuracy and an uncertain background.

In section III. 2 several spectra of protons from (n,p) reactions have been presented. In this particular experiment the nature of the particle being detected is fairly well established. However, in desirable extensions of the work this no longer remains true. In Fig. III. 4 the background is seen to rise as the channel number drops below 20 (which corresponds to the absorption of 4 Mev. protons in the scintillator). When spectra similar to those of Fig. III. 4, but at lower pulse heights,

were measured the background was observed to rise more rapidly and soon exceed the signal due to protons. This background is due to electrons. In another proposed extension of this work, the measurement of alpha particle spectra the number of proton pulses will greatly exceed that of alpha pulses. Because of the smallness of the total thickness of material necessary to absorb an alpha particle or a low energy proton it would be difficult to build a two scintillator device with the first scintillator sufficiently thin for use in either of the proposed experiments.

However, our particular problem as well as the more general one of the preceeding paragraph could be resolved if further information could be extracted from the shape of the pulse from a single scintillator. It is therefore of practical, as well as theoretical, interest to consider whether there is any variation for different particles in τ, the mean life of the main pulse in CsI(Tl), a commonly used scintillating material. (Although the fluorescent efficiency of CsI(Tl) is less than that of NaI(Tl), its excellent physical and mechanical properties make it preferable in most applications.)

Van Sciver and Hofstadter (1951), using an RCA 5819 photomultiplier, have found a value for τ of 1.1 ± 0.1 μ sec for fast electrons in CsI(Tl), whereas Bonanomi and Rossel (1952), using the same type of photomultiplier, give a value of 0.6 μsec for polonium alpha particles. Knoepfel et al.(1956), using an RCA 6655, and also measuring τ for alpha particles obtain a value of 0.55 μsec. Possibly these results have not been inter-

preted as due to difference in particle, because it is known that other factors can significantly influence the measured lifetime.

Knoepfel et al. (1957) have found that τ for alpha particles in CsI(Tl) varies with temperature. Eby and Jentschke (1954) have shown that τ is the same for alphas and electrons in NaI(Tl), but varies with thallium concentration. From these last results, it would be reasonable if the different values of τ measured in CsI(Tl) were at least partly due to a difference in the concentration of thallium in the crystals used. Kallmann and Brucker (1957), using an RCA 5819, have measured τ for fast electrons and alpha particles in a range of organic and inorganic crystals not including CsI(Tl) and find no significant difference.

Summarizing the results of all the above experiments, it can be stated that while different values of τ have been observed for alpha particles and electrons in CsI(Tl), no such effect has been found in the main current pulse of other scintillators, and the measured values of τ may be expected to vary with temperature, concentration of thallium and, possibly, type of photomultiplier.

In the experiments described below, these last three factors were kept constant, and τ has been measured for different energies of alpha particles, protons, and electrons.

(b) Experimental Method

The CsI(Tl) crystal was obtained from the Harshaw Chemical Company who stated that the molar concentration of thallium was 0.1%. The dimensions of the crystal were 1.5 cmx0.9 mm

and it was mounted by fine wires on a DuMont 6292 photomultiplier parallel to the photocathode at a distance of 3.5 cm. A highly reflecting aluminium cylinder, 3.5 cm. in diameter by 3.5 cm. in length, with a very thin aluminium end window was used as a light reflector.* This arrangement has been found to give good pulse height resolution for photomultipliers with photocathodes which are not quite uniformly sentitive.

The current pulses from the photomultiplier were integrated, the leakage time constant being 86 μsec. The integrated current pulses, or voltage pulses, were then fed through a cathode follower and a matched delay line of 1.7 μsec to a Tektronix 517A cathode-ray oscilloscope. Measurements were made on three time scales, 0.2 μsec cm^{-1}, 0.5 μsec cm^{-1} and 2 μsec cm^{-1}. The pulses on the oscilloscope were photographed, projected on a large screen and carefully traced on fine graph paper.

The time base speeds on the Tektronix oscilloscope were compared with the period of a crystal controlled, standard frequency oscillator, Furzehill type G415. This was done by using the crystal controlled oscillator to check the frequency scale of a variable frequency oscillator, type Advance 62. Using convenient frequencies for each time base, the train of sine waves was randomly triggered, photographed and then projected and traced in the same way as the pulses from the CsI(Tl). The probable error in the calibration was ± 1%. The time base speeds indicated on the oscilloscope appeared to be systematically 2% higher than those given by our calibration. Our results have been corrected for this difference.

*This was the crystal-target assembly of section III. 2 (see Fig. III. 1).

The electron source was the photopeak and Compton spectrum in the crystal for Cs^{137} gamma rays (E = 661 kev.). A polonium source (5.3 Mev.) was used at different distances from the crystal to give alpha particles of different energies. Higher energy alpha particles were obtained by bombarding boron 10 with 500 kev. deuterons. From other experiments with a multichannel pulse height analyser, we have verified that most of the pulses in a limited region of the energy spectrum can be attributed to the reaction $^{10}B(d, \alpha)^{8}Be$ (Q = 17.8, 14.91 Mev.). High energy protons were obtained from the reaction $^{10}B(d, p)^{11}B$ (Q = 9.23, 7.09, 4.77 Mev.).*

Five different values of the photomultiplier voltage were used to make the pulse height on the oscilloscope about the same for 1 Mev. alpha particles, 4.8 Mev. alpha particles, 660 kev. electrons, 2 Mev. protons and 8.5 Mev. protons. The change in photomultiplier gain at these different voltages was later measured using a Hutchinson-Scarrott 100-channel pulse height analyser. Knowing the differences in gain at the five voltages, all of the graphs of the voltage pulses could be normalized to the same gain.

(c) Results

When the photographs of the voltage pulses were projected on a large screen, it was immediately obvious that the pulses due to alpha particles were rising more rapidly than those due to electrons, and that the rise time of the proton pulses lay somewhere between the two.

---

* See sections II. 2 and II. 3 and in particular Fig. II. 8 for the actual spectrum used.

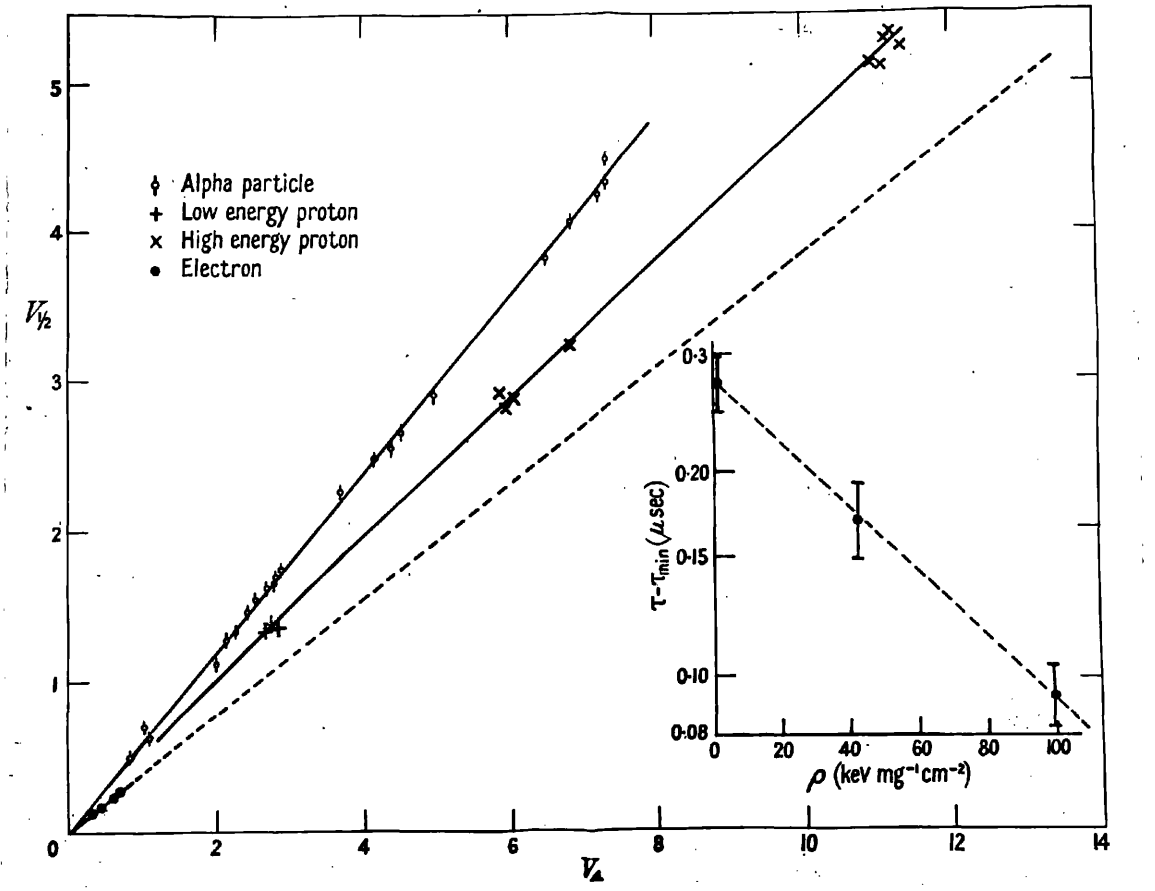

Fig. IV. 1 The minimum mass separation using CsI(Tl) as a single crystal detector. $V_{\frac{1}{2}}$ and V_4 are the voltage pulse heights at 0.5 μsec and 4 μsec respectively. Inset: $\tau - \tau_{min}$ as a function of ρ the average ionization density.

The graphs of the voltage pulses were analysed in two ways. In the first method, voltage pulse heights $V_{\frac{1}{2}}$ and V_4 were measured at 0.5 μsec and 4 μsec. These values were then normalized to allow for the changes in gain of the photomultiplier at the different voltages used in the experiments. When this was done, the values of $V_{\frac{1}{2}}$ were plotted against V_4, and the result is shown Fig. IV. 1 in which different symbols are used for points arising from different types of particles. It can be seen that there are three distinct loci for the points, one for each type of particle. The width of the loci can be calculated, if the number of photoelectrons released from the photocathode per unit proton energy is known. From the width of the peaks in the pulse height spectra measured on a multichannel pulse height analyser, we estimate this number to be greater than 5000 per 10 Mev. Choosing a fixed value of $V_{\frac{1}{2}}$ for 10 Mev. protons, the percentage spread in the corresponding value of V_4 is therefore about 1% since $V_{\frac{1}{2}} \approx \frac{1}{2}V_4$. Only pile up of pulses at very high counting rates can further increase the width of the loci. Fig. IV. 1 can be obtained directly using the X and Y plates of an oscilloscope and the mass separation can be further increased by a suitable choice of bandwidths of amplifiers for $V_{\frac{1}{2}}$ and V_4.

In the second method of analysis, the graphs were corrected for the leakage time constant of 86 μsec, and then carefully differentiated to obtain the shape of the current pulses. This was done for electrons of 660 kev. protons of

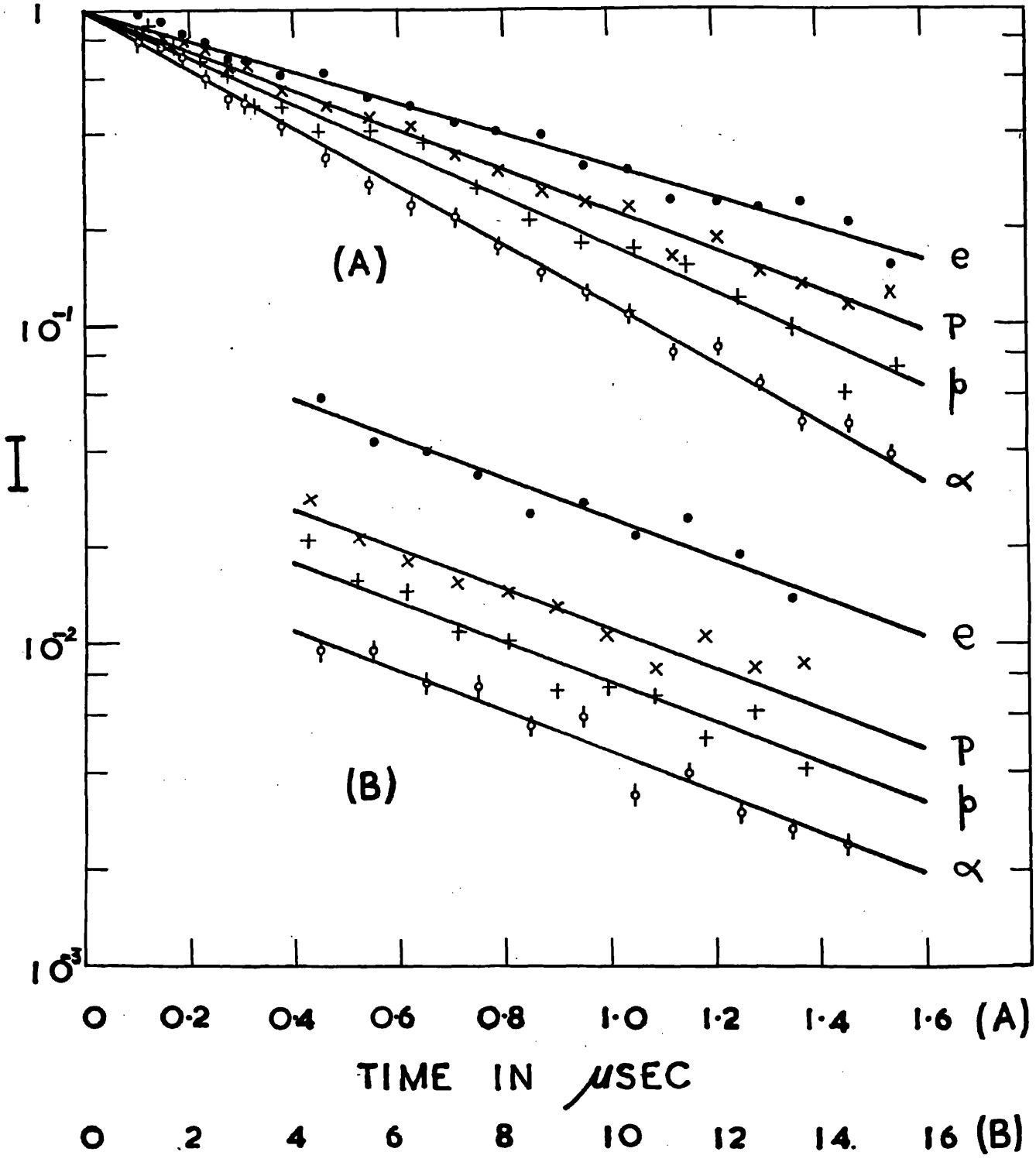

Fig. IV. 2 Decay curves in CsI(Tl) for different particles.

8.6 and 2.2 Mev. and alpha particles of 4.8 Mev. two pulses being analyzed in each case. The advantage of measuring the voltage pulse and then differentiating it, rather than measuring the current pulse directly is that it allows a flexible compromise between time resolution and charge fluctuation. When the derivatives of the voltage pulses were plotted, it was found that the current pulses rose with a time constant of 50 ± 10 μsec, which is attributed to the bandwidth of the delay cable and transit time variations in the DuMont 6292. The effect of this rise time on the measured values of τ was very small, but the initial decay rates were corrected to allow for its effect. All of the derived current pulses were then normalized to unity at time zero, and the results for the different particles plotted in Fig. IV. 2. Values have not been plotted for the region 1.6-4 μsec because residual mismatch of the delay line may render them uncertain.

It can be seen from Fig. IV. 2 that the decay of the current pulse can be conveniently described in terms of two components in each case, an initial fast decay and a slow component. If a third component exists with mean life of 2-3 μsec. we estimate that it must contribute less than about 5% to the total voltage pulse at 17 μsec. The subtraction of the common slow component which has a value of 7 ± 0.5 μsec from the initial decay shown in Fig. IV. 2, gives the results shown in the table, for the average lifetime τ during the time interval 0.1 μsec-1.6 μsec. For comparison, the energy of the

particles used and the average ionization density ρ defined as the energy divided by the range, are also given in table IV. 1.. The range for the electron taken from the empirical formula of Katz and Penfold (1952) has been increased by a factor of two to try to allow for electron scattering in the crystal.

Table IV. 1

	e	p	p	a
Particle	Electron	Proton	Proton	Alpha
Energy E (Mev.)	0.66	8.6	2.2	4.8
ρ(kev. mg^{-1} cm^{-2})	1.1	42.5	100	680
τ(μsec)	0.70±0.025	0.60±0.02	0.52±0.01	0.425±0.01
$\tau_{eqn.}$(μsec)	0.695	0.60	0.519	0.423
$\epsilon_{1.5}$	1±0.05	1.56±0.08	1.49±0.08	0.75±0.04
ϵ_{∞}	1±0.05	1.18±0.05	1.04±0.05	0.48±0.03
I_{max}/E	1.0±0.1	1.75±0.2	1.9 ±0.2	1.15±0.1
R	0.50	0.35	0.30	0.25

The variation of τ with ρ encourages us to believe that τ may be a continuous function of ρ. Consideration of the number and accuracy of the points available does not permit us to derive the function very accurately. However the general behaviour is illustrated by the empirical formula $\tau - \tau_{min} = (\tau_{max} - \tau_{min}) \exp(-\rho/\rho_o)$ which is suggested by the values in table IV.1 and also by the loci of Fig. IV.1 The inset in Fig. IV.1 is a logarithmic plot of $\tau - \tau_{min}$ against ρ. The value of ρ_o obtained from this graph is $\rho_o = 95 \pm 15$ kev. $mg^{-1}cm^{-2}$,

if τ_{min} = 0.415 μsec and τ_{max} = 0.685 μsec, our best estimates of τ for alphas and electrons respectively. The values τ_{eqn} in table IV. 1 are calculated from the empirical formula using the above values.

Since all of our results could be normalized to the same electronic gain, we have been able to estimate the relative voltage pulse height per unit energy (or efficiency) for the different particles. Two efficiencies are given in the table IV. 1: $\epsilon_{1.5}$ is defined as the efficiency for light emitted in the time range up to 1.5 μsec, and ϵ_{∞} is the efficiency for infinite time based on the assumption that there are no contributions from components longer than the common 7 μsec component. Derived values of I_{max}/E, the relative peak currents per unit energy, and of R the ratio of the light output in the long component to the total light output are also given in this table.

(d) Discussion

Our results show that in CsI(Tl) the efficiency and the decay time of the fluorescence vary with the density of ionization. It might be thought that both effects would be related and arise from the same cause. Kallmann and Brucker (1957) have shown that in a wide variety of scintillators which exhibit efficiency quenching effects which vary with ionization density there is no evidence for any variation in the decay time. Kallmann concludes that the main part of the quenching, at least in the organic scintillators, is finished before any

appreciable amount of light is emitted. It might be expected that a similar fast quenching effect occurs to some extent in inorganic scintillators, but that in CsI(Tl) there may also be a slower mechanism for quenching, which competes with the process of emission during the time of emission. Since the efficiency of CsI(Tl) (and also LiI Eu), Schenck and Heiler 1954) appears to first increase with ionization and then decrease, while the fast quenching mechanisms observed in the organic crystals lead to a monotonic decrease in efficiency, it is necessary to look for a slow quenching mechanism, which will result in the efficiency increasing with increasing ionization density. If the observed variation of τ with ionization is attributed to a transport (or recombination) mechanism (Curran 1953), slow quenching occurring during the transport time to the emitting centres would result in a greater decrease in efficiency for smaller ionization densities, which correspond to longer decay times. Thus, qualitatively, this interpretation of our results would explain the observed variations of efficiency and lifetime with ionization density. Such a mechanism, including fast quenching, contains so many adjustable parameters that it is possible that the results for CsI(Tl) could be explained quantitavely, particularly as a transport mechanism would lead to a hyperbolic decay law which would be in rough agreement with our results. However, we have estimated transport or recombination times for CsI(Tl) and these are very much shorter than the observed decay times. Because of this fundamental discrepancy it seems unlikely that our results

can be explained in terms of this mechanism.

Since the efficiency variation appears to depend mainly on the fast quenching which is expected to be independent of the emission process, we now go on to consider a possible interpretation of the variation of τ with ρ independently of the variation of efficiency.

The dependence of τ on so many different factors, and the limitations of the present experiments make it necessary to be cautious in comparing the observed variation of τ with ionization density and the results of others in experiments on CsI(Tl) crystals. There is, however, a very striking similarity between the variation of τ for alpha particles in CsI (1% Tl) as a function of temperature measured by Knoepfel et al. (1957) using an RCA 6655 and our own results for the variation of with ionization density at constant temperature. Knoepfel et al. find that τ for alpha particles decreases to a limiting value τ_L as the temperature is increased to room temperature. We have plotted the logarithm of $\tau - \tau_L$ as a function of temperature using their results, and find that

$$\tau - \tau_L \propto \exp(-T/T_0)$$

where $T_0 = 13.5^\circ C \pm 1^\circ C$. This empirical expression can be compared with our own results expressed as $\tau - \tau_L \propto \exp(-\rho/\rho_0)$ where $\rho_0 = 95 \pm 15$ kev. mg^{-1} cm^{-2}. The similarity of the two expressions, in each of which τ_L is the value found for alpha particles suggests that the effect of changing the particle ionization density is to change the effective local temperature

at which the emission takes place. If the change in local temperature is proportional to ρ then it is possible to deduce our results for different particles at the same temperature from those of Knoepfel et al. for the same particle at different temperatures.

Our results may be explained in terms of a simple model employing two sets of electron traps at different energy levels. Decay of the trap occurs when it receives enough thermal energy to reach an excited state, decay from which leads to fluorescence. It is supposed that the higher energy trap is responsible for the short lifetimes, while the lower energy trap gives rise to the 7 μsec lifetime. The difference in the two lifetimes is due to the energy difference between the trap and the levels responsible for fluorescence. It would be expected that the trap with the smaller energy difference would be more susceptible to temperature changes than the other one. This would explain the difference in the short lifetimes for different particles if different values of ρ correspond to different effective temperatures in the material surrounding the track, and would also account for the common long lifetime.

In the table R is the ratio of the light emitted due to the long lifetime (7 μsec) to the total light emitted. It is seen that the shorter the initial lifetime, the less there is of the long component. This effect, also seen in Fig. IV. 2 suggests that the lower energy trap is fed from the higher one

in competition with the normal transition to the radiating state. In this case, the lifetime for decay from one trap to another must be of the order of 1 μsec.

This interpretation of our results would lead us to expect a considerably greater change in the values of τ for different particles in CsI(Tl) than are given here if the crystal temperature is lowered below room temperature. This result follows from the behaviour of τ as a function of temperature observed for alpha particles by Knoepfel et al. and would result in a considerable increase in the particle separation shown in Fig. IV. 1.

If this preliminary interpretation of our results is correct, it seems likely that similar effects may occur in other crystals in which non-radiating states are involved. It is possible, however, that it is only in CsI(Tl) that the characteristics of the resonance energy transfer are such as to result in a conveniently large variation in τ as a function of available temperatures, and thus to a useful variation of τ for different particles.

Another quite different interpretation of our results is that the variation in ionization density results in a different distribution in the initial population of radiating states. The observed variation in the value of τ would then reflect the different contributions of many radiating states with different decay times. The simplest and most extreme case would be two radiating states corresponding to the values

of τ observed for alpha particles and electrons. It is not possible from our present results to deduce from the straightness of the log plots of the current pulses due to protons whether the values of τ observed for protons are due to a combination of two lifetimes or one single lifetime. However, the order of magnitude of the values of τ observed seems more consistent with those to be expected for traps rather than for radiating states.

A possible interpretation of the results given here could have been that the original decay of the main light pulse from the tracks of the particles is the same but complex. Since the path length of the light passing through the crystal to the photocathode increases in our experiments with increasing ρ, differential absorption of the longer components in the light pulse would tend to a shorter measured decay time for higher values of ρ. However, Wells (private communication) of this department, has found substantially the same values of τ as we have for alpha particles and electrons in a different CsI (0.1%Tl) crystal, obtained from the Harshaw Chemical Company six months later than the one used in the experiments described here. The crystal which Wells used was about three times the thickness of our crystal and was mounted using silicone grease. In both cases we believe that the crystals were cut from the interior of a much larger block of material and therefore that the thallium concentration is uniform throughout our crystals.

It is hoped that further measurements, particularly on the emission spectrum for the different particles, will help to

elucidate the mechanism involved. Further experiments will also be designed from the point of view of improving the mass separation.

Part V CONCLUSIONS

It is appropriate in this final part of the thesis to consider what has been achieved and what should be undertaken next in order to further our understanding of these problems.

As discussed in section I. 5 the initial experiment was based to some extent on the assignment by Bashkin et al. (1955) of a 5/2 spin to the 7.61 Mev. capture level. The analysis of the experimental evidence in section II. 1 shows that the spin of this level is in fact $\frac{1}{2}$ or 3/2. Accordingly, it appears that to obtain sufficient information to determine the spins and parities of the first three excited states it will be necessary to measure in detail the transitions from the higher capture levels which are beyond the range of the present accelerator. However, since the work of Marion et al. (1955) suggests that the resolution may not have been adequate in the early experiments which determined the number of energy levels, a careful experiment should be undertaken to determine, if possible, whether the 5.27 Mev. level is not in fact a doublet before further angular distributions are carried out. Such an experiment would require the use of the (d,n) reaction and the method of Bonner and Cook (1954) for slow neutron thresholds.

In general the (p,γ) reaction is a valuable source of information and much work remains to be done. However, most of this requires measurement of angular distributions or

correlations with considerable accuracy in a region where several gamma rays contribute to the spectra. Since the 5 in. NaI(Tl) detector (if necessary with collimation) gives the best separation of the gamma ray contributions it will be widely used in future work.

The $^{10}B(d,p\gamma)^{11}B$ measurements have been successfully interpreted in terms of ordinary stripping theory and of an incoherent contribution from deuteron capture chiefly at a "broad level" of 25.7 Mev. excitation in ^{12}C. The lack of agreement between the phase shifts of the deBorde formula and the agreement with the strong coulomb stripping theory so far as this could be tested suggests simply that in the $^{24}Mg(d,p)^{25}Mg$ reaction the deBorde formula is not an adequate approximation. It may, however, prove satisfactory at higher energies where the coulomb effects are weaker. Although the present interpretations of our experimental data on low energy deuteron experiments have been in general successful it must be remembered that this is a very small and perhaps not too typical example of that potentially available. Considerable further experimental work will therefore be required to establish these various descriptions with certainty and to delimit the region of applicability for each. From a theoretical point of view the expected variation of the phase shifts of the deBorde formula as the coulomb effects increase must be investigated more thoroughly for comparison with the theory and to ensure that they tend toward the strong coulomb description

of Ter Martirosian and of Biedenharn et al. The latter requires as a priority the development of a method of calculating the angular distributions for non zero values of the angular momentum of the captured nucleon. In the intermediate case it must be assumed that the ordinary stripping is replaced by a suitable coulomb distorted stripping in the combination with the compound nucleus contribution. In this complex region accurate and extensive measurements are required to obtain the values of the many parameters which will be present. Although the (d,p) reaction has been used to investigate nuclear level parameters in a limited sense in this present work its full use as a tool in nuclear spectroscopy awaits more complete understanding of the reaction mechanism.

By careful attention to the reduction of background a high efficiency single scintillator method of measuring the proton spectra from (n,p) reactions has been developed and applied to several isotopes. The possible extension of this technique to measurement of the spectra of the other possible charged products emitted by an excited nucleus (in the unavoidable presence of the yield from this dominant (n,p) reaction) has been indicated by the demonstration of the variation of the decay time characteristic of CsI(Tl) with the nature of the particle absorbed. Since this work was completed Mr. C. Robertson of this laboratory has developed an apparatus which is able to distinguish electronically between alpha particles

and electron pulses and to record the spectrum separately of either in the presence of the other. Mr. Robertson also plans measurement of alpha particle spectra in (n, α) reactions. Measurements such as this of different charged particle spectra and measurements over a wide range of excitation energies of the compound nucleus will do much to establish an exact description of the evaporation process and will lead to a more quantitative equation of state for nuclei.

Apart from its obvious importance in nuclear detection technique the decay characteristic of CsI(Tl) has considerable intrinsic interest. We have suggested that the variation observed may be due to a local heating effect. It is obvious that more information about this possibility may be obtained by measuring the decay time at a series of different ambient temperatures. This is being carried out in detail by Mr. C. Wells of this laboratory whose preliminary results indicate that the effect becomes larger as the temperature is reduced below 0° C. In a similar manner the effect on this phenomenon of other relevant variables such as the portion of the spectra of the light emitted from the scintillator may also be investigated.

APPENDIX A

Geometrical Analysis of (n, p) Apparatus

In order to obtain the absolute value of $\sigma(n, p)$ (θ_p, E_p) (barns per nucleus per Mev. interval of Ep) it was necessary to calculate certain geometrical factors which relate the monitored pulse height spectra measured in the experiment to this desired reaction parameter. Usually nuclear reaction products are measured in circumstances in which the detector subtends a constant solid angle to various parts of the source and in which the effects of finite solid angle are negligible. Moreover, this geometry results in the particle beam detected being sufficiently parallel that the loss of energy in any absorbing layer which may separate source and detector is effectively the same for all particles of the same initial energy. In other words, yields are usually sufficiently great that a simple geometry may be obtained at the expense of detection efficiency. In our experiment efficiency was so essential that it was not possible to satisfy any of the above simplifying assumptions in the final form of the apparatus. Moreover, no description of our geometry was found in the literature of the subject. The following analysis was therefore undertaken by the author. If the average neutron flux in a volume V in which (n, p) reactions are being considered is N_f per sec. per cm^2 and the number of protons produced per sec. per ster. per Mev. interval per Cm^3 is $N_p(\theta_p, E_p)$ then

$$N_p(\theta_p, E_p)\,dV\,d\Omega\,dE\,dt = \frac{N_f\ \sigma(\theta_p, E_p)\ A_o}{W}\,dV\,d\Omega\,dE\,dt \qquad (A1)$$

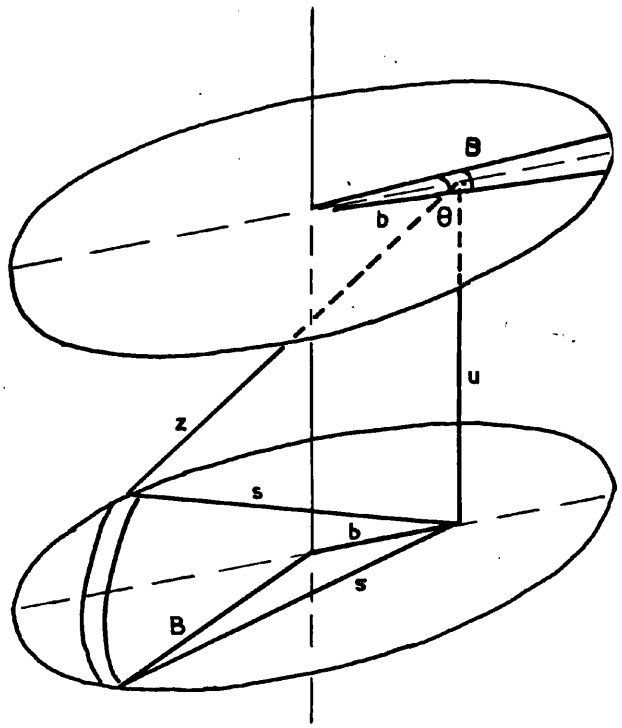

(a)

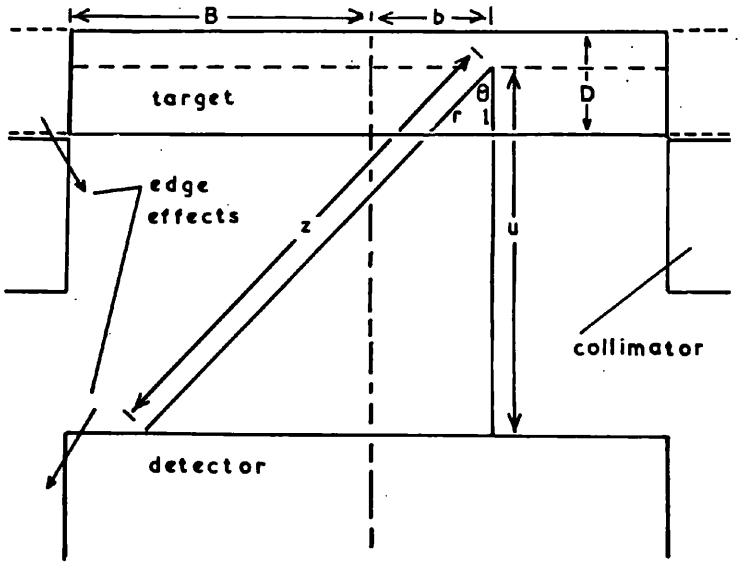

(b)

Fig. A1 Diagrams illustrating the detailed geometry of the (n,p) apparatus (see text).

where $\sigma(\theta_p, E_p)$ is the cross section per Mev. per ster. for proton production, W and ρ are the atomic weight and density of the target material and A_o is Avogadro's number. Our particular geometry consists of two colinear discs of equal diameters. One, the target in which the protons are produced and the other two scintillator in which they are detected. In Fig.A1(a) the lower circle represents the adjacent face of the scintillator and the upper circle a plane within the target disc at a distance l above its lower surface. In Fig.A1(b) the thickness D of the target disc is exaggerated in order to show the quantity r which is the measure of proton energy loss occurring before the proton leaves the target. In order to simplify the calculation we set $\sigma(\theta_p, E_p) = \sigma(E_p)$ and say that any proton incident on the adjacent face of the scintillator is adequately detected, but these assumptions will be discussed later.

The number of protons produced in a volume $dV = dl\ dA_t$ in the target per sec. per Mev. interval and incident on an area dA_s of the scintillator face is

$$\frac{N_f \sigma(E_p) A_o \rho}{W} (dl\ dA_t) \left\{\frac{dA_s \cos\theta}{z^2}\right\} \qquad (A2)$$

Substituting and integrating we find the total number of detected protons produced in the layer dl and emitted between θ and $\theta + d\theta$ to be.

$$\frac{N_f \sigma(E_p) A_o \rho}{W} dl \quad 2\pi \sin\theta d\theta \int_0^D 2\phi\, bdb \qquad (A3)$$

where since $\phi = \cos^{-1} \frac{u^2 \tan^2 \theta + b^2 - B^2}{2 bu \tan \theta}$ (A4)

$\int_0^B 2 \phi \, b \, db$ may be set equal to $\pi B^2 F(\theta, u, E)$

The total number of protons detected per unit solid angle per Mev. interval may be then written as

$$2 \pi \sigma(E_p) \frac{N_0 A_0 \rho}{W} \left[\frac{1}{D} \int_0^D dl \int_0^{\cos^{-1}[1/R(E_p)]} \sin \theta F(\theta, u, E) \, d\theta \right] \quad (A5)$$

The upper limit shown is valid because r must be less than $R(E_p)$ for detection but $F(\theta)$ vanishes at $\theta = \tan^{-1}\left(\frac{2B}{D}\right)$ and in the geometries used this gave the effective upper limit for $E_p \gtrsim$ 6 Mev.

Since the electrical pulse obtained when a proton passes through a CsI (Tl) detector is closely proportional to the energy expended in the crystal, the energy spectrum of protons emitted in a (n, p) reaction $\sigma(E_p)$ can be obtained from the pulse height spectrum with corrections only for the energy loss in the target material. These are evaluated in terms of r which is that part of the proton track which falls within the target volume. That is, if a proton is produced with an energy E_p and expends an amount of energy ϵ_ρ in the detector then for each E_p there will be a distribution $n(\epsilon_\rho, E_p)$ which can be found from the corresponding distribution $n(r, E_p)$.

$n(r, E_p)$ may be found by substituting $dl = \cos \theta \, dr$ in eqn. (3) and integrating over θ. Thus

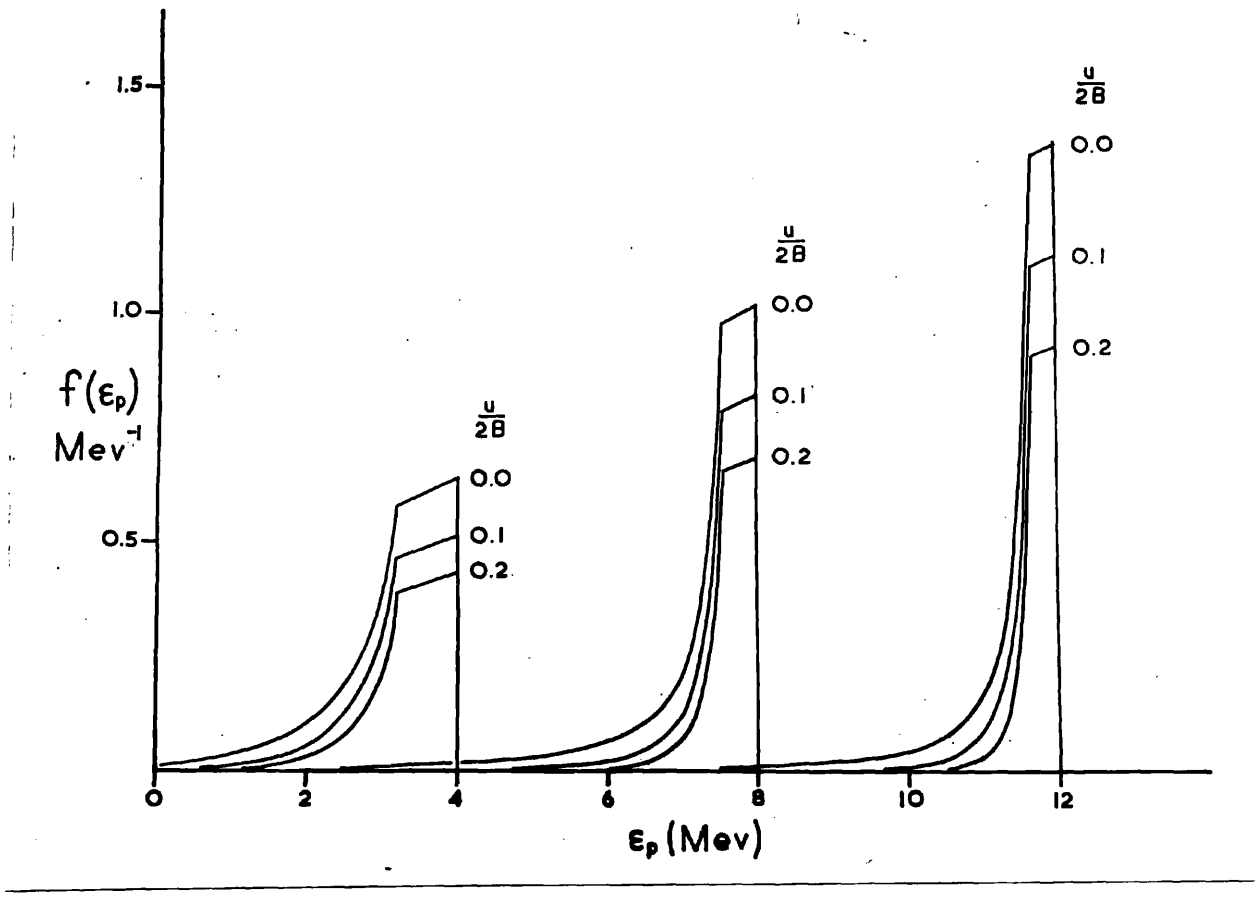

Fig. A2 Calculated pulse height spectra for monoenergetic proton groups at E_p = 4, 8, and 12 Mev. $\frac{u}{2B}$ is the ratio of the target-detector spacing to the mutual diameter.

$$n(r, E_p) = 2\pi\sigma(E_p)\frac{N_f A_o \rho V}{W}\left[\frac{1}{D}\int_{\cos^{-1}\left(\frac{D}{r}\right)}^{90^\circ}\frac{\sin 2\theta}{2}F(\theta,u,B)d\theta\right] \quad (A6)$$

the lower limit being 0° for $0<r<D$. In the limit for "2π geometry" $F(\theta) = 1$ and we have for the value of the integral

$$\frac{1}{2}, \quad 0<r<D \qquad \text{and}$$

$$\frac{D^2}{2r^2}, \quad D<r<R$$

It is also interesting to note that in this limit the total number of protons detected per sec. per Mev. interval of E_p can be obtained as

$$2\pi\sigma(E_p)\frac{N_f A_o \rho V}{W}\left(1 - \frac{D}{2R}\right) \quad (A7)$$

by integrating (7) over r in (6) as well as substituting in (5)

If $r + r_1 = R$ (r_1 is the residual range corresponding to the energy loss in the detector, then

$$n(\epsilon_p, E_p) = 2\pi\sigma(E_p)\frac{N_f A_o \rho V}{W} f(\epsilon_p, E_p) \quad (A8)$$

where

$$f(\epsilon_p, E_p) = \frac{1}{(dR/dr_1)D}\int_{\cos^{-1}\left(\frac{D}{R - r_1}\right)}^{90^\circ}\frac{\sin 2\theta}{2}F(\theta,u,B)\,d\theta \quad (A9)$$

Trapezoidal numerical integration has been used to obtain $f(\epsilon_p, E_p)$ for D = 15 mg. cm.$^{-2}$ in copper (R (E) and dE/dr_1 were obtained from Allison and Warshaw (1953) and Rich and Madey (1954) for a few values of E_p and $u/2B$. These are shown in Fig.A2. It is seen that increasing u/2 B or E_p reduces the characteristic low energy tail. The area under a curve

$F(\epsilon_p) = \int_0^{\epsilon_p} f(\epsilon_p, E_p)\, d\epsilon_p$ is equal to the ratio of the number of protons detected in the particular circumstances to the number which would be detected in a 2π geometry with D/R = 0. Subject to the initial assumptions $f(\epsilon_p, E_p)$ describes completely the geometrical effects on the relation between the observed pulse height spectrum $n_1(\epsilon_p)$ and $\sigma(E_p)$. That is,

$$n_1(\epsilon_p) = \frac{N_0 A_0 \rho V}{E_0} \int_{\epsilon_p}^{E_p} 2\pi\sigma(E_p)\, f(\epsilon_p, E_p)\, dE_p \qquad (A10)$$

Since $F(\theta,u,E) = F(S/2B)$, it is convenient to calculate the latter. The $F(u,E,\theta)$ needed for the numerical integration of (5) to (10) can be readily obtained from this. A brief attempt was made to find $F(S/2B)$ analytically. This having failed, numerical integrations were performed using Simpson's and Weddle's Rules with intervals of 0.1B, and using Gauss's Method with five values of the integrand (see, for example Margenau and Murphy (1943). The values obtained were in agreement to about one percent. The more accurate values obtained using Gauss's Method are given in Table A1. These are accurate to about 5 units in the fourth figure after the decimal point.

S/2B	F(S/2B)
0.0	1.0000
0.1	.8728
0.2	.7469
0.3	.6237
0.4	.5044
0.5	.3910
0.6	.2849
0.7	.1883
0.8	.1042
0.9	.0374
1.0	.0000

Table A1

Since in this experiment the energy spectra of protons emitted from the compound nucleus are being studied, it is necessary to avoid, as far as possible, contributions from the direct effect. At this time the contribution to the total cross section from this source is estimated to be about 10%. Because the efficiency of our apparatus becomes very small and then vanishes as θ approaches 90° the actual direct contributions to our spectra depend on the degree of anisotropy of the direct effect. It has been numerically calculated by evaluating

$$\frac{1}{\pi}\int_{0}^{\cos^{-1}(1/R)} \cos^{-1}\left(\frac{\cos(\theta_p \text{ max})}{\sin\theta}\right) F(\theta,u,B)\, d\theta \quad \text{for} \quad \frac{u}{2B} = 0.15$$

that if the direct emission may be approximated by

$$\sigma_{\text{dir.}}(\theta_p) = k, \quad 0 \leq \theta_p \leq (\theta_p \text{ max}) \quad \text{and } 180^{\circ} - (\theta_p \text{ max}) \leq \theta_p \leq 180^{\circ}$$

$$\sigma_{\text{dir.}}(\theta_p) = 0, \quad (\theta_p \text{ max}) \leq \theta_p \leq 180^{\circ} - (\theta_p \text{max})$$

then the actual direct contribution falls to 8% for θ_p max = 50° and to 4% for θ_p max = 30°. Since there is some evidence that direct protons are emitted in predominantly forward directions and that this tendency increases with increasing E_p it is therefore expected that the contributions of the direct effect to our spectra will be small.

Two types of edge effects are possible and have been indicated in Fig. I(b). In both these cases the part of the track r_1 in the scintillator is less than (R - r) and this results in a further distortion of the energy spectrum. A

numerical calculation has been performed for a typical experimental case E_p = 11.4 Mev., $R(E_p)$ = 0.075 cm.(in CsI (Tl)) = 0.05 x (2B) and the magnitude of the effects obtained as 4% in the scintillator edge and 2% due to absorption in the bismuth collimator. The latter effect only occurs, of course, when the target protrudes beyond the edge of the collimator.

APPENDIX B

The Preparation of Thin Plastic Scintillators

Before CsI(Tl) became available plastic scintillators were widely used for charged particle detection. Often it is required in the form of a very thin sheet, for background reduction, for a dE/dx measuring element in a proton telescope, or for a hydrogenous radiator in a neutron telescope. Since it was difficult to produce such items by machining and polishing from a large piece of plastic the author decided to attempt to obtain them by heating samples of material until it partially softened and then slowly pressing it until the thickness required was achieved.

Initially the sample of plastic scintillator was cut to the correct volume for the thin disc desired. It was then carefully cleaned. The edges were rounded and the surfaces smoothed to avoid trapping air. Two alternative methods of pressing were used. In one of these the sample was placed between two pieces of plate glass and lead blocks piled on top provided sufficient pressure. In the other, brass blocks were used as flats and screws connecting them tightened to effect the pressing. Shims were used to control the final thickness. It became increasingly difficult to part the flats at the end of the process without damaging the thin disc as the thickness was reduced. Various substances were tried as release agents. Silicone oil was very unsatisfactory and although silicone grease was effective, the surface

of the plastic was usually not as clear as desired. Since the softening temperature of polyethylene terephthalate (mylar or melinex) is greater than 200° C., films of this material could be placed between the plastic scintillator and the flats. They showed no tendency to adhere to either and gave very smooth surfaces. The temperature and pressure required will, of course, depend on the type of plastic (usually polystyrene or polyvinyltoluene), on the time allowed for the process to occur and on the final thickness required. In practice a combination of fairly low temperature (about 120° - 140° C.) and high pressures (about 100 lb. per sq. in.) were found desirable. This was because at much higher temperatures small bubbles were produced (probably due to the decomposition of some additive associated with the scintillation process) and if mylar was used high pressures were found to be necessary to prevent it from wrinkling. Some of the first samples although clear when initially produced, later developed crazing effects. Because of this the later ones were cooled very slowly to avoid internally stressing the plastic. Using the above process the author produced many different sizes of disc including some about $1\frac{1}{2}$" in diameter and less than 0.005" thick. None of these showed any diminution of light output compared to machined samples.

REFERENCES

Ajzenberg, F., and Lauritsen, T., 1955, Rev. Mod. Phys. 27,77.

Allan, D. L., 1957, Proc. Phys. Soc. A,70,195; 1958, Nuc. Phys. 6,464.

Allan, H. R., and Sarma, N., 1955, Proc. Phys. Soc. A,68,535.

Allison, S. K., and Warshaw, S. D., 1953, Rev. Mod. Phys. 25,779.

Austern, N., Butler, S., and McManus, H., 1953, Phys. Rev. 92,350.

Bame, S. J., Jr., Haddad, E., Perry, J. E., Jr., and Smith, R.K., 1957, Rev. Sci. Instr. 28,997.

Band, W., 1955, "Quantum Statistics" (New York: VanNostrand).

Bashkin, S., Carlson, R. R., and Nelson, E. B., 1955, Phys. Rev. 99,107.

Bethe, H. A., 1937, Rev. Mod. Phys. 9,69; 1938, Phys. Rev. 53,39.

Bhatia, A. B., Huang, K., Huby, R., and Newns, H. C., 1952, Phil. Mag. 43, 485.

Biedenharn, L. C., Boyer, K., and Goldstein, M., 1956, Phys. Rev. 104,383.

Biedenharn, L. C., and Rose, M. E., 1953, Rev. Mod. Phys. 25,729.

Bilaniuk, O., and Hensel, J. C., to be published.

Blatt, J. M., and Biedenharn, L. C., 1952, Rev. Mod. Phys. 24,258.

Blatt, J. M. and Weisskopf, V. F., 1952, "Theoretical Nuclear Physics" (New York: Wiley).

Blin-Stoyle, R. J., 1951, Proc. Phys. Soc. A,64,700.

Blin-Stoyle, R. J., Grace, M. A., and Halban, H., 1953,"Progress in Nuclear Physics 3", (London: Pergamon Press)

Bloch, C., 1954, Phys. Rev. 93,1094.

Bohr, A., and Mottelson, B., 1953, Kgl. danske Vid. Selsk., mat-fys. Medd. 27, No. 16.

Bonanomi, J. and Rossel, J., 1952, Helv. Phys. Acta 25,725.

Bonner, T. W., and Cook, C. F., 1954, Phys. Rev. 96,122.

Bocock, J. E., 1956, Proc. Phys. Soc. A,68,512.

Breit, G., and Wigner, E. P., 1936, Phys. Rev. 49,519.

Brown, G., Morrison, G. C., Muirhead, H., and Morton, W. J., 1957, Phil. Mag. 2,785.

Brown, G., and Muirhead, H., 1957, Phil. Mag. 2,473.

Brown, G. E., and Dominicis, C. T., 1958, Proc. Phys. Soc. 72,70.

Bruechner, K. A., 1955, Phys. Rev. 105,1949.

Buechner, W. W., Strait, E. N., Stergiopoulos, C. G., and Sperduto, A, 1948, Phys. Rev. 74,1569

Burke, W. Risser, J. R., and Phillips, G.C., 1954, Phys. Rev. 93,188.

Burrows, H. B., Gibson, W. M., and Rotblat, J., 1950, Phys. Rev. 80,1095

Butler, S. T., 1951, Proc. Roy. Soc. A,208,559.

Chadwick, J., 1932, Proc. Roy. Soc. A,136,692.

Cockcroft, J. D., and Walton, E. T. S., 1930, Proc. Roy. Soc. A,129,477; 1932, ibid, 136,619.

Cohen, B. L., 1957, Phys. Rev., 105,1549.

Colli, L., Facchini, U., Micheletti, S., 1957, Nuovo Cim. 5,502.

Colli, L., Facchini, U., Iori, I., Marcazzan, A., and Sona, A., 1958 Nuovo Cim. 7,400

Conner, J. P., 1953, Phys. Rev. 89,712.

Curran, S. C., 1953,"Luminescence and the Scintillation Counter" (London: Butterworths)

deBorde, A. H., 1955, Private Communication.

Deuchars, W. M., and Wallace, K. A., 1955, see Deuchars, Ph.D. thesis, unpublished.

Devons, S., and Goldfarb, L. J. B., 1957, Handbuch der Physik XL11,362.

Devons, S., and Hine, M. G. N., 1949, Proc. Roy. Soc. A,199,56.

Eby, F. S. and Jentschke, W. K., 1954, Phys. Rev. 96,911.

Moore, W. C., and Sands, M., 1949, "Electronics" (New York: McGraw Hill).

Elton, L., and Gomes, L. C., 1957, Phys. Rev. 105,1027.

Endt, P. M., and Braams, C. M., 1957, Rev. Mod. Physics 29,683.

Evans, N. T. S., and French, A. P., 1958, Phys. Rev. 109,1272.

Evans, N. T. S., and Parkinson, W. C. 1954, Proc. Phys. Soc. A,67,684.

Evans, W. H., Green, T. S., and Middleton, R., 1953, Proc. Phys. Soc. A,66,108.

Feenberg, E., and Phillips, M., 1937, Phys. Rev. 51,597.

Fermi, E., 1950, "Nuclear Physics" (Chicago: The University Press).

Feshbach, H., Porter, C. E., and Weisskopf, V. F., 1953, Phys. Rev. 90,166 1954, Phys. Rev. 96,448.

Flügge, S., (Ed.) 1957, "Handbuch der Physik" (Berlin: Springer Verlag).

Forbes, S. G., 1952, Phys. Rev. 88,1309.

French, A. P. and Newton, J. O., 1952, Phys. Rev. 85,1041.

Geiger, H. and Marsden, E., 1909, Proc. Roy. Soc. A82,495.

Ghoshal, S. N., 1950, Phys. Rev. 80,939.

Gorodetsky, S., Gallman, A., Croissiaux, F., and Armbruster, R., 1956, J. Phys. Rad. 17,550.

Grant, I. P., 1954, Proc. Phys. Soc. A67,981; 1955, ibid. A68,244.

Graves, E. R., and Rosen, L., 1953. Phys. Rev. 89,343.

Gugelot, P. C., 1954, Phys. Rev. 93,425.

Halbert, E. C. and French, J. B., 1957, Phys. Rev. 105,1563.

Hamilton, D. R., 1948, Phys. Rev. 74,782.

Haxel, O., Jensen, J. H. D., and Suess, H. E., 1949, Phys. Rev. 75,1766.

Lagakawa, S., Kawai, M., and Kikuchi, K., 1955, Prog. Theor. Phys. Japan 13,415.

Heitler, W., 1944 "The Quantum Theory of Radiation" (Oxford: University Press).

Hensel, J. C., and Parkinson, W. C., 1958, Phys. Rev. 110,128.

Heusinkveld, M., and Freier, G., 1952, Phys. Rev. 85,80.

Hofstadter, R., 1956, Rev. Mod. Phys. 28,214.

Holt, J. H., and Marsham, I. N., 1953, Proc. Phys. Soc. A66,1032.

Horowitz, J., and Messiah, A. M. L., 1953, J. Phys. Rad. 14,695.

Huby, R., 1953, "Progress in Nuclear Physics 3" (London: Pergamon Press).

Hughes, I. S., and Grant, P. J., 1954, Proc. Phys. Soc. A67,481.

Hutchinson, G. W., and Scarrott, G. G., 1951, Phil. Mag., 42,792.

Jack, W., 1958, Conference of the Physical Society on Nuclear Reactions (Cambridge, April, 1958).

Johnson, C. H., Robinson, G. P., and Moak, C. D., 1952, Phys. Rev. 85,931.

Jones, G. A., and Wilkinson, D. H., 1952, Phys. Rev. 88,423.

Kallmann, H., and Drucker, G. J., 1957, Phys. Rev. 108,1122.

Katz, L., and Penfold, A. S., 1952, Rev. Mod. Phys. 24,28.

Knoepfel, H., Leopfe, E., and Stoll, P., 1956, Helv. Phys. Acta 29, 241; 1957, Z Naturf. 12a,348; 1957, Helv. Phys. Acta 30,521.

Lagiss, C., 1956, Nucleonics 14, No. 3,66.

Lane, A. M., and Radicati, L. A., 1954, Proc. Phys. Soc. A67,167

Lane, A. M., and Thomas, R. G., 1958, Rev. Mod. Phys. 30,257.

Lane, A. M. and Wilkinson, D. H., 1955, Phy . Rev. 97,1199.

Lang, J. M. B., and LeCouteur, K. J., 1954, Proc. Phys. Soc. A67,586.

Litherland, A. E., Paul, E. B., Bartholomew, G. A., and Gove, H. E., 1956, Phys. Rev. 102,208.

March, P. V., and Morton, W. T., 1958a, Phil. Mag. 3,143; 1958b, ibid, 3,557.

Margenau, H., and Murphy, G. M., 1943, "The Mathematics of Physics and Chemistry" (New York: Van Nostrand).

Marion, J. B., Brugger, R. M., and Bonner, T. W., 1955, Phys. Rev. 100,46.

Mayer, M. G., 1949, Phys. Rev. 75,1969.

Morse, P. M., and Feshbach, H., 1953 "Methods of Theoretical Physics" (New York: McGraw-Hill).

Newton, T. D., 1956, Can. Jour. Phys. 30,53.
1952, Can. Jour. Phys. 34,804.

Oppenheimer, J. R., and Phillips, M. 1935, Phys. Rev. 48,500.

Overley, J. C., Pixley, R. E., and Whaling, W., 1956, Bull. Am. Phys. Soc. 1,387.

Paris, C. H., Valckx, F. P. G., and Endt, P. W., 1954, Physica 20,573.

Paul, E. B., and Clarke, R. L., 1953, Can. Jour. Phys. 31,267.

Pratt, W. W., 1954, Phys. Rev. 93,816.

Redman, W. C., 1950, Phys. Rev. 79,6.

Rich, M., and Madey, R., 1954, "Range Energy Tables" (U.C.R.L. 2301)

Robertson, C., 1958, Private Communication

Rose, M. E., 1953, Phys. Rev. 91,610.

Rutherford, E., 1911, Phil. Mag. 21,669.

Sargent, C. P., and Bertozzi, W., 1957, Proceedings of the International Conference on the Neutron Interactions with the Nucleus, Columbia Univ. Sept., 1957.

Satchler, G. R., and Spiers, J. A., 1952, Proc. Phys. Soc. A65,980.

Schenck, J., and Neiler, J. H., 1954, Nucleonics 12, No. 3,28.

Segre, E., (Ed.), 1953, "Experimental Nuclear Physics I" (New York: Wiley).

Siegbahn, K., (Ed.), 1955, "Beta and Gamma-Ray Spectroscopy" (Amsterdam: North Holland)

Serber, R., 1947, Phys. Rev. 72,1008.

Sharp, W. T., Kennedy, J. M., Sears, B. J., and Hoyle, M. G., 1953, "Tables of Coefficients for Angular Distribution Analysis" (Chalk River: Atomic Energy of Canada Ltd.)

Sharpe, J., 1955, "Nuclear Radiation Detectors" (London: Methuen)

Simon, A., and Welton, T. A., 1953, Phys. Rev. 90,1036.

Sinclair, R. M., 1954, Phys. Rev. 93,1082.

Ter Haar, D., 1954, "Elements of Statistical Mechanics" Rinehart and Co., New York, 1954.

Ter Martirosian, K. A., 1956, Soviet Physics, 2,620.

Thirion, J., 1953, Annales de Physique 8,489.

Thompson, L. C., 1954, Phys. Rev. 96,369.

Thomson, D. L., 1957, Proc. Phys. Soc. A69,447.

Tobocman, W., and Malos, M. H., 1955, Phys. Rev. 97,132.

Van de Graaff, R. J., 1931, Phys. Rev. 38,1919; 1933, ibid,43,149

Van Seiver, W., and Hofstadter, R., 1951, Phys. Rev. 84,1062.

Varma, J., and Jack, W., 1956, Physica 22, 1139(A).

Wäffler, H., 1950, Helv. Phys. Acta 23,239.

Wallace, K. A., 1957, Ph. D. Thesis.

Way, K., King, R. W., McGinnis, C. L, and van Lieshout, R., 1955, "Nuclear Level Schemes" (U.S.A.E.C. TID-5300).

Weisskopf, V. F., 1937, Phys. Rev. 52,295, 1951, ibid, 83,1073.

Wells, G., 1958, Private Communication.

Wigner, E. P., and Feenberg, E., 1941, Rep. Prog. Phys. 8,274.

Wilkinson, D. H., 1956, Phil. Mag. 1,127; 1957, Phy. Rev. 105,666.